Pharmaceutical aspects of subvisible particles in protein formulations
Weinbuch, D.

Citation
Weinbuch, D. (2016, December 13). *Pharmaceutical aspects of subvisible particles in protein formulations*. Retrieved from https://hdl.handle.net/1887/44780

Version:	Not Applicable (or Unknown)
License:	Licence agreement concerning inclusion of doctoral thesis in the Institutional Repository of the University of Leiden
Downloaded from:	https://hdl.handle.net/1887/44780

Note: To cite this publication please use the final published version (if applicable).

Cover Page

Universiteit Leiden

Author: Weinbuch, D.
Title: Pharmaceutical aspects of subvisible particles in protein formulations
Issue Date: 2016-12-13

Pharmaceutical aspects of subvisible particles in protein formulations

DANIEL WEINBUCH

Pharmaceutical aspects of subvisible particles in protein formulations

Farmaceutische aspecten van microscopisch fijne deeltjes in eiwitformuleringen
(met een samenvatting in het Nederlands)

Proefschrift

ter verkrijging van
de graad van Doctor aan de Universiteit Leiden,
op gezag van Rector Magnificus Prof. Mr. C.J.J.M. Stolker,
volgens besluit van het College voor Promoties
te verdedigen op 13. December 2016 des middag te 12.30 uur.

door

Daniel Weinbuch

Geboren op 1 mei 1985 te Illertissen, Duitsland

Promotor

Prof. Dr. W. Jiskoot

Co-promotor

Dr. A. Hawe

Promotiecommissie

Prof. Dr. J.A. Bouwstra, Leiden University, Chair
Prof. Dr. M. Danhof, Leiden University, Secretary
Prof. Dr. W. Friess, Ludwig Maximilian University of Munich, Germany
Prof. Dr. A.M. Juppo, University of Helsinki, Finland
Prof. Dr. C.J. Roberts, University of Delaware, USA
Prof. Dr. A.P. IJzerman, Leiden University

"I am a part of all that I have met."

(Alfred Lord Tennyson)

Table of contents

CHAPTER 1

GENERAL INTRODUCTION

Immunogenicity of therapeutic proteins

Since the introduction of insulin as the first protein-based pharmaceutical product in the 1920s, the market for and the number of biopharmaceutical drugs has been rapidly growing. At present, about 100 different therapeutic proteins have been approved for clinical use by the US Food and Drug Administration (FDA) and they have acquired a key role in the treatment of various diseases such as several types of cancer, autoimmune and inflammatory diseases, and metabolic disorders (1). The first therapeutic proteins originated from non-human sources, such as equine antisera and insulin from bovine or porcine pancreas. Even though effective for therapy in humans, the large drawback of such proteins was their low purity and foreign structure to the human immune system, resulting in immune reactions in patients against the therapeutics (2). Extensive research has been performed in the past 30 years to improve safety and efficacy of biopharmaceuticals. With the development of improved molecular biology methods, recombinant expression techniques and better purification protocols, it has become possible to obtain highly pure recombinant human proteins. It was believed that those recombinant human proteins will not be recognized as foreign by the human immune system and will therefore not reveal the immunogenicity-related problems of former therapeutic proteins. However, clinical and post-market studies show that even these "human" products still induce immune responses in patients, suggesting that not just "foreignness" alone is responsible for the unwanted immunogenicity (3–5).

As we know now, unwanted immunogenicity of therapeutic proteins is a complex issue depending on patient-related factors (e.g., type of disease, genetic background), treatment-related factors (e.g., administration route, dosage regime), and product-related factors (e.g., product modifications, contaminants, and impurities) (6–8). An introduction of biological mechanisms potentially underlying unwanted immunogenicity can be found in Chapter 3. While it is still not entirely clear how each factor contributes to a drug product's potential for immunogenicity, it is generally recognized that the presence of aggregates is one of the main product-related risk factors for inducing immune reactions in patients (9–12).

Protein degradation and aggregation

Protein degradation can occur throughout the life cycle of a drug product, including manufacturing, storage, handling and administration to patients. The protein can thereby undergo various ways of degradation (13). Chemical modification for example include reactions such as deamidation, oxidation, isomerization, and peptide bond cleavage.

These can compromise the primary structure and thereby the conformational stability of a protein. Conformational stability can also be influenced by physical degradation including exposure to elevated temperatures, solid-liquid and liquid-air interfaces. In many instances, protein degradation results in protein aggregation.

Protein aggregation can follow a number of different mechanisms and pathways (Figure 1). These mechanisms are not mutually exclusive and can occur in parallel within the same product. The predominant mechanisms depends not only on the protein itself, but also on a variety of other factors, such as the formulation, the presence of impurities or contaminants, and the exposure to chemical or physical stress mentioned above (14–16). It is currently not fully understood how different aggregation mechanisms and the thereby resulting structural differences of aggregates influence their potential immunogenicity.
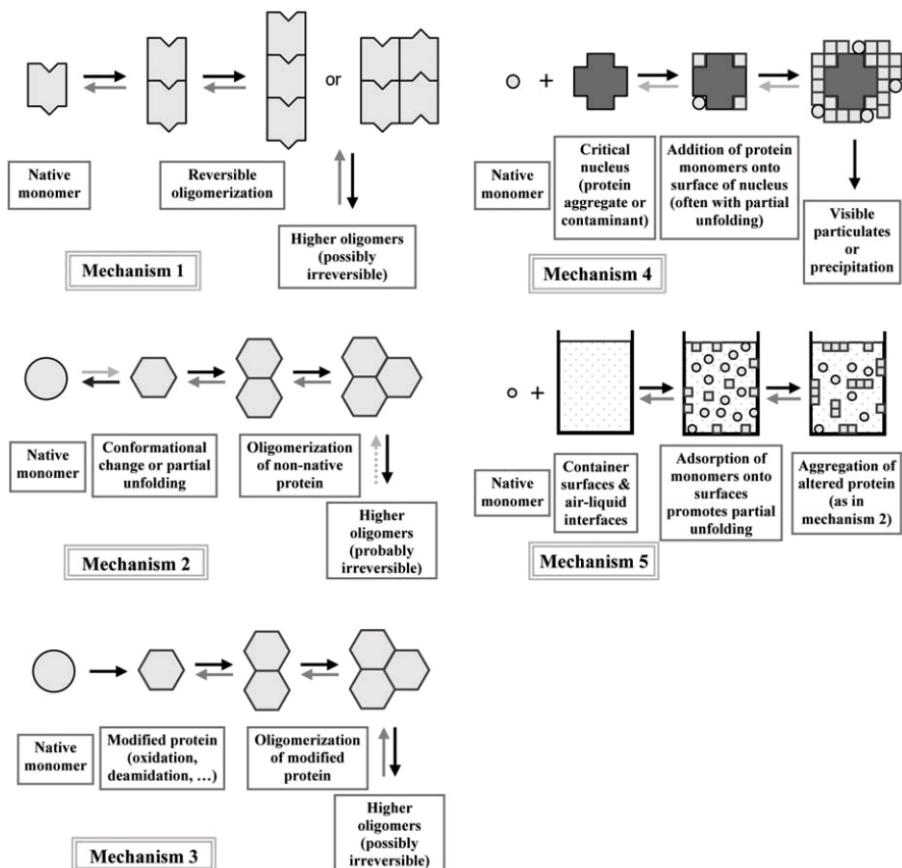

Figure 1: Schematic illustration of five common aggregation mechanisms (14).

Formulation development, an integral part of every biopharmaceutical drug product development program, aims to obtain a product that, amongst other things, maintains the stable and functional state of a therapeutic protein throughout the intended shelf life, while suppressing the potentially harmful degradation pathways. A detailed introduction into formulation development can be found in Chapter 2.

Analytical challenges

One major challenge during protein formulation development is the reliable characterization and quantification of potential degradation products, particularly aggregates and particles in the size range between around 0.1 to 10 µm (17,18). Importantly, proteinaceous particles in this size range are potentially the most immunogenic class of protein aggregates and are thus generally considered a critical quality attribute (19–22). While instrument manufacturers have worked on providing new analytical techniques to overcome an analytical gap in the subvisible size range identified in 2009 (19), there is a large demand of their critical scientific evaluation (23–26). Additionally, subvisible particles can be composed of non-proteinaceous material, such as particle sheds from pumps or primary packaging materials (including silicone oil droplets in prefilled syringes) or particles formed by degradation of excipients (e.g., polysorbate). While those are not necessarily harmful themselves, they can negatively impact protein stability and thereby compromise product quality (27–32). The presence of non-proteinaceous particles can also be indicative of problems during the production process (33). Unlike the compendial specification for particles ≥ 10 µm and ≥ 25 µm (34,35), there are currently no specifications for particle concentrations in the size range < 10 µm. It is therefore necessary for developers of innovator as well as biosimilar products to assess the nature and criticality of potentially present aggregates and particles case-by-case.

Aim and outline of this thesis

The aim of the work presented here was to evaluate and improve established and emerging analytical techniques for the characterization of aggregates and particles in the nm- and µm-size range, which are to be employed during research and development of biopharmaceutical drug products. These analytical techniques are then applied:

(i) to characterize particles in the nm- and µm-size range present in protein formulations and

(ii) to study the effect of nanoparticulate impurities from excipients on the stability of therapeutic proteins.

Chapter 2 is an introduction into the field of protein formulation development. It reviews literature on current protein formulation development strategies and summarizes current challenges formulation scientists are facing. **Chapter 3** is an introduction into the concept and underlying mechanisms of unwanted immunogenicity, as well as a review of various models currently employed to predict immunogenicity during the different stages of research and development of biopharmaceutical drug products. In **Chapter 4**, an improved version of the commonly applied subvisible particle counting technique light obscuration is investigated for its applicability to analyze formulations with high protein concentrations. The influence of sample viscosity on the results of different system setups is studied using highly concentrated drug products and model solutions with enhanced viscosity, which are spiked with polystyrene beads. **Chapter 5** is a comparative evaluation of Micro-Flow Imaging and Resonant Mass Measurement as emerging techniques for the differentiation of protein particles and silicone oil droplets in biopharmaceutical formulations. Artificially formed protein aggregates and silicone oil droplets in various concentrations and size ranges are analyzed individually and in different combinations by both systems. Furthermore, a novel mathematical filter, differentiating the particle types based on morphology, is developed and evaluated in comparison to currently used algorithms. In **Chapter 6**, four of the most relevant flow-imaging microscopy instruments are compared with the goal of identifying their differences, benefits and shortcoming. Artificially formed protein aggregates and silicone oil droplets as well as counting and sizing standards are used to test the instruments with respect to their accuracy and precision regarding size and concentration determination as well as their capability of differentiating particles of different morphology. In **Chapter 7**, an interference of sugar-containing formulations with light scattering based detection of nm-sized protein aggregates is investigated. The root cause of this interference is studied by using various different sugars, purification techniques and analytical instruments. In **Chapter 8**, nanoparticulate impurities found in pharmaceutical-grade sucrose are investigated and their effect on the stability of four therapeutic monoclonal antibodies currently on the market is studied in a time and concentration dependent fashion. In **Chapter 9**, the main findings are summarized and perspectives for further developments of analytical techniques and improvements of scientific knowledge in the field of subvisible particle analysis are briefly discussed.

References

1.   Kinch MS. An overview of FDA-approved biologics medicines. Drug Discov Today. 2015;20(4):393–8.

2.   Fineberg SE, Galloway JA, Fineberg NS, Goldman J. Effects of species of origin, purification levels, and formulation on insulin immunogenicity. Diabetes. 1983;37(7 I):592–9.

3.   Greenfield JR, Tuthill a, Soos M a, Semple RK, Halsall DJ, Chaudhry a, et al. Severe insulin resistance due to anti-insulin antibodies: response to plasma exchange and immunosuppressive therapy. Diabet Med. 2009 Jan;26(1):79–82.

4.   Renard E, Scheen AJ. Circulating insulin antibodies : influence of continuous subcutaneous or intraperitoneal insulin infusion , and impact on glucose control. Diabetes Metab Res Rev. 2009;(June):491–501.

5.   Bertolotto A, Deisenhammer F, Gallo P, Sölberg Sørensen P. Immunogenicity of interferon beta: differences among products. J Neurol. 2004 Jun;251 Suppl(S2):II15–24.

6.   Schellekens H. The immunogenicity of therapeutic proteins and the fabry antibody standardization initiative. Clin Ther. 2008 Jan;30(SUPPL. 2):S50–1.

7.   Schellekens H. Factors influencing the immunogenicity of therapeutic proteins. Nephrol Dial Transplant. 2005;20(SUPPL. 6).

8.   Sauerborn M, Brinks V, Jiskoot W, Schellekens H. Immunological mechanism underlying the immune response to recombinant human protein therapeutics. Trends Pharmacol Sci. 2010 Feb;31(2):53–9.

9.   Ratanji KD, Derrick JP, Dearman RJ, Kimber I. Immunogenicity of therapeutic proteins: Influence of aggregation. J Immunotoxicol. 2013 Aug 6;6901(2012):1–11.

10.   Rosenberg AS. Effects of protein aggregates: an immunologic perspective. AAPS J. 2006 Jan;8(3):E501–7.

11.   Wang W, Singh SK, Li N, Toler MR, King KR, Nema S. Immunogenicity of protein aggregates--concerns and realities. Int J Pharm. Elsevier B.V.; 2012 Jul 15;431(1-2):1–11.

12.   Moussa EM, Panchal JP, Moorthy BS, Blum JS, Joubert MK, Narhi LO, et al. Immunogenicity of Therapeutic Protein Aggregates. J Pharm Sci. Elsevier Ltd; 2016;105(2):417–30.

13.   Mahler HC, Friess W, Grauschopf U, Kiese S. Protein aggregation: Pathways, induction factors and analysis. J Pharm Sci. Elsevier Masson SAS; 2009;98(9):2909–34.

14.   Philo JS, Arakawa T. Mechanisms of protein aggregation. Curr Pharm Biotechnol. 2009;10:348–51.

15.   Roberts CJ. Protein aggregation and its impact on product quality. Curr Opin Biotechnol. 2014;30:211–7.

16.   Morris AM, Watzky M a, Finke RG. Protein aggregation kinetics, mechanism, and curve-fitting: a review of the literature. Biochim Biophys Acta. Elsevier B.V.; 2009;1794(3):375–97.

17.   Narhi LO, Schmit J, Bechtold-Peters K, Sharma D. Classification of protein aggregates. J Pharm Sci. 2012 Feb;101(2):493–8.

18.   Zölls S, Tantipolphan R, Wiggenhorn M, Winter G, Jiskoot W, Friess W, et al. Particles in therapeutic protein formulations, Part 1: overview of analytical methods. J Pharm Sci. 2012 Mar;101(3):914–35.

19.   Carpenter JF, Randolph TW, Jiskoot W, Crommelin DJA, Middaugh CR, Winter G, et al. Overlooking subvisible particles in therapeutic protein products: gaps that may compromise product quality. J Pharm Sci. 2009 Apr;98(4):1201–5.

20.   Singh SK, Afonina N, Awwad M, Bechtold-Peters K, Blue JT, Chou D, et al. An industry perspective on the monitoring of subvisible particles as a quality attribute for protein therapeutics. J Pharm Sci. 2010;99(8):3302–21.

21.   Narhi LO, Jiang Y, Cao S, Benedek K, Shnek D. A critical review of analytical methods for subvisible and visible particles. Curr Pharm Biotechnol. 2009 Jun;10(4):373–81.

22.   Kirshner LS. Regulatory expectations for analysis of aggregates and particles. In: Colorado Protein Stability Conference. Breckenridge, CO; 2012.

23.   Filipe V, Hawe A, Jiskoot W. Critical evaluation of Nanoparticle Tracking Analysis (NTA) by NanoSight for the measurement of nanoparticles and protein aggregates. Pharm Res. 2010 May;27(5):796–810.

24.   Nishi H, Mathäs R, Fürst R, Winter G. Label-Free Flow Cytometry Analysis of Subvisible Aggregates in Liquid IgG1 Antibody Formulations. J Pharm Sci. 2013 Nov 11;103(1):1–10.

25.   Narhi LO, Corvari V, Ripple DC, Afonina N, Cecchini I, Defelippis MR, et al. Subvisible (2-100 μm) particle analysis during biotherapeutic drug product development: Part 1, considerations and strategy. J Pharm Sci. 2015;104(6):1899–908.

26.   Weinbuch D, Zölls S, Wiggenhorn M, Friess W, Winter G, Jiskoot W, et al. Micro-flow imaging and resonant mass measurement (archimedes) - complementary methods to quantitatively differentiate protein particles and silicone oil droplets. J Pharm Sci. 2013;102(7):2152–65.

27.   Mehta SB, Lewus R, Bee JS, Randolph TW, Carpenter JF. Gelation of a monoclonal antibody at the silicone oil-water interface and subsequent rupture of the interfacial gel results in aggregation and particle formation. J Pharm Sci. 2015;104(4):1282–90.

28.   Ludwig DB, Carpenter JF, Hamel J-B, Randolph TW. Protein adsorption and excipient effects on kinetic stability of silicone oil emulsions. J Pharm Sci. 2010 Apr;99(4):1721–33.

29.   Britt KA, Schwartz DK, Wurth C, Mahler HC, Carpenter JF, Randolph TW. Excipient effects on humanized monoclonal antibody interactions with silicone oil emulsions. J Pharm Sci. 2012 Sep 16;101(12):4419–32.

30.   Li Y, Hewitt D, Lentz YK, Ji J a, Zhang TY, Zhang K. Characterization and stability study of polysorbate 20 in therapeutic monoclonal antibody formulation by multidimensional ultrahigh-performance liquid

chromatography-charged aerosol detection-mass spectrometry. Anal Chem. 2014 May 20;86(10):5150–7.

31.   Siska CC, Pierini CJ, Lau HR, Latypov RF, Fesinmeyer RM, Litowski JR. Free fatty acid particles in protein formulations, Part 2: Contribution of polysorbate raw material. J Pharm Sci. 2015 Sep 5;104(2):447–56.

32.   Kerwin BA. Polysorbates 20 and 80 used in the formulation of protein biotherapeutics: structure and degradation pathways. J Pharm Sci. 2008 Aug;97(8):2924–35.

33.   Saller V, Matilainen J, Grauschopf U, Bechtold-Peters K, Mahler HC, Friess W. Particle Shedding from Peristaltic Pump Tubing in Biopharmaceutical Drug Product Manufacturing. J Pharm Sci. 2015;104(4):1440–50.

34.   Ph.Eur. 2.9.19. General, particulate contamination: sub-visible particles. In: The European Pharmacopoeia,. 7th ed. 2011.

35.   USP <787>. Subvisible particulate matter in therapeutic protein injections. In: The United States Pharmacopoeia, National Formulary.

CHAPTER 2

INTRODUCTION INTO FORMULATION DEVELOPMENT OF BIOLOGICS

Daniel Weinbuch[1,2], Andrea Hawe[1], Wim Jiskoot[2], Wolfgang Friess[3]

[1] Coriolis Pharma, Am Klopferspitz 19, 82152 Martinsried-Munich, Germany

[2] Division of Drug Delivery Technology, Leiden Academic Centre for Drug Research (LACDR), Leiden University, P.O. Box 9502, 2300 RA Leiden, The Netherlands

[3] Department of Pharmacy, Pharmaceutical Technology and Biopharmaceutics, Ludwig Maximilian University, 81377 Munich, Germany

Abstract

Formulation development is an essential part of every biopharmaceutical development program and important for the therapeutic and commercial success of a promising protein drug product. Assuring the quality, safety, and efficacy of a therapeutic product throughout the intended shelf life are thereby major goals. Formulation development is composed of multiple phases, interacting with other product development exercises as early as discovery research all the way until and beyond market approval. Every drug product demands a tailor-made formulation, due to the complexity of degradation pathways potentially affecting the product stability, the specific characteristics of the active pharmaceutical ingredient, the demands for patient compliance, and even marketing considerations. Formulation development can be approached using various strategies, based on a rational design, relying on scientific knowledge in low or medium throughput, or high-throughput formulation (HTF) approach screening of hundreds or even thousands of conditions employing miniaturized analytical methods. In this chapter an introduction to the field of protein formulation development is given, literature on current protein formulation development strategies is reviewed, and current challenges are summarized.

Introduction

Protein formulation development aims to render a therapeutic protein product robust for manufacturing, storage, handling and administration to patients. So, formulation development is essential for the therapeutic and commercial success of a promising protein molecule: "it is a medicine, not a molecule, that we are giving to the patient" (1). With this chapter, the reader is introduced to general concepts related to formulation development of biologics. The focus is on liquid and lyophilized protein formulations for parenteral use, as those comprise the vast majority of our current arsenal of marketed biologics. Nevertheless, most of the concepts described in this chapter also apply to other biologics, such as vaccines and DNA- and RNA-based products. Issues specific for the challenges of protein delivery systems for non-invasive administration and particles for sustained release and targeting are beyond the scope of this chapter; the interested reader is referred to the literature (2–6).

Within this chapter we discuss various elements of protein formulation development, formulation strategies during several stages of development and challenges that can be encountered. Rather than going into great detail, the intention is to present the complexity of the topic and important aspects that should be considered during formulation development (see Table 1).

Formulation Development Strategies and Approaches

Protein Formulation: Beyond Stabilization

One of the major challenges in the formulation of therapeutic proteins is to assure their stability, not only during storage but also during manufacturing, shipment, handling and administration. Nevertheless, it should be realized that the 'optimal' formulation is not necessarily the one that is most stable, but rather should fit the purpose depending on several factors. These include, besides sufficient stability, the stage of development, clinical requirements, regulatory requirements, packaging, and device configuration, economical issues, marketing considerations or the freedom to operate within the patent landscape (Table 1). As an example, what is 'best' in terms of a product's stability is not necessarily good from a patient's or economical perspective. For instance, suppose a certain product would be most stable in 50 mM sodium citrate, pH 4.0. If the product is meant for subcutaneous administration, this formulation probably would be not preferred, because the unfavorable combination of low pH and hypotonicity may cause pain at the injection site (7). The same formulation might, however, be acceptable if the product were intended to be diluted in an infusion liquid prior to intravenous

administration, provided that the product is stable in use and compatible with the infusion system. Another example: if a lyophilizate in a vial would be stable for five years but the same molecule could be formulated as an aqueous solution in a prefilled syringe with two years shelf life, the latter might be preferred over the more stable formulation for economical and marketing reasons and due to easier patient self-administration.

Table 1: Critical factors to be considered during formulation development.

Factor	Description / attributes / examples
Analytical methods	High- versus low-throughput, stability-indicating, QC, extended characterization
API	Type of protein, physico-chemical properties, e.g., molecular weight, pI, hydrophobicity, solubility, post-translational modifications, pegylation
Clinical factors	Patient population (e.g., age, indication, concomitant medication), therapeutic window, self-administration versus administration by professional, compatibility with infusion solution
Competitive landscape	Originator versus biosimilar product, patent situation, competitive drugs
Dosage form	Single- or multi-dose, prefilled syringe, dual chamber cartridge, pen cartridge
Drug substance	API concentration, formulation composition, available amount, purity
Excipients	Pharmaceutical quality, safety record (for intended administration route and dose), manufacturer, tested for critical impurities, stability
Manufacturing capabilities	Disposable/non-disposable technologies, dedicated equipment, filling line / pumping
Other factors	Budget, time(lines), manufacturability, company policy, marketing strategy, regulatory requirements
Phase of development	Preclinical, early clinical, late clinical, commercial
Primary packaging material	Glass, polymers, rubber, silicone oil, metals, leachables (anti-oxidants, plasticizers, etc.)
Route of administration	Subcutaneous, intravenous injection or infusion, intramuscular, intravitreal, intraarticular, intradermal
Target dose and dosing regime	Concentration, volume, indication (e.g., one-time application or chronical application)
Type of formulation	Liquid, lyophilizate, frozen liquid

Since a liquid formulation is often faster and cheaper to produce and is more user-friendly, generally it is preferred over a lyophilizate. However, it may be impossible to develop a sufficiently stable liquid formulation, either because of time constraints during (early) product development or because the molecule turns out to be insufficiently stable even after extensive formulation development exercises. The obvious alternative in such cases is a dry formulation (apart from an early-stage frozen liquid formulation), which is almost exclusively achieved by lyophilization, a process requiring dedicated formulation development.

From a formulation scientist's perspective, in an ideal world already at the earliest stage of development the final dosage form, the required stability profile as well as other needs (see Table 1) have been defined, high-throughput, stability-indicating analytical methods are in place, and material, time and resources are available in unlimited amounts. However, the real world is quite different. Consequently, the first formulation used during preclinical studies (e.g., toxicity studies) is likely going to be different from the formulation applied during later clinical phases and the final formulation used for commercialization. This may be explained, besides by the above-mentioned reasons, by changes in the dosing regime, the route of administration or the primary packaging material (e.g., switch from vials to syringes) or by instabilities occurring in a not-yet-optimized formulation as well as additional insight gained into the stability of the protein molecule and/or the excipients. Nevertheless, it is highly favored to have the final formulation composition defined as early as possible during drug product (DP) development to avoid additional studies, regulatory efforts and to align drug substance (DS) and DP composition. To this end, it is imperative that the formulation scientist acquires knowledge about the clinical needs, marketing considerations as well as regulatory requirements. Moreover, the more is known about the physical and chemical stability of a protein molecule as function of major formulation variables and external stress factors (temperature, mechanical stress, freezing and thawing etc.) early in the development, the less complex, costly and time-consuming it will be in a later stage of development to accommodate a formulation to the needs of the molecule and the product.

 "There isn't just one way of doing it" holds true for formulation development of biologics and there are numerous ways and philosophies how to come to a stable and robust formulation. No matter which approach is followed for achieving a satisfactory formulation, the selection of analytical methods plays a crucial role. Already early in the process the critical routes of instability need to be identified in order to establish the important stability indicating analytical methods as well as the appropriate formulation strategy to tackle the instability issues. Formulation development usually evolves during a drug development program, and often thereafter, and can generally be divided in the following activities: preformulation, formulation development for DS, DP formulation development for preclinical phases, for early clinical phases, for late stage/commercialization, and finally formulation activities during the life cycle of a product (Figure 1). Of course, there certainly is an overlap between these phases and wherever applicable, considerations for a later stage should be reflected as early in the development process as possible. In the following sections, we describe first what typically

forms part of a protein formulation and then discuss several phases and approaches of formulation development.
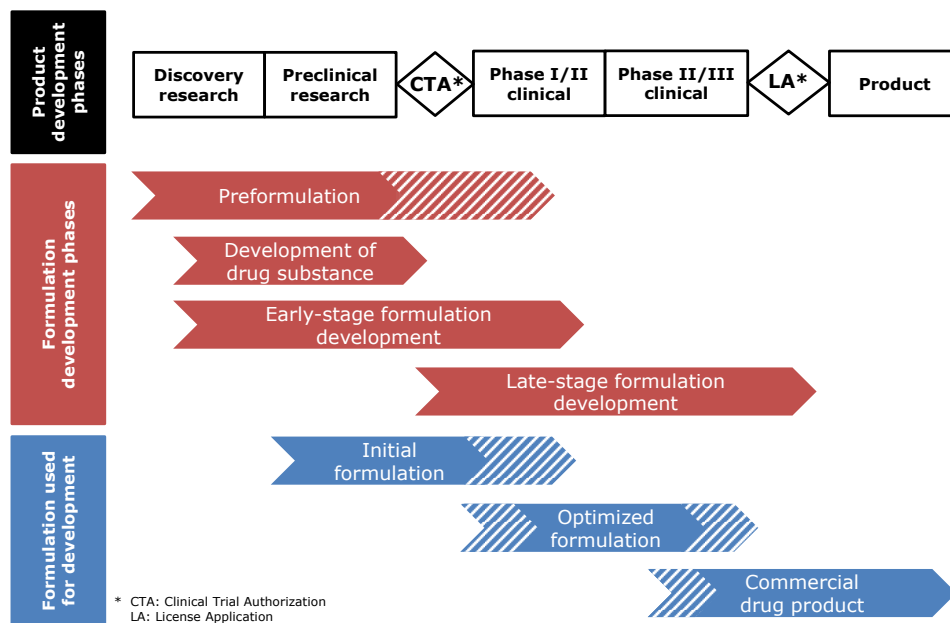
Figure 1: Diagram of a formulation development process. Modified from (8).

Components of a Protein Formulation

Active pharmaceutical ingredient and drug substance

The term active pharmaceutical ingredient (API) refers to the molecule of interest e.g., a peptide, monoclonal antibody or enzyme. In a pure state, the API would typically be a solid powder, as often found for peptides. This state however, is extremely impractical to obtain and/or presents an unstable state for most biologics. Therefore, a DS, a (sometimes frozen) liquid formulation containing the API is used for purified bulk storage. A DS typically results from a chromatographic or ultra-diafiltration step at the end of a purification process. In commercial-scale production, the formulation composition of the DS is often very similar to that of the final DP, but this can obviously not be the case when formulation development has yet to be completed. This may have consequences for DP formulation screening.

Excipients

One rule in formulation development is to avoid putting anything into the formulation that is not needed. In other words, a formulation should be kept as simple as possible and

each excipient, as well as its quantity, should be justified. Having mentioned this, it is not an easy task to combine the right excipients in the right concentration, because a stabilizing excipient potentially exhibits a destabilizing effect on a different protein instability pathway, and excipients potentially influence each other's action. For instance, polysorbates added for protection against interface related protein aggregation may contain oxidizing species, which may promote chemical instability (9). Whereas sodium chloride could help reducing a formulation's viscosity, it may negatively affect a protein's colloidal stability and also be detrimental upon freezing or lyophilization as upconcentrated in the freeze-concentrated solution (10). Finally, the most frequently used excipient, water for injection, is a natural solvent for proteins but at the same time mediates most if not all possible protein degradation reactions, reason why many products are lyophilized to reduce the water content to minimal amounts.

Table 2 gives an overview of the most commonly used excipient classes and their functions in protein formulations. Importantly, it is common practice to choose among excipients that are approved and commonly used in protein formulations (see examples in Table 2) in comparable doses and dosing frequencies for the intended route of administration. Although it would be interesting to explore novel excipients in order to expand the options for a formulation scientist, including a new excipient in a formulation is often a 'no go'. The reason is that it would greatly increase development time and cost, because – besides the need for a justification to use it instead of a more common excipient – its safety would have to be evaluated in order to get the product approved for clinical trials and registration. The same may hold true for unusually high doses of a certain excipient. Furthermore, the quality of excipients should be considered critically and their stability in the specific formulation should be assessed. For instance, sucrose might not be included in liquid formulations below pH 6, because its hydrolysis rate during storage may become significant, leading to the formation of fructose and glucose; the latter degradant can form glycation products with the protein via the Maillard reaction (11). While excipients preferably should comply with compendial standards, additional requirements may apply for specific protein formulations.

Excipients can exert several functions, e.g., glycine can act as stabilizer, buffer and tonicity modifier and may have several modes of action. The need for their inclusion in a protein formulation mainly depends on the critical instability pathways of the protein and other not protein stability related needs, such as tonicity requirements and lyophilizate appearance. Furthermore, certain excipients that may be useful in liquid formulations should be avoided in lyophilizates (e.g., volatile buffers such as acetate, or salts that lower the glass transition temperature of the maximally freeze-concentrated solution (Tg') of

amorphous formulation), whereas some excipient functions are specific for lyophilized products, e.g., bulking agent, lyoprotector.

Table 2: Common excipients encountered in protein formulations.

Excipient class	Function	Examples
Solvents	Dissolution	Water for injection
Buffers	pH control, tonicity	Acetate, citrate, glutamate, histidine, phosphate, succinate, glycine, aspartate
Salts	Tonicity, solubilization, stabilization, viscosity reduction	Sodium chloride
Sugars, polyols	Tonicity, stabilization, cryoprotection, lyoprotection*, bulking agent*	Mannitol, sorbitol, sucrose, trehalose
Surfactants	Solubilization, stabilization, adsorption prevention, reconstitution improvement*	Polysorbate 20, polysorbate 80, Poloxamer
Amino acids	Solubilization, stabilization, tonicity, viscosity reduction, pH control, bulking agent*	Arginine, glycine, glutamate, histidine, lysine, succinate
Anti-oxidants	Oxidation prevention	Methionine, sodium edetate
Preservatives	Antibacterial action (multi-dose formulations)	Benzyl alcohol, meta-cresol, phenol

* specifically for lyophilized products

Buffer species may have specific destabilizing or stabilizing effects on proteins, besides offering buffer capacity. So, buffer type and concentration should be carefully selected during formulations screening and the decision depends not only on the desired pH (typically well within about ± 1 unit from the pKa of the buffer species), but also on the protein, the route of administration, and whether it is a liquid or a lyophilized formulation. Furthermore, in high-concentration protein formulations one could consider not to include any buffer. Especially in slightly acidic, highly concentrated (>50 mg/ml) antibody formulations, the total number of His, Glu, and Asp residues in the API may provide sufficient buffer capacity to provide a stable pH value (12).

Primary Packaging Material

Since the primary packaging material may affect the quality of the DP, it is an important and integral part of the formulation development program. Obviously, the primary packaging material depends on the dosage form (see Table 1 for some examples), which in turn impacts the way a drug is administered and its user-friendliness. Implications of the primary container on formulation development, e.g., the set-up of mechanical stress

studies, are addressed in the section "*Selection of Analytical Methods and Stress Conditions*" of this chapter.

Preformulation

Preformulation studies are a prerequisite "to know your molecule", which is vital for the entire development cycle of a therapeutic protein. On the short term, preformulation studies may be used for candidate selection and will help in the optimization of upstream and downstream processes for the selected candidate molecule as well as in the development of a sufficiently stable formulation for DS, preclinical and first-in-human clinical trials. At later stages of development and after commercialization, the fundamental knowledge acquired with preformulation activities will support the rational design of (an) optimized formulation(s) and the assessment of the shelf life under appropriate storage conditions.

The term preformulation is used rather flexible and differently among research groups with respect to its transition to, or its position within, formulation development. Preformulation studies are performed in close collaboration with discovery research and should start as early as a promising drug candidate has been obtained. Preformulation studies are meant to gain insight into critical physico-chemical properties of the protein drug candidate (see Table 1), such as primary, secondary, and higher-order structure, molecular weight, extinction coefficient, isoelectric point, post-translational modifications, hydrophobicity, and biophysical properties, such as conformational and colloidal stability. Moreover, they are aimed to determine the criticality of various environmental factors, such as pH, ionic strength and buffer species, and the API's sensitivity to pharmaceutically relevant stress conditions (Table 3). The latter involves assessment of the predominant degradation pathways. The critical predominant degradation pathways, as well as the sensitivity to pH and ionic strength, may be quite different between proteins, even for relatively similar ones such as monoclonal antibodies (13–16). Preformulation should ultimately lead to the development of suitable stress conditions and a toolbox of stability-indicating analytical methods, enabling the differentiation between good and bad formulations in upcoming, more comprehensive formulation development studies. In some cases, selected excipients may already be screened to improve the stability of the molecule against critical stress factors.

Table 3. Accelerated stability and forced-degradation studies used in protein formulation screening.

Stress type	Exemplary stress conditions	Anticipated instability types
Temperature	Real-time/intended temperature, e.g., at 2-8°C. Accelerated testing, e.g., at 15, 25 or 40°C	Aggregation, conformational changes, chemical changes
Mechanical, shaking	50-500 rpm, 2 h to >48 h	Aggregation, adsorption, conformational changes
Mechanical, stirring	50-500 rpm, < 1 h to 48 h	Aggregation, adsorption, conformational changes
Mechanical, freeze-thawing	1-5 cycles, e.g., between 25°C and -20°C to -80°C	Aggregation, adsorption, conformational changes
Oxidation	H_2O_2, 1-5 % for 1-2 days, oxygen purge	Chemical changes (oxidation), aggregation, conformational changes
Humidity*	0-100% RH	Aggregation, conformational changes, chemical changes, moisture content

* specifically for lyophilized products

Preformulation includes the testing of the thermal stability, e.g., by (micro-)differential scanning calorimetry (DSC) or dynamic scanning fluorimetry (DSF) as well as the testing of colloidal stability, including aggregation propensity and viscosity, e.g., by determination of the 2nd virial coefficient or the interaction parameter kd by static light scattering (SLS), dynamic light scattering (DLS) or analytical ultracentrifugation (AUC) (17,18). DSC and DSF are often applied to assess thermal events, such as unfolding, which is helpful to define relevant conditions for accelerated stability studies. However, although thermal stability studies are routinely used in formulation screening, for several reasons thermal stability may not correlate with storage stability. For example, Bam et al. (19) observed an excellent stabilization against agitation by polysorbates, although DSC experiments showed lower unfolding temperatures in presence of the surfactant. Furthermore, the ranking of melting temperatures does not always predict the order of conformational stability at storage temperature (20,21). Therefore, preformulation should include mechanical stress e.g., by shaking or stirring at temperatures, far below the Tm value (Table 3). Moreover, chemical degradation can arise from the fully native structure even without the application of thermal or mechanical stress and might in specific cases be more problematic than conformational or colloidal instability (22). Preformulation should thus test for such pathways e.g., by forced oxidation (Table 3).

Formulation Development

Formulation development strategies
Formulation development involves studying the influence of formulation variables on potential critical quality attributes upon intended storage, accelerated and forced-degradation conditions in order to identify a stable and robust formulation based on previous experience with the same API or similar molecules and the preformulation work. There are several ways and philosophies to reach a stable and robust formulation. One is a rational design methodology testing well-selected formulation conditions in low or medium throughput and a defined number of excipients based on the properties of the molecule, as established in preformulation studies. The alternative high-throughput formulation (HTF) approach involves the empirical screening of hundreds or even thousands of different formulations under accelerated conditions preferably employing miniaturized analytical methods. Finally, for some well-known molecule formats (e.g., monoclonal antibodies), platform approaches might be suitable by applying standard formulation conditions with a high chance, but no guarantee of success. For novel protein molecule designs, such a fast-track formulation approach may not be feasible, as a better understanding of the physico-chemical properties and the routes of instability is required to identify appropriate formulation conditions.

Independent of the formulation strategy followed, once a suitable formulation has been identified, its shelf life must be confirmed in real-time and accelerated stability studies and its robustness assessed under relevant stress conditions. Accelerated stability studies can never replace real-time stability assessment, because rates of the degradation routes may have different temperature dependency potentially affected by a change in protein conformation with temperature (8). Consequently, the predominant degradation pathway at elevated temperature, e.g., 25 °C/60 °C, could differ from that under refrigerated conditions (2-8 °C). Therefore, and because protein degradation processes can mutually influence each other in a complex fashion, Arrhenius kinetics often do not apply to protein formulations (23).

Early-stage formulation development
Time pressure, limited resources, the risk of a drug to drop out during the development program, or plans to sell a drug candidate after clinical phase 1, are only some arguments to define an early-stage DP for preclinical phase or clinical phase 1 without extensive formulation development. In this case, within a relatively short time frame the formulation scientist should aim to deliver such an initial formulation that can be reproducibly manufactured with a standard container closure system, while leaving enough flexibility to, e.g., alter the dosage regime and the route of administration at later

development stages. Lyophilization and reconstitution with a different volume is one approach to allow dosing flexibility and setting up different protein concentrations (24,25). The shelf life requirement of this early DP is mainly determined by the logistics of supplying the drug for clinical trials. Stability of the API in the DP until at least the end of the trial must be supported by stability data. Importantly, the more is known at this stage about the intended commercial formulation (e.g., administration route, dosage form, and primary packaging material), the better.

In preformulation and early formulation development, HTF screening can be beneficial, especially if there is no or very limited pre-existing knowledge about the sensitivity of the API to formulation and stress conditions. The high number of test formulations can be handled when working with automated pipetting systems or robots ideally combined with stress testing/stability testing in plates and plate-reader based analytics requiring low sample volumes. Typical analytical methods for this purpose are UV spectroscopy (protein content, turbidity), fluorescence spectroscopy (intrinsic or extrinsic with dyes), and DLS, all of which can be performed fully automated in multi-well plates. Moreover, intermediate-throughput methods, such as HPLC/UPLC and DSC, when performed with autosampler devices, can be conveniently used (26–28).

Late-stage formulation development
While the protein in its initial formulation is tested in clinical trials, the formulation scientist will already be working on an optimized, commercially viable formulation. This formulation should, beyond the stability required for the initial formulation, ultimately be robust against external stresses during the desired shelf life, administration (sometimes using product specific application devices), and to potential protein-specific degradation pathways. In order to test robustness, forced degradation studies at relevant stress conditions (Table 3) combined with a tailored set of stability indicating analytical methods, defined during preformulation, are employed. In this context, design of experiment (DOE) approaches can be applied to optimize experimental setups and reduce the number of required sample measurements (29). While forced degradation studies do not reflect real-life conditions, they are useful to reveal differences in stability between formulations and to give justification on why excipients are added and at which quantity. In late-stage formulation development, tasks of the preformulation phase might still be ongoing and specific molecule characterization tasks may be intensified. Since the DS is at this stage available in larger quantities (and often higher purity), the formulation scientist is not anymore tied to low-volume analytical methods used in early-stage development, but can also employ resource consuming or high-volume methods e.g. AF4, AUC, FTIR-spectroscopy, MS, and particle characterization (30) to test the stability of the protein

more in detail. Knowledge from clinical trials on application route, dosage regime, and the potential use of an application device will also influence the formulation design. The investigation of processing stability should include filter tests, tubing tests, handling test, and fill-finish tests to assure robustness towards stresses during manufacturing, if not already, at least in parts, performed during early-stage development. Finally, real-time stability studies at relevant storage conditions (e.g., 2-8 °C) using the DP in its primary container system from different production batches are to be conducted to define and justify the product's shelf-life. This is stated in the ICH guideline QC5 and for most DPs a shelf life of at least 18 - 24 months is desired.

Formulation development after commercialization

When a commercial DP has successfully entered the market, formulation development might still be needed e.g., for life cycle management to change protein concentration, packaging material, or route of administration and to support changes in the manufacturing process. In this case, knowledge from pre-, early stage, and late stage formulation activities is key to enable fast and effective formulation change and comparability studies. Since slight changes in formulation conditions potentially affect the safety and efficacy of the DP, it is necessary to perform detailed studies to assure that product quality and degradation profile have not quantitatively worsened or even qualitatively altered. If analytical characterization and non-clinical comparability studies are not sufficient for this claim, the ICH Guideline Q5E demands additional clinical comparability studies.

Challenges during Formulation Development

Amount and Quality of DS

One challenge in preformulation and early-stage formulation studies is the typically limited availability of API. The required amount depends in part on the product development stage as well as on the formulation strategy. Vice versa, if substantially limited amounts are available, this may unavoidably lead to a change in formulation strategy and/or a reduction of the number of stress testing methods applied, formulations screened, and analytical methods used (30). Obviously, analytical methods that require little sample are preferred, including well-plated based spectroscopic and light-scattering based methods as well as electrophoretic and chromatographic techniques (28).

Another challenge is the potential variation in DS quality during product development, which may be due to coinciding development and changes in production cell line, cultivation conditions, and downstream processes. In particular during early stages of

product development, the quality of the DS may not reflect that of later-stage (pilot or full-scale production) batches. In particular, aggregate and particle levels in pre-GMP technical batches do not always meet the minimum standards, such as those defined by the USP Chapter 787, which impedes proper assessment of a formulation's capability to avoid aggregation (31). Moreover, the level of impurities or contaminants may have major effects on product stability (32). For instance, variations in residual protease activity will especially affect the stability of the API in a liquid DP. Similarly, a relatively high residual lipase activity may lead to unexpectedly rapid degradation rates of polysorbates (33,34). If the root cause of such degradation processes would be identified in an early stage, one could choose to first develop a frozen liquid or lyophilized DP for early-stage (pre)clinical development, while optimizing the upstream and downstream processes in the meantime. This, however, would take additional resources and time. Ultimately, there is the risk that formulation development is focused on inhibiting a degradation process that turns out to be irrelevant as soon as higher-quality DS batches become available.

For DP formulation screening the available DS formulation will have to be exchanged with the formulations of interest e.g. by column chromatography, dialysis or ultra-/diafiltration. Such processes, which may also involve dilution or concentration of the API, pose stress upon the molecule. Consequently, it should be investigated whether the chosen method compromises the protein quality. Furthermore, in buffer exchange and concentration procedures using a semi-permeable membrane, especially at high protein concentrations, the final formulation composition may significantly differ from the intended one because of unequal partitioning of excipients. This may be due to volume exclusion, non-specific interactions and for ionic solutes, such as salts and buffer components, the Donnan effect (35). The presence of a surfactant such as polysorbates in the DS formulation e.g. introduced in the downstream process to protect the API against interfacial stress would pose a particular challenge, as it is practically impossible to remove surfactants quantitatively and they may accumulate in an unpredictable way during membrane concentration processes (36). Thus, quantification methods for each of the excipients that are part of DS and DP should be in place for guiding the proper design of formulation screening methodologies. Furthermore, once a suitable final DP formulation is chosen, the polishing step in the downstream process can be adjusted to bring the DS formulation in line with that of the DP.

Selection of Analytical Methods and Stress Conditions

The paradigm "formulation is characterization" refers to the fact that only with a proper analytical toolbox one can differentiate between good and poor formulations within the

limited time frame of a short accelerated stability and stress program. But how should one set up the analytical package and appropriate stress conditions?

Analytical methods

No matter which formulation approach is followed, the availability of low-volume, high-throughput methods is advantageous, especially in preformulation and early-stage formulation studies. Techniques used in these stages preferable provide a general indicator for stability, such as melting temperature by DSF or DSC, or colloidal stability by light scattering. Since proteins can undergo a variety of degradation reactions (22), complementary analytical methods should be used for monitoring the formation of all potential degradation products when performing stability and forced-degradation studies. Filipe et al. (30) gave an excellent overview of commonly used analytical methods outlining their measurement parameter, their sample requirement, and whether they can be operated in high-throughput. The interested reader is also referred to books by Jiskoot and Crommelin (37), and by Houde and Berkowitz (38) providing details about analytical methods beyond the scope of this chapter. Especially in later stages of formulation development, orthogonal methods should be used to verify the validity of specific methods. For instance, size-exclusion chromatography (SEC) methods only cover a limited size range of relatively small protein aggregates (up to about 100 nm) and may not detect reversible aggregates within this range (39,40). Consequently, regulatory agencies expect SEC data to be confirmed by orthogonal methods, such as AUC and AF4 (30,41). In addition, until recently the use of compendial methods such as light obscuration has been focused on the analysis of subvisible particles larger than 10 micron. However, safety concern with respect to protein aggregates and other particulates in the size range of 2 – 10 μm and more recently also the submicron size-range has facilitated the development of new particle analysis methods e.g., micro flow imaging, nanoparticle tracking analysis, and resonant mass measurement that are now increasingly being applied in formulation development (30,41–44). This has also been acknowledged by regulatory bodies and has lead to new and updated guidelines such as the USP <787> and the educational chapter USP <1787>, suggesting quantification and qualitative characterization of particles in this size range by orthogonal methods (45). With the analytical methods comes the challenge of setting specifications and their justification. For many quality attributes assessed throughout the whole manufacturing process of a DP like appearance, color, pH, sterility, osmolality, visible particles, or subvisible particles, the pharmacopoeial monographs apply. Other specifications e.g., the SEC monomer content, are not ultimately defined at early stage. A specification of more than e.g., 95 % monomer can be accepted at early stage development, may be set in accordance with platform technology experience and revised reflecting experience and stability data gathered on the way to commercialization.

Stability testing and forced-degradation studies

How to select appropriate stress conditions? The answer to this question is not straightforward, because it depends, amongst others, on the purpose, the protein, the formulation, the dosage form, and the development stage (23). For formulation screening, the stress conditions should be discriminative and allow ranking of formulations, which implies that they should be harsh enough to induce detectable changes, but at the same time not so harsh that all formulations show similar, nearly complete degradation. Preexisting knowledge from the literature and in-house experience with similar molecules may be extremely valuable to set up appropriate stress conditions. Moreover, the relevance of the stress conditions should be kept in mind. For instance, exposing a protein to a temperature above its unfolding temperature over a longer storage period would be as irrelevant as pyrolyzing a small molecule; and if a formulation is shown to be resistant to rigorous shaking for several days, rather than continuing the applied stress for another few weeks, one may conclude that the formulation is robust towards this mechanical stress factor.

Setting up appropriate stress conditions may be part of preformulation and could be done with the DS. Typical stressors include thermal, freeze-thawing, mechanical, and oxidation stress. Table 3 gives some rough indications of possible conditions that could be applied for each of these stress factors. Although extreme pH and ionic strength are sometimes mentioned as stress factors, those are in fact formulation variables that are typically studied in preformulation studies, often in combination with exposure to elevated temperatures. The outcome of such extreme pH/ionic strength exposure studies is relevant to define the design space not only in formulation development but also in downstream processing steps, such as elution conditions in chromatographic procedures, viral inactivation, hold times, and conditions between purification steps.

Light stress may be added at later-stage formulation studies and essential protection is finally provided by the secondary packaging material. One may consider using also less harsh conditions than those according to ICH, in order to assess subtle differences between formulations. If the final container is known, this may be advantageous, especially for mechanical stress studies. For instance, the influence of shaking stress (conditions) is highly dependent on not only the shaking frequency and the incubation temperature, but on container dimensions, filling volume, and solution viscosity as well.

For lyophilized formulations, storage of lyophilizates with different residual moistures levels under accelerated testing conditions needs to be considered. Moreover, the effect of freeze-thawing stress to the corresponding liquid formulation (with conditions used during lyophilization) needs to be studied. Furthermore stress stability testing after

reconstitution is highly valuable to reflect light, temperature, and mechanical stress, which the liquid could potentially be exposed to in the clinics and by the patients.

While forced degradation or accelerated stress studies are valid means to compare formulation conditions during development and are recommended by the ICH Q1 guidelines, they have limited predicting value to the stability of a protein at real-time storage conditions. Thus, one can use these data to understand degradation pathways and to define and justify formulation conditions, for instance the use of an excipient in a certain concentration, but one should not exaggerate forced degradation studies. Instead, a promising formulation should be tested by long-term studies testing at relevant storage conditions as early as possible since these studies are the basis for the determination of the product's shelf life and demonstrate the relevance of the different degradation pathways.

Manufacturability and Formulability

Formulation development has the goal to obtain a DP that serves the patient's needs and promotes stability of the protein. However, manufacturability should also play a role when defining a final formulation, because the product needs to be manufactured at large scale and commercially viable. Some steps and procedures that can be performed with ease in small scale or on a lab bench might be difficult to implement in a large-scale production facility. For example, filtration steps using very low pore size filters are easily performed in the lab, but low volume throughput and the costs of industry-sized filter systems might make implementation problematic in production scale. Also, high-concentration and viscous formulations could be difficult to handle during manufacturing and might cause problems during release testing by required compendial methods such as light obscuration. Contrary, low-concentration formulations might face the problem of protein loss through surface absorption, a factor that can become more relevant in a production facility. The same holds true for excipients in low concentrations e.g., substantial loss of polysorbate to filters at the beginning of a filling process can occur. The scale up to a commercial facility can create additional problems not observed in small scale. For example, mixing solutions in a large stainless steel tank, pumping solutions through stainless steel tubing, filtration, and filling through a high-speed filling machine can introduce unexpected stresses to the protein. In addition, the introduction of particles, e.g., by pump systems has been observed. Therefore, the relevance of such scale-up related problems should be assessed early during process development and should be considered during formulation development. Since some, if not all, of the factors mentioned above can show a certain batch-to-batch variability, regulators require stability data from multiple production batches before approval of the final DP.

Data Handling and Analysis

From the above it should be clear that protein formulation screening will involve the generation, analysis, and interpretation of huge data sets. The two goals of a formulation scientist are to make analytical data manageable as well as interpretable. For the first, a streamlined data analysis is important, which should include standardized export and analysis templates for each analytical technique (either using standard office software or dedicated data analysis programs). In addition, meaningful data folder and file structures as well as traceable sample names are crucial when handling huge data sets. For the second goal, singular-value decomposition analysis can help to condense complex data sets, e.g., spectroscopic data, by vector algorithms to a few descriptive values without loosing information. Further, visualization tools such as empirical phase diagrams and radar plots (46,47) will improve data interpretation and will allow the formulation scientist to identify the best formulation more quickly.

Conclusions

Protein formulation activities are an important part of a protein drug development process. Formulation development should start early in product development. Selecting 'the right' formulation requires extensive exercises, including analytical method development, forced-degradation studies, and accelerated and real-time stability studies. Moreover, clinical needs, company policy, and marketing strategy should be taken into consideration during formulation development. Knowledge gained during preformulation activities will help the scientist to identify potential hurdles in the subsequent formulation development program and to design a formulation to overcome those, by selecting a limited number of required excipients in appropriate amounts. Since the definition of 'the right' formulation depends in part on the development stage, early stage formulations typically differ from late-stage and commercial formulations. Despite its complexity, if formulation development is done properly, the final result is often a simple liquid or lyophilized formulation in a dosage form for parenteral administration.

References

1.   Brown MB. The lost science of formulation. Drug Discov Today. 2005 Nov 1;10(21):1405–7.

2.   Antosova Z, Mackova M, Kral V, Macek T. Therapeutic application of peptides and proteins: parenteral forever? Trends Biotechnol. 2009 Nov;27(11):628–35.

3.   Jiskoot W, Randolph TW, Volkin DB, Middaugh CR, Schöneich C, Winter G, et al. Protein instability and immunogenicity: roadblocks to clinical application of injectable protein delivery systems for sustained release. J Pharm Sci. 2012 Mar;101(3):946–54.

4.   Mitragotri S, Burke PA, Langer R. Overcoming the challenges in administering biopharmaceuticals: formulation and delivery strategies. Nat Rev Drug Discov. 2014 Sep;13(9):655–72.

5.   Pisal DS, Kosloski MP, Balu-Iyer SV. Delivery of therapeutic proteins. J Pharm Sci. 2010 Jun;99(6):2557–75.

6.   Schweizer D, Serno T, Goepferich A. Controlled release of therapeutic antibody formats. Eur J Pharm Biopharm. 2014 Oct;88(2):291–309.

7.   Laursen T, Hansen B, Fisker S. Pain perception after subcutaneous injections of media containing different buffers. Basic Clin Pharmacol Toxicol. 2006;98(2):218–21.

8.   Chang BS, Hershenson S. Practical approaches to protein formulation development. In: Carpenter JF, Manning MC, editors. Rationale Design of stable protein formulations-theory and practice. New York: Kluwer Academic/Plenum; 2002. p. 1–20.

9.   Kerwin BA. Polysorbates 20 and 80 used in the formulation of protein biotherapeutics: structure and degradation pathways. J Pharm Sci. 2008 Aug;97(8):2924–35.

10.   Sarciaux JM, Mansour S, Hageman MJ, Nail SL. Effects of buffer composition and processing conditions on aggregation of bovine IgG during freeze-drying. J Pharm Sci. 1999;88(12):1354–61.

11.   Monnier VM. Nonenzymatic glycosylation, the Maillard reaction and the aging process. J Gerontol. 1990;45(4):B105–11.

12.   Gokarn YR, Kras E, Nodgaard C, Dharmavaram V, Fesinmeyer RM, Hultgen H, et al. Self-buffering antibody formulations. J Pharm Sci. 2008 Aug;97(8):3051–66.

13.   Fesinmeyer RM, Hogan S, Saluja A, Brych SR, Kras E, Narhi LO, et al. Effect of ions on agitation- and temperature-induced aggregation reactions of antibodies. Pharm Res. 2009 Apr;26(4):903–13.

14.   Yadav S, Sreedhara A, Kanai S, Liu J, Lien S, Lowman H, et al. Establishing a link between amino acid sequences and self-associating and viscoelastic behavior of two closely related monoclonal antibodies. Pharm Res. 2011 Jul;28(7):1750–64.

15.   Neergaard MS, Kalonia DS, Parshad H, Nielsen AD, Møller EH, van de Weert M. Viscosity of high concentration protein formulations of monoclonal antibodies of the IgG1 and IgG4 subclass - prediction

of viscosity through protein-protein interaction measurements. Eur J Pharm Sci. 2013 Jun 14;49(3):400–10.

16.   Yadav S, Shire SJ, Kalonia DS. Viscosity behavior of high-concentration monoclonal antibody solutions: correlation with interaction parameter and electroviscous effects. J Pharm Sci. 2012 Mar;101(3):998–1011.

17.   Yadav S, Scherer TM, Shire SJ, Kalonia DS. Use of dynamic light scattering to determine second virial coefficient in a semidilute concentration regime. Anal Biochem. 2011 Apr 15;411(2):292–6.

18.   Saito S, Hasegawa J, Kobayashi N, Kishi N, Uchiyama S, Fukui K. Behavior of monoclonal antibodies: relation between the second virial coefficient (B (2)) at low concentrations and aggregation propensity and viscosity at high concentrations. Pharm Res. 2012 Feb;29(2):397–410.

19.   Bam NB, Cleland JL, Yang J, Manning MC, Carpenter JF, Kelley RF, et al. Tween protects recombinant human growth hormone against agitation-induced damage via hydrophobic interactions. J Pharm Sci. 1998 Dec;87(12):1554–9.

20.   Privalov PL, Khechinashvili NN. A thermodynamic approach to the problem of stabilization of globular protein structure: a calorimetric study. J Mol Biol. 1974 Jul 5;86(3):665–84.

21.   Freire E, Schön A, Hutchins BM, Brown RK. Chemical denaturation as a tool in the formulation optimization of biologics. Drug Discov Today. 2013 Oct;18(19-20):1007–13.

22.   Manning MC, Chou DK, Murphy BM, Payne RW, Katayama DS. Stability of protein pharmaceuticals: an update. Pharm Res. 2010 Apr;27(4):544–75.

23.   Hawe A, Wiggenhorn M, van de Weert M, Garbe JHO, Mahler H-C, Jiskoot W. Forced degradation of therapeutic proteins. J Pharm Sci. 2012 Mar;101(3):895–913.

24.   Andya J, Cleland JL, Hsu CC, Lam XM, Overcashier DE, Shire SJ, et al. Stable Isotonic Lyophilized Protein Formulation. WO 9704801, 1997.

25.   Krishnan S, Pallitto MM, Ricci M. Development of formulations for therapeutic monoclonal antibodies and Fc fusion proteins. In: Jameel J, Hershenson S, editors. Formulation and Process Development Strategies for Manufacturing Biopharmaceuticals. New Jersey, NJ: John Wiley & Sons; 2010. p. 383–427.

26.   Nayar R, Manning MC. High Throughput Formulation: Strategies for Rapid Developent of Stable Protein Products. In: Carpenter JF, Manning MC, editors. Rationale Design of stable protein formulations - theory and practice. New York, NY: Kluwer Academic/Plenum; 2002. p. 177–99.

27.   Capelle MAH, Gurny R, Arvinte T. High throughput screening of protein formulation stability: practical considerations. Eur J Pharm Biopharm. 2007 Feb;65(2):131–48.

28.   Samra HS, He F. Advancements in high throughput biophysical technologies: applications for characterization and screening during early formulation development of monoclonal antibodies. Mol Pharm. 2012 Apr 2;9(4):696–707.

29.   Grillo AO. Late-stage formulation development and characterization of biopharmaceuticals. In: Jameel F, Hershenson S, editors. Formulation and Process Development Strategies for Manufacturing Biopharmaceuticals. Hoboken, NJ, USA: John Wiley & Sons; 2010.

30.   Filipe V, Hawe A, Carpenter JF, Jiskoot W. Analytical approaches to assess the degradation of therapeutic proteins. TrAC Trends Anal Chem. Elsevier Ltd; 2013 Sep;49:118–25.

31.   USP <787>. Subvisible particulate matter in therapeutic protein injections. In: The United States Pharmacopoeia, National Formulary.

32.   Wang W, Ignatius AA, Thakkar S V. Impact of Residual Impurities and Contaminants on Protein Stability. J Pharm Sci. 2014 Mar 12;(2):1315–30.

33.   Khossravi M, Kao Y-H, Mrsny RJ, Sweeney TD. Analysis methods of polysorbate 20: A new method to assess the stability of polysorbate 20 and established methods that may overlook degraded polysorbate 20. Pharm Res. 2002 May;19(5):634–9.

34.   Labrenz SR. Ester hydrolysis of polysorbate 80 in mAb drug product: Evidence in support of the hypothesized risk after the observation of visible particulate in mAb formulations. J Pharm Sci. 2014 Jun 17;103(8):2268–77.

35.   Stoner MR, Fischer N, Nixon L, Buckel S, Benke M, Austin F, et al. Protein-solute interactions affect the outcome of ultrafiltration/diafiltration operations. J Pharm Sci. 2004 Sep;93(9):2332–42.

36.   Mahler H-C, Printz M, Kopf R, Schuller R, Müller R. Behaviour of polysorbate 20 during dialysis, concentration and filtration using membrane separation techniques. J Pharm Sci. 2008 Feb;97(2):764–74.

37.   Jiskoot W, Crommelin D. Methods for Structural Analysis of Protein Pharmaceuticals. Springer; 2005.

38.   Houde DJ, Berkowitz SA. Biophysical Characterization of Proteins in Developing Biopharmaceuticals. 1st ed. Elsevier B.V.; 2014.

39.   Carpenter JF, Randolph TW, Jiskoot W, Crommelin DJA, Middaugh CR, Winter G. Potential inaccurate quantitation and sizing of protein aggregates by size exclusion chromatography: essential need to use orthogonal methods to assure the quality of therapeutic protein products. J Pharm Sci. 2010 May;99(5):2200–8.

40.   Philo JS. A critical review of methods for size characterization of non-particulate protein aggregates. Curr Pharm Biotechnol. 2009 Jun;10(4):359–72.

41.   Den Engelsman J, Garidel P, Smulders R, Koll H, Smith B, Bassarab S, et al. Strategies for the assessment of protein aggregates in pharmaceutical biotech product development. Pharm Res. 2011 Apr;28(4):920–33.

42.   Zölls S, Tantipolphan R, Wiggenhorn M, Winter G, Jiskoot W, Friess W, et al. Particles in therapeutic protein formulations, Part 1: overview of analytical methods. J Pharm Sci. 2012 Mar;101(3):914–35.

43. Carpenter JF, Randolph TW, Jiskoot W, Crommelin DJA, Middaugh CR, Winter G, et al. Overlooking subvisible particles in therapeutic protein products: gaps that may compromise product quality. J Pharm Sci. 2009 Apr;98(4):1201–5.

44. Mahler HC, Jiskoot W. Analysis of Aggregates and Particles in Protein Pharmaceuticals. Wiley; 2011.

45. Kirshner LS. Regulatory expectations for analysis of aggregates and particles. In: Colorado Protein Stability Conference. Breckenridge, CO; 2012.

46. Joshi SB, Bhambhani A, Zeng Y, Middaugh RC. An Empirical Phase Diagram -High-Trhoughput Screening Approach to the Characterization and Formulation of Biopharmaceuticals. In: Jameel F, Hershenson S, editors. Formulation and Process Development Strategies for Manufacturing Biopharmaceuticals. Hoboken, NJ, USA; 2010.

47. Kalonia C, Kumru OS, Kim JH, Middaugh CR, Volkin DB. Radar chart array analysis to visualize effects of formulation variables on IgG1 particle formation as measured by multiple analytical techniques. J Pharm Sci. 2013 Dec 9;102(12):4256–67.

CHAPTER 3

PRECLINICAL MODELS USED FOR IMMUNOGENICITY PREDICTION OF THERAPEUTIC PROTEINS

Vera Brinks[1], Daniel Weinbuch[2], Matthew Baker[3], Yann Dean[4], Philippe Stas[5], Stefan Kostense[6], Bonita Rup[7], Wim Jiskoot[2]

[1] Department of Pharmaceutics, Utrecht Institute for Pharmaceutical Sciences (UIPS), Utrecht University, Universiteitsweg 99 3584 CG Utrecht, The Netherlands

[2] Division of Drug Delivery Technology, Leiden Academic Centre for Drug Research (LACDR), Leiden University, P.O. Box 9502, 2300 RA Leiden, The Netherlands

[3] Antitope Ltd, Babraham Research Campus, Babraham Cambridge CB22 3AT, UK

[4] Eclosion SA, Chemin des Aulx, 14 1228 Plan-les-Ouates, Geneva, Switzerland

[5] BLA Consult bvba, Kortestraat 62 9473 Welle, Belgium

[6] Crucell Holland BV, Leiden, The Netherlands

[7] Protein Bioanalytics, Pfizer Inc., Andover Massachusetts, USA

Abstract

All therapeutic proteins are potentially immunogenic. Antibodies formed against these drugs can decrease efficacy, leading to drastically increased therapeutic costs and in rare cases to serious and sometimes life threatening side-effects. Many efforts are therefore undertaken to develop therapeutic proteins with minimal immunogenicity. For this, immunogenicity prediction of candidate drugs during early drug development is essential. Several *in silico*, *in vitro,* and *in vivo* models are used to predict immunogenicity of drug leads, to modify potentially immunogenic properties, and to continue development of drug candidates with expected low immunogenicity. Despite the extensive use of these predictive models, their actual predictive value varies. Important reasons for this uncertainty are the limited/insufficient knowledge on the immune mechanisms underlying immunogenicity of therapeutic proteins, the fact that different predictive models explore different components of the immune system, and the lack of an integrated clinical validation. In this review, we discuss the predictive models in use, summarize aspects of immunogenicity that these models predict, and explore the merits and the limitations of each of the models.

Introduction

Therapeutic proteins are very successful in treating a wide variety of life-threatening diseases such as multiple sclerosis, diabetes, chronic kidney failure and a wide variety of cancers. In contrast to small molecule drugs, they do not possess intrinsic toxicity due to harmful metabolites or off-target effects, and their side effects are mainly caused by exaggerated pharmacodynamic effects (1). Because of their success and versatility, therapeutic proteins are the fastest growing class of drugs and make up about one third of the drug market.

One of the major attention points of therapeutic proteins is immunogenicity. Anti-drug antibodies (ADAs) induced by nearly all therapeutic proteins can interfere with drug-efficacy, alter PK/PD or induce severe, sometimes life-threatening, side-effects in a subset of the patients (2–5). The potential danger of immunogenicity of therapeutic proteins caught public attention around 2002 when an increased number of patients treated with Eprex® (epoetin alpha) were reported to form antibodies that cross-reacted with endogenous erythropoietin. As a result red blood cell production arrested and blood transfusions were vital for these patients' survival (5–7). Besides the apparent risk for patient safety, immunogenicity also poses a financial burden.

In order to minimize side effects caused by ADA formation, immunogenicity assessment of therapeutic proteins during drug development is critical. By identifying immunogenic properties at an early stage, and subsequently modifying those properties, immunogenicity in patients could be minimized. Many efforts have been undertaken to develop *in silico*, *in vitro,* and *in vivo* models that predict different aspects of immunogenicity of therapeutic proteins (8–10). However, current limited knowledge on the general principles that apply to the induction of antibodies by these drugs makes it very difficult to determine the risk factors for immunogenicity and predict the clinical consequences of immunogenicity of a new protein drug (11). Also, the clinically observed immunogenicity against specific drugs is variable depending on other factors such as the disease treated, concomitant treatment and patient background (12). In addition, direct clinical evidence showing that use of these predictive models to guide drug development actually helps to lower immunogenicity is largely missing, as few drug candidates are clinically tested and therefore direct comparisons of candidates showing predicted high and low risk are rarely obtained. Despite these limitations, several *in silico*, *in vitro,* and *in vivo* models are currently applied for different aspects of preclinical immunogenicity prediction (13–15) (Table 1).

Table 1: Main applications and limitations of current *in silico*, *in vitro* and *in vivo* predictive tools for protein immunogenicity.

Category	What does it predict?	Advantages	Disadvantages
In silico	Presence of potential CD4+ T cell epitopes	Fast, low cost	Focus on primary structure; no information on contribution of other factors (e.g., glycosylation, formulation, aggregation)
	Presence of neoepitopes	Fast, low cost	Does not address the actual T-cell activation
In vitro	Presence of CD4+ T cell epitopes	Relatively fast, low cost	Focus on activation of specific immune cells
	Presence of neoepitopes	Measures biological effects	Large donor sets needed
	Activation of T cells	Can be used to screen product-related factors other than primary structure	Assay variability
In vivo			
Conventional animals	Relative immunogenicity	*In vivo* correlate of immunogenicity	Per definition a classical immune response against therapeutic proteins Overestimation of immunogenicity Time consuming, expensive Non-human immune system
Non-human primates	Relative immunogenicity	Express similar proteins as humans, therefore may have similar immune mechanism underlying immunogenicity	Predictive value strongly depends on protein
	Likely the presence of neoepitopes	*In vivo* correlate of immunogenicity	Time consuming, expensive
	Breaking of tolerance (depends on protein)	*In vivo* correlate of immunogenicity	Needs clinical validation
Transgenic immune	Presence of neoepitopes	Express protein of interest similar to tolerant mice humans, can be used to study breaking of tolerance	Mice respond with murine immune system
	Relative immunogenicity	*In vivo* correlate of immunogenicty	Time consuming, expensive
	Breaking of tolerance	*In vivo* correlate of immunogenicty	Needs clinical validation
Human immune system xenograft models	Presence of neoepitopes	Express many human immune proteins that xenograft models are (potential) therapeutic targets, can be used to study breaking of tolerance.	For most models human T cells lack the ability to recognize antigens in a HLA-restricted manner (i.e. no value to predict T cell-de pendent ADA), BLT mice are exception.
	Relative immunogenicity	Mice respond with a (reconstituted) human immune system	Time consuming, expensive
	Breaking of tolerance (if human protein is expressed due to xenografting)	*In vivo* correlate of immunogenicty	Needs clinical validation

This review summarizes the models in use and potential future models to predict immunogenicity of therapeutic proteins. It gives insight into the rationale of each of the models and discusses the specific aspects of immunogenicity predicted by them. It ends with recommendations on future studies that need to be performed in order to improve predictability.

Models predicting CD4+ T cell epitopes and CD4+ T cell activation

Most of the *in silico* and *in vitro* models used to predict immunogenicity of therapeutic proteins focus on identifying CD4+ T helper cell epitopes and measuring activation of CD4+ T cells (Table 1). In an adaptive immune response against foreign proteins, CD4+ T cells and their epitopes are crucial for the induction of an immune response, which is characterized by isotype switched antibodies such as IgG, by affinity maturation, and the formation of immunological memory. The observation that some patients treated with therapeutic proteins produce high affinity, isotype switched antibodies, suggests that ADA immunogenicity in these cases is driven via a CD4+ T cell dependent mechanism (16), involving T cell epitopes present in the protein sequence. Presentation of these epitopes by major histocompatibility complex (MHC) class II molecules on antigen presenting cells (APC) can engage T cells to initiate a cascade of events resulting in an ADA response by B cells. Assuming that therapeutic proteins evoke an antibody response via this T cell-dependent mechanism, the prediction of T cell epitopes and a corresponding T cell response could be an effective way to identify immunogenic sequences and, by eliminating them, reduce the potential for immunogenicity. The main methods employed in detecting CD4+ T cell epitopes and CD4+ T cell responses to proteins are (i) *in silico* analysis of MHC class II binding peptides and (ii) *in vitro* T cell stimulation. Both techniques enable CD4+ T cell epitopes to be predicted in the context of human MHC class II.

In silico models

In silico models use the amino acid sequence of therapeutic proteins to predict the presence of peptides in these proteins that bind to MHC molecules. Several first-generation models are based on quantitative matrices. They use experimental data of the many peptides known to bind to specific HLA allotypes and in addition they score each of the amino acids depending on their position in the binding groove. Even though this approach has been mainly applied to MHC class I (which is driving cytotoxic responses), *in silico* tools for predicting the presence of MHC class II-binding epitopes such as Tepitope, MHCPred, Epimatrix and SVMHC are also developed (17–20). More recently, *in silico* models based on artificial neural networks (ANN) have been developed, which involve

data modeling tools able to "learn" which peptides could bind to MHC. The information needed during a learning phase is provided by a set of peptide sequences from both known MHC binders and confirmed non-binders, and is used by the ANN to find patterns for a prediction of new sequences. Examples of such models are ANNPrep and Comprep (21). Several neural network servers are available, such as NetCHOP, NetCTLpan and NetMHCpan (http://tools.immuneepitope.org). The ANN methods are very adaptive and have the ability to self-improve.

A drawback of the above mentioned methods is their reliance on extremely large data sets, which require intensive experimental work. To overcome this problem, some structure-based methods have been developed that also examine the three dimensional structures of the binding groove of the HLA molecules using force field analysis based on crystal structures and other structural approaches. Up until now, two models applying to HLA class II molecules have been described: Epibase and the methods developed by Davies and colleagues (22,23).

The latest *in silico* algorithms aim to combine T cell epitope identifications with predictors of proteasomal cleavage sites and transport efficiency of the peptides to the endoplasmic reticulum (where peptides are loaded onto MHC class I molecules). Combined prediction methods could indeed lead to a bridging between pure T cell epitope prediction and the actual T-helper cell stimulation by the loaded peptides, as these also take into account processes involved in antigen presentation (24). Unfortunately, the reliability of the currently available models (e.g. Fragpredict, PAProC) is still very low. Moreover, applications are mostly available for MHC class I prediction and more research on their applicability for MHC class II binding is needed.

In general, *in silico* methods allow a rapid and relatively low-cost analysis of protein sequences for peptides that bind to MHC class II. They are very useful in modeling interactions between known CD4+ T cell epitopes (identified from *in vitro* T cell assays) and MHC class II, and have shown similar epitopes as identified with *in vitro* methods (discussed later) (25–29). The use of *in silico* tools has enabled the generation of a number of therapeutic proteins in which the CD4+ T cell epitopes have been removed by mutations that disrupt binding to MHC class II. However, whereas good accuracy can be reached with some of these tools in generating a peptide map of the peptides that are capable to bind MHC class II receptors *in vitro* based on the primary protein structure, the application of the tools is limited. The major reason is that these tools are largely restricted to the prediction of interactions between peptide sequences and MHC molecules and therefore do not take into account other factors that affect immune responses, such as antigen uptake and processing by the APC, T cell activation through the

T cell receptor (TCR), tolerance of T cells to epitopes encountered during development in the thymus, and the involvement of other immune cells. Therefore, *in silico* methods are suitable to predict the presence of potential CD4+ T cell epitopes on a given protein sequence, however, information on subsequent activation of T cells and interactions among other immune components is lacking. Because these tools use primary amino acid sequence information, they do not take into account the effect of non-sequence related factors such as formulation, impurities, and aggregates on antibody response (Table I).

In vitro models

The limitation of *in silico* methods in providing information on activation of CD4+ T cells can be partly overcome by *in vitro* T cell assays. *In vitro* T cell assays are used to assess the potential of whole proteins to activate CD4+ T cells, as well as map T cell epitopes using peptides spanning the sequence of interest. The assays typically involve large numbers of patient or healthy donors to represent a large proportion of human leucocyte antigen (HLA) allotypes in the world population and to reach sufficient statistical power (Table 1). There are many different methods in practice, but in general, peripheral blood mononuclear cells (PBMCs), including APCs and T cells from patients, naïve donors or antigen-exposed individuals are harvested and brought into contact with either the whole antigen or peptide fragments (mostly 15 residues per peptide overlapping 10 or 12 amino acids). Subsequently, the type and strength of the immune response can be determined by various intracellular and extracellular T cell markers. A method commonly used for the determination of T cell activation is ELISPOT. This ELISA based method detects cytokines secreted by activated T cells, such as IL-2, IL-4, or INF-γ, where INF-γ ELISPOT seems to be favored by many researchers (30,31). More recently, flow cytometry was implemented as a more direct method for detection of T cell activation by analyzing the expression of CD25 at the cell surface of CD4+ T cells (32). There is evidence that the repertoire of epitopes presented in patients is similar to the epitopes identified *in vitro*. Two independent research groups have identified CD4+ T cell epitopes in the C1 and A2 domains of Factor VIII using *in vitro* primed T cells from healthy donors (33,34). These observations have enabled the use of community donor blood for mapping T cell epitopes and determining the T cell activation potential by whole proteins (Table 1). Data from *in vitro* T cell assays, such as the number and potency (immunodominance) of individual T cell epitopes or proteins, are therefore used to predict the relative risk of activating a T cell dependent immune response between multiple variants of a therapeutic protein during pre-clinical development.

In general, the use of *in vitro* T cell assays allows the qualitative and quantitative measurement of T cell epitopes and their role in the activation of T-helper cells, which in

turn enables strategies such as T cell epitope removal to be employed. In addition, *in vitro* T cell assays can be used to monitor T cell activation and proliferation of differently formulated products or in presence of aggregates, which is not possible with *in silico* methods. However, as these assays are based on cell material from donors, batch-to-batch and donor variability makes standardization an issue (Table 1). The use of large donor pools is a requirement, making the tools relatively low-throughput at this time (20).

Combined use

Often, CD4+ T cell based *in silico* and *in vitro* tools are combined in preclinical immunogenicity prediction. Because these models simplify the complexity of the immune system and its responses, they are used to assess relative potential for immunogenicity due to the presence of CD4+ T cell epitopes and activation, between similar products directed against the same target. *In silico* tools are particularly used to screen early stage drug candidates or libraries, in order to exclude the protein variants or designs that show a significantly higher number of potential T cell epitopes compared to other variants. *In vitro* models in particular are also used to study the effect of product-related factors other than primary structure on T cell activation. They are, however, less suitable to predict aspects of immunogenicity that involve complex immune processes such as breaking of immune tolerance (discussed later on), incidence of antibody formation, and clinical consequences of ADAs.

Models Predicting B cell epitopes and B cell activation

B cell epitopes are important in eliciting an immune response against bacteria and viruses. A repeated array of B cell epitopes on the surface of these microorganisms can bind to multiple B cell receptors on the B cell surface, and by crosslinking them, directly activate B cells to give an antibody response. This type of immune response is different from the classical T cell dependent immune responses in many ways, but two of the most important features are that T cells are not necessarily involved in antibody formation and that immunological memory formation against foreign antigens is absent (35). Clinical studies on patients treated with therapeutic interferon beta and an anti-TNF antibody have shown that patients being antibody positive during first treatment did not show a fast increase in antibody titers when treatment was restarted. This indicates that no immunological memory was formed (36,37). Although a limited number of patients was included, the data suggest that repeated B cell epitopes and crosslinking of B cell receptors could be important in immunogenicity. It might be hypothesized that protein aggregates could

express repeated cell epitopes needed to crosslink B cell receptors and activate B cells. This has been suggested as a mechanism for breaking of immune tolerance (38).

Models predicting individual B cell epitopes are available, however, taking into account that the structure of proteins is highly dependent on production conditions, formulation, and handling and that, with changing structure, other B cell epitopes can form, it seems almost impossible with our current knowledge to accurately predict B cell epitopes using *in silico* models (39–41). Nonetheless, advances in their predictive value are made (42). Also it is questionable if these models would have any value for immunogenicity prediction, because individual epitopes are incapable of crosslinking B cell receptors; instead, repeated epitopes are needed for this. Models looking at repeated protein structure are therefore more likely suitable in predicting immunogenicity of therapeutic proteins. While current *in silico* methods are unsuitable for this, *in vitro* B cell models could be a solution. However, the maintenance of B cells *in vitro* is a highly complicated task and current assays using PBMCs in short term suspension or in monolayer format, do not represent *in vivo* behavior sufficiently (43).

So, for now no models are available that could predict immunogenicity of therapeutic proteins due to repeated structures or repeated B cell epitopes. Moreover, if such models would become available, they would likely encounter similar limitations as the T cell epitope models in that they would focus on a single component aspect of the immune response, and not take into account the biological complexity of the entire immune system.

In vivo models

In vivo models used to predict immunogenicity of therapeutic proteins have the advantage over *in silico* and *in vitro* tools that immunogenicity can be studied in an organism with an intact immune system. In contrast to the simplified nature of *in silico* and *in vitro* models, *in vivo* models allow the interplay between immune cells and complex processes underlying antibody formation against therapeutic proteins. However, because preclinical assessment of immunogenicity *in vivo* is expensive and time consuming, animal models are less suitable for large-scale screening. Moreover, care has to be taken that the animal models are representative for the immune processes taking place in humans. They are therefore mostly used after lead selection by *in silico* and *in vitro* models (Table 1). Similar to the models described before, the predictive value of animal models depends on the items that need prediction, on the type of therapeutic protein and on the similarity of the processes underlying immunogenicity compared to those in humans. These include the similarities or differences in pharmacokinetics, pharmacodynamics, and target binding

between humans and the species of animal model. Similar to the *in silico* and *in vitro* models, animal models cannot be used to predict incidence of immunogenicity in patients. Also the specificity of humoral antibody responses and therefore potential for clinical effect will be hard to predict. However, they might be used to assess relative immunogenicity, presence of 'neo-epitopes' and breaking of immune tolerance (Table 1). We assume that animal models with an immune system that is genetically most similar to the human immune system are most predictive. Therefore, conventional animal models such as rats and mice would have least predictive value, while transgenic animal models and non-human primates would have highest predictive value. Recently developed animal models such as the human xenograft mouse models are being investigated for immunogenicity prediction.

Conventional Animal Models

Animal models such as rats and mice have been often used in the early years of preclinical immunogenicity prediction. However, most human therapeutic proteins are foreign proteins (i.e. have limited sequence homology) for these animals and as a result they will usually develop an ADA response against a foreign protein. This may not be informative, as the exact mechanisms underlying immunogenicity might be different in humans (38). Even when the therapeutic protein is foreign in both humans and the animal model (e.g., plant derived or bacterial proteins), species differences in the immune system, and restriction in genetic diversity between animals (in the case of inbred strains) might introduce false results.

When assessing the predictive value of conventional animal models, it is expected that they overestimate immunogenicity development in patients since rats and mice are likely to form antibodies against all (recombinant human) therapeutic proteins (44). This also implies that the ADAs will mostly be neutralizing. Therefore these animals are insensitive to discriminate between binding and neutralizing antibody responses which both can occur in patients and are therefore unsuitable to predict clinical relevance of antibody formation. In addition, Katsutani et al. (45) have shown that wildtype mice seem unsuitable to assess the presence of neoepitopes. Using human tissue plasminogen activator as antigen, they have shown that site specific modification does not lead to increased recognition of epitopes in these mice. Because these animals already recognize multiple epitopes due to foreignness of the protein, the prediction of neo-epitopes is very difficult, especially when taking into account species differences in MHC class II. However, for some proteins, rats and mice might be of value to determine the relative immunogenicity between products of the same class. For example, Bellomi et al. (46) have used BALB/c mice to assess relative difference between interferon beta 1a formulations.

They found that a new formulation of interferon beta 1a was less immunogenic compared to commercially available formulations, Avonex and Rebif.

Mice Rendered Immune Tolerant to Human Proteins

In order to prevent therapeutic proteins from inducing an ADA response in mice due to their foreignness, transgenic mice that express a human protein have been developed. As a result these mice are, like humans, immune tolerant for the particular human protein they express. Studies in such mice have shown that the immunogenicity of clinical preparations of recombinant human interferon alpha, interferon beta and monoclonal antibodies (mAbs) is significantly enhanced by the presence of aggregates (47–50). In particular, aggregates induced by metal catalyzed oxidation and aggregates composed of monomers that still exhibit native structural elements appear most immunogenic. However, by using these models it is not possible to predict what level of aggregation is needed to induce an antibody response in patients. These models have shown to predict relative immunogenicity of interferon beta products (51), with the most immunogenic product in patients (Betaferon) being more immunogenic in these mice compared to other products such as Avonex and Rebif. However absolute incidences of antibody positive individuals differed between the immune tolerant mice and patients.

Transgenic mouse models also have been shown to predict neo-epitopes when given a modified form of human insulin and tissue plasminogen activator (52,53). So, these models can therefore be used to determine relative immunogenicity of protein variants and formulations. Moreover, studies conducted with immune tolerant mice have shown that although being tolerant for human growth hormone, an immune response could be induced when these mice were treated with a sustained-release formulation. This illustrates that – in addition to predicting immunogenicity due to aggregation, relative immunogenicity, and neo-epitopes – these models can be used to study breaking of immune tolerance (54). Immune tolerant murine models are, however, limited by their inability to predict the incidence of immunogenicity or clinical consequences of ADA formation (Table 1).

A major disadvantage of the immune tolerant mice is that they, like conventional animal models, respond against a therapeutic protein via a rodent immune system. If the mechanisms underlying immunogenicity are T cell (epitope) triggered, absence of human MHC class II in these mice likely limits the usefulness of such models. In turn, differences in B cell repertoire might affect prediction for B cell epitopes if these appear to be the trigger for immunogenicity (Table 1).

Non-human primates

Because proteins expressed in humans and non-human primates show a high degree of homology, non-human primates are expected to be immune tolerant for most human proteins. Also their immune system is more similar to the human immune system compared to rodent models and transgenic mice. Therefore, the mechanisms underlying the antibody response in non-human primates would, in theory, better reflect the human immune response against therapeutic proteins. Non-human primates such as chimpanzees and rhesus monkeys have been shown to predict the presence of neo-epitopes and relative immunogenicity of protein structural variants of various human proteins such as tissue plasminogen activator, growth hormone and insulin (45,55,56). In theory, they might also be suitable to study breaking of immune tolerance for therapeutic proteins, which are similar to their endogenous proteins. In one occasion non-human primates have also been shown to predict development of neutralizing (cross-reactive) antibodies to thrombopoietin that was also observed clinically (57). However, is questionable if this is generally applicable to other therapeutic proteins (Table 1). Despite their apparent superiority as predictive model, non- human primates are incapable of predicting incidence of immunogenicity in patients. Moreover, non-human primates cannot be used to predict immunogenicity of all therapeutic proteins; apparently their predictive value strongly depends on the protein in question. For example, for interleukin 3 they have shown very poor predictability (58). This implies that the predictive value of these models is only known for already tested proteins (Table 1).

HLA Transgenic Mice

Mice expressing specific human HLA allotypes (and lacking endogenous mouse MHC class II) have been developed and used for research to evaluate the involvement of human HLA alleles in indications such as allergy and autoimmune diseases (59,60). Applications of these models in predicting the immunogenicity of protein therapeutics are currently being developed. These models will be particularly valuable when immunogenicity is driven by CD4+ T cell epitopes. To improve the suitability of these mice, they should be crossed with mice where immune tolerance against a specific recombinant therapeutic or class of therapeutics is induced by either transgenic expression of the protein of interest or induction of tolerance during neonatal development (61,62). For example, in order to produce a model that might be suitable to predict the potential immunogenicity of mAbs, transgenic mice that express (monoclonal) human immunoglobulin could be bred with transgenic mice that express human HLA alleles (63–66). In order to avoid generating mice that are tolerant to both human and murine mAb variable region sequences, these mice should not express endogenous mouse MHC class II and mouse immunoglobulins.

However, obtaining HLA-diversity, which is comparable to that of the human population, will be a significant challenge.

Human Immune System Xenograft Models

As an alternative to transgenic mice, models based on immunodeficient NOD scid IL2Rγ/- or Rag2−/−γc−/− mice are being developed. These mice lack functional mouse T- and B cells, have no functional complement system, have diminished mouse NK functioning, and lack mouse macrophage activity. These mice have shown to be very successful for engraftment of human immune cells and therefore have a functional human-like immune system (67,68). Neonatal immunodeficient mice are used for engraftment of CD34+ human hematopoetic progenitor cells, which can be isolated from fetal human tissue. This engraftment leads to the reconstitution of 40–60% of human CD45+ mononuclear cells in peripheral blood and spleen, and gives sizable compartments of human B cells, T cells, natural killer cells, monocyte/macrophages, and dendritic cells. Since these mice express human MHC class II and should be tolerant to human immunoglobulins, they might be suitable for the prediction of the immunogenicity of therapeutic proteins including mAbs. In addition, as the biological activity of the therapeutic target probably plays an important role in immunogenicity (e.g., soluble versus membrane-bound), these models offer the advantage to express many therapeutic targets (e.g., TNF, BAFF, CD3, CD20) as human (69–71).

There are, however, limitations in using some of the currently available engraftment models. First, they are not tolerant against all human proteins. Second, there is no germline transfer of genes encoding human immune cells, so each mouse has to be generated on an individual basis. As shown in some studies, this may lead to considerable variability in immune responses to antigens that stimulate potent responses in humans. Furthermore, some strains of these mice do not express HLA molecules on thymic epithelial cells. Consequently, human T cells developing in these humanized mice lack the ability to recognize antigens in an HLA-restricted manner, precluding the investigation of human T cell responses against therapeutic proteins (72). However BLT mice, which are immunodeficient mice in which human liver and thymus fragments are implanted under the renal capsule and which are given additional haematopoietic stem cells intravenously, do have HLA restricted T cells (73). However B cell responses in these BLT mice appear to be generally limited to IgM, potentially due to immature lymph node architecture.

General Conclusions and Recommendations

The main limitations in predictive value of the models presented in this paper are (i) insufficient knowledge on the interplay of immune mechanisms underlying immunogenicity of therapeutic proteins and (ii) insufficient clinical validation. Future studies should therefore address these two topics.

The mechanisms underlying immunogenicity of therapeutic proteins are not well studied. For example, it is still uncertain whether the primary mechanism by which therapeutic proteins induce antibodies is driven via a T cell dependent mechanism, via repeated B cell epitopes, via another yet unknown mechanism, or whether immunogenicity is a combination of all of these. We also do not know whether there is a general immune mechanism explaining immunogenicity of all (recombinant human) therapeutics, or if this mechanism is product specific. Special attention should be taken when considering proteins that are non-human, vs. human proteins in patients with endogenous counterparts vs. human proteins used in replacement therapy for patients deficient in the endogenous counterpart. To answer these questions, more studies in animals, but also more in depth studies in patients are needed. One of the priorities should be to elucidate to what extent T- and B cell epitopes are triggering ADA formation, and if there is HLA restriction in this response. Also we should focus on understanding contributions of aggregates. These are considered one of the major risk factors of immunogenicity. However, despite numerous publications we still do not know which specific types of aggregates are immunogenic and why they can induce ADAs. Is this because of better uptake by APC or are they capable of directly activating B cells? It is also not clear whether low levels of aggregates found in many therapeutic proteins play a role in the protein immunogenicity. In addition, insight in treatment and patient-related factors affecting immunogenicity should be gained. For example, we do not know if a patient forming antibodies against a certain drug can be retreated with that same or a similar drug on a later occasion without having a memory response. For now this is (almost) not studied, although sparse clinical data suggests that this might be possible for some therapeutic proteins (36,37). We also need more data on why some individuals form ADAs and others do not, while being treated with the same drug.

Another focus should be on validating the current predictive models. Data from *in silico*, *in vitro,* and *in vivo* models should be combined with clinical data in order to answer questions like: Does the removal of T cell or B cell epitopes lower immunogenicity in patients? And to what extent are *in vivo* models capable of predicting immunogenicity in patients? Clinical immunogenicity data comparing the original and corresponding "deimmunized" variants of the same protein species should give insight into the effect of

predicted epitope removal on immunogenicity. Also comparing predicted CD4+ T cell epitopes, *in silico,* and *in vitro*, with actual peptides recognized by MHC II in patients would be needed to validate the suitability of epitope prediction by these models. The assessment of predictive value of animal models might be achieved by comparing antibody incidences of different products between animals and patients. As mentioned before, parameters such as antibody titer and clinical effect of ADAs might not be suitable in assessing predictive value. Foundations such as the European Immunogenicity Platform (www.e-i-p.eu) gather experts in the field to discuss these items and to start collaborations aiming to answer some of the questions mentioned above. However, the studies comparing *in silico*, *in vitro*, *in vivo* and clinical data encounter some challenges. *In silico*, *in vitro,* and *in vivo* models are used to predict relative potential for immunogenicity between different products during developmental stages. In order to compare these results with clinical data, the same products should be given to patients. This poses a problem. Clinical testing will not involve multiple drug lead candidates. Also chances are that drugs given to patients in clinical testing will have different formulation, impurities and aggregation profiles than those during early development. A solution would be to include a reference drug during preclinical testing that has a known immunogenicity profile in patients. It is critical that such reference exhibits similar characteristics to the test product, such as target binding, size, and protein class, since these characteristics could all influence immunogenicity. For new drugs, having a reference with similar characteristics might be very challenging. These references, however, are very likely available for biosimilar development in the form of the original product against which the biosimilar should be tested.

Conclusion

The predictive value of the current *in silico*, *in vitro,* and *in vivo* models used to assess immunogenicity of therapeutic proteins is uncertain and in several cases only partial answers are obtained. In order to gain more knowledge about their predictive value and to potentially improve existing models, clinical validation and increased insights into the immune mechanism underlying immunogenicity should be aimed for. Predicted immunogenicity in these models may therefore not lead to a go/no go decision on individual drug leads, but instead could be used in the selection of one drug candidate over another for further (clinical) development. *In silico*, together with *in vitro* models would be most suitable to screen multiple drug leads for potential immunogenicity due to T- or B cell epitopes, activation of T- and B cells or due to a particular formulation. A selection of these leads, with assumed lowest immunogenicity potential, would then be tested for capability to form ADAs in animal models. These models could give an indication

of their relative potential immunogenicity by studying antibody incidences. Ideally for all predictive models, a reference product with known immunogenicity in patients would be tested in parallel. It is critical that such a product exhibits similar characteristics, such as target binding, size, and protein class. With the use of such a reference, better insight into immunogenicity potential of drug leads might be possible, however, it appears unlikely that for new drugs such reference products would be available. For now, clinical testing will stay critical for determining actual immunogenicity in patients.

References

1. Clarke JB. Mechanisms of adverse drug reactions to biologics. Handbook of Experimental Pharmacology. 2010. p. 453–74.

2. Bartelds GM, Wijbrandts C a, Nurmohamed MT, Stapel S, Lems WF, Aarden L, et al. Anti-infliximab and anti-adalimumab antibodies in relation to response to adalimumab in infliximab switchers and anti-tumour necrosis factor naive patients: a cohort study. Ann Rheum Dis. 2010;69(5):817–21.

3. Bertolotto A, Deisenhammer F, Gallo P, Sölberg Sørensen P. Immunogenicity of interferon beta: differences among products. J Neurol. 2004 Jun;251 Suppl(S2):II15–24.

4. De Vries MK, Wolbink GJ, Stapel SO, de Vrieze H, van Denderen JC, Dijkmans B a C, et al. Decreased clinical response to infliximab in ankylosing spondylitis is correlated with anti-infliximab formation. Ann Rheum Dis. 2007;66:1252–4.

5. Schellekens H. Immunologic mechanisms of EPO-associated pure red cell aplasia. Best Pract Res Clin. 2005;18(3):473–80.

6. McKoy JM, Stonecash RE, Cournoyer D, Rossert J, Nissenson AR, Raisch DW, et al. Epoetin-associated pure red cell aplasia: Past, present, and future considerations. Transfusion. 2008. p. 1754–62.

7. Yang J, Joo KW, Kim YS, Ahn C, Han JS, Kim S, et al. Two cases of pure red-cell aplasia due to anti-erythropoietin antibodies. J Nephrol. 2005;18(1):102–5.

8. Brinks V, Jiskoot W, Schellekens H. Immunogenicity of therapeutic proteins: The use of animal models. Pharmaceutical Research. 2011. p. 2379–85.

9. Bryson CJ, Jones TD, Baker MP. Prediction of immunogenicity of therapeutic proteins: validity of computational tools. BioDrugs. 2010 Jan;24(1):1–8.

10. Wullner D, Zhou L, Bramhall E, Kuck A, Goletz TJ, Swanson S, et al. Considerations for optimization and validation of an *in vitro* PBMC derived T cell assay for immunogenicity prediction of biotherapeutics. Clin Immunol. 2010;137(1):5–14.

11. Schellekens H. How to predict and prevent the immunogenicity of therapeutic proteins. Biotechnology Annual Review. 2008. p. 191–202.

12. Schellekens H. Factors influencing the immunogenicity of therapeutic proteins. Nephrol Dial Transplant. 2005;20(SUPPL. 6).

13. Stas P, Lasters I. Strategies for preclinical immunogenicity assessment of protein therapeutics. IDrugs. 2009;12(3):169–73.

14. De Groot a S, Knopp PM, Martin W. De-immunization of therapeutic proteins by T-cell epitope modification. Dev Biol (Basel). 2005;122:171–94.

15. Perry LCA, Jones TD, Baker MP. New approaches to prediction of immune responses to therapeutic proteins during preclinical development. Drugs in R and D. 2008. p. 385–96.

16.   Baker MP, Reynolds HM, Lumicisi B, Bryson CJ. Immunogenicity of protein therapeutics: The key causes, consequences and challenges. Self Nonself. 2010;1(4):314–22.

17.   Bian H, Hammer J. Discovery of promiscuous HLA-II-restricted T cell epitopes with TEPITOPE. Methods. 2004 Dec;34(4):468–75.

18.   De Groot AS, Jesdale BM, Szu E, Schafer JR, Chicz RM, Deocampo G. An interactive Web site providing major histocompatibility ligand predictions: application to HIV research. AIDS Res Hum Retroviruses. 1997 May;13(7):529–31.

19.   Dönnes P, Kohlbacher O. SVMHC: a server for prediction of MHC-binding peptides. Nucleic Acids Res. 2006 Jul;34(Web Server issue):W194–7.

20.   Van Walle I, Gansemans Y, Parren PWHI, Stas P, Lasters I. Immunogenicity screening in protein drug development. Expert Opin Biol Ther. 2007 Mar;7(3):405–18.

21.   Lata S, Bhasin M, Raghava GPS. Application of machine learning techniques in predicting MHC binders. Methods Mol Biol. 2007 Jan;409:201–15.

22.   Davies MN, Sansom CE, Beazley C, Moss DS. A novel predictive technique for the MHC class II peptide-binding interaction. Mol Med. 9(9-12):220–5.

23.   Desmet J, Meersseman G, Boutonnet N, Pletinckx J, De Clercq K, Debulpaep M, et al. Anchor profiles of HLA-specific peptides: analysis by a novel affinity scoring method and experimental validation. Proteins. 2005 Jan;58(1):53–69.

24.   Lundegaard C, Hoof I, Lund O, Nielsen M. State of the art and challenges in sequence based T-cell epitope prediction. Immunome Research. 2010.

25.   Fonseca SG, Coutinho-Silva A, Fonseca LAM, Segurado AC, Moraes SL, Rodrigues H, et al. Identification of novel consensus CD4 T-cell epitopes from clade B HIV-1 whole genome that are frequently recognized by HIV-1 infected patients. AIDS. 2006;20(18):2263–73.

26.   Fonseca CT, Cunha-Neto E, Goldberg AC, Kalil J, De Jesus AR, Carvalho EM, et al. Identification of paramyosin T cell epitopes associated with human resistance to Schistosoma mansoni reinfection. Clin Exp Immunol. 2005;142(3):539–47.

27.   Veeraraghavan S, Renzoni E a, Jeal H, Jones M, Hammer J, Wells a U, et al. Mapping of the immunodominant T cell epitopes of the protein topoisomerase I. Ann Rheum Dis. 2004;63(8):982–7.

28.   Iwai LK, Yoshida M, Sidney J, Shikanai-Yasuda MA, Goldberg AC, Juliano MA, et al. *In silico* Prediction of Peptides Binding to Multiple HLA-DR Molecules Accurately Identifies Immunodominant Epitopes from gp43 of Paracoccidioides brasiliensis Frequently Recognized in Primary Peripheral Blood Mononuclear Cell Responses from Sensitized Ind. Mol Med. 2003;9(9-12):209–19.

29.   Kapoerchan V V., Wiesner M, Hillaert U, Drijfhout JW, Overhand M, Alard P, et al. Design, synthesis and evaluation of high-affinity binders for the celiac disease associated HLA-DQ2 molecule. Mol Immunol. 2010;47(5):1091–7.

30.   Anthony D. T-cell epitope mapping using the ELISPOT approach. Methods. 2003 Mar;29(3):260–9.

31.   Mashishi T, Gray CM. The ELISPOT assay: an easily transferable method for measuring cellular responses and identifying T cell epitopes. Clin Chem Lab Med. 2002 Sep;40(9):903–10.

32.   James EA, LaFond R, Durinovic-Bello I, Kwok W. Visualizing antigen specific CD4+ T cells using MHC class II tetramers. J Vis Exp. 2009 Jan;(25).

33.   Hu G-L, Okita DK, Conti-Fine BM. T cell recognition of the A2 domain of coagulation factor VIII in hemophilia patients and healthy subjects. J Thromb Haemost. 2004;2(11):1908–17.

34.   Jones TD, Phillips WJ, Smith BJ, Bamford CA, Nayee PD, Baglin TP, et al. Identification and removal of a promiscuous CD4+ T cell epitope from the C1 domain of factor VIII. J Thromb Haemost. 2005;3(5):991–1000.

35.   Mond JJ. T cell independent antigens. Current Opinion in Immunology. 1995. p. 349–54.

36.   Perini P, Facchinetti A, Bulian P, Massaro AR, Pascalis DD, Bertolotto A, et al. Interferon-beta (INF-beta) antibodies in interferon-beta1a- and interferon-beta1b-treated multiple sclerosis patients. Prevalence, kinetics, cross-reactivity, and factors enhancing interferon-beta immunogenicity *in vivo*. Eur Cytokine Netw. 2001;12(1):56–61.

37.   Ben-Horin S, Mazor Y, Yanai H, Ron Y, Kopylov U, Yavzori M, et al. The decline of anti-drug antibody titres after discontinuation of anti-TNFs: Implications for predicting re-induction outcome in IBD. Aliment Pharmacol Ther. 2012;35(6):714–22.

38.   Sauerborn M, Brinks V, Jiskoot W, Schellekens H. Immunological mechanism underlying the immune response to recombinant human protein therapeutics. Trends Pharmacol Sci. 2010 Feb;31(2):53–9.

39.   Blythe MJ, Flower DR. Benchmarking B cell epitope prediction: underperformance of existing methods. Protein Sci. 2005 Jan;14(1):246–8.

40.   De Groot AS, McMurry J, Moise L. Prediction of immunogenicity: *in silico* paradigms, ex vivo and *in vivo* correlates. Curr Opin Pharmacol. 2008 Oct;8(5):620–6.

41.   Greenbaum JA, Andersen PH, Blythe M, Bui H, Cachau RE, Crowe J, et al. Towards a consensus on datasets and evaluation metrics for developing B-cell epitope prediction tools. J Mol Recognit. 2007;20(2):75–82.

42.   Giaco L, Amicosante M, Fraziano M, Gherardini PF, Ausiello G, Helmer-Citterich M, et al. B-Pred, a structure based B-cell epitopes prediction server. Adv Appl Bioinform Chem. 2012;5:11–21.

43.   Giese C, Lubitz A, Demmler CD, Reuschel J, Bergner K, Marx U. Immunological substance testing on human lymphatic micro-organoids *in vitro*. J Biotechnol. 2010;148(1):38–45.

44.   Koren E, Zuckerman L a, Mire-Sluis a R. Immune responses to therapeutic proteins in humans--clinical significance, assessment and prediction. Curr Pharm Biotechnol. 2002;3(4):349–60.

45.   Katsutani N, Yoshitake S, Takeuchi H, Kelliher JC, Couch RC, Shionoya H. Immunogenic properties of structurally modified human tissue plasminogen activators in chimpanzees and mice. Fundam Appl Toxicol. 1992;19(4):555–62.

46.   Bellomi F, Mute A, Palmieri G, Focaccetti C, Dianzani C, Mattel M, et al. Immunogenicity comparison of Interferon Beta-1a preparations using the BALB/c mouse model: Assessment of a new formulation for use in multiple sclerosis. New Microbiol. 2007;30(3):241–6.

47.   Braun A, Kwee L, Labow MA, Alsenz J. Protein aggregates seem to play a key role among the parameters influencing the antigenicity of interferon alpha (IFN-alpha) in normal and transgenic mice. Pharm Res. 1997;14(10):1472–8.

48.   Hermeling S, Schellekens H, Maas C, Gebbink MFBG, Crommelin DJA, Jiskoot W. Antibody response to aggregated human interferon alpha2b in wild-type and transgenic immune tolerant mice depends on type and level of aggregation. J Pharm Sci. 2006 May;95(5):1084–96.

49.   Van Beers MMC, Sauerborn M, Gilli F, Brinks V, Schellekens H, Jiskoot W. Oxidized and aggregated recombinant human interferon beta is immunogenic in human interferon beta transgenic mice. Pharm Res. 2011;28(10):2393–402.

50.   Filipe V, Jiskoot W, Basmeleh AH, Halim A, Schellekens H, Brinks V. Immunogenicity of different stressed IgG monoclonal antibody formulations in immune tolerant transgenic mice. MAbs. 2012;4(6):740–52.

51.   Van Beers MMC, Sauerborn M, Gilli F, Hermeling S, Brinks V, Schellekens H, et al. Hybrid transgenic immune tolerant mouse model for assessing the breaking of B cell tolerance by human interferon beta. J Immunol Methods. Elsevier B.V.; 2010 Jan;352(1-2):32–7.

52.   Ottesen JL, Nilsson P, Jami J, Weilguny D, Dührkop M, Bucchini D, et al. The potential immunogenicity of human insulin and insulin analogues evaluated in a transgenic mouse model. Diabetologia. 1994 Dec;37(12):1178–85.

53.   Stewart TA, Hollingshead PG, Pitts SL, Chang R, Martin LE, Oakley H. Transgenic mice as a model to test the immunogenicity of proteins altered by site-specific mutagenesis. Mol Biol Med. 1989 Aug;6(4):275–81.

54.   Lee HJ, Riley G, Johnson O, Cleland JL, Kim N, Charnis M, et al. *In vivo* characterization of sustained-release formulations of human growth hormone. J Pharmacol Exp Ther. 1997;281(3):1431–9.

55.   Zwickl CM, Cocke KS, Tamura RN, Holzhausen LM, Brophy GT, Bick PH, et al. Comparison of the immunogenicity of recombinant and pituitary human growth hormone in rhesus monkeys. Fundam Appl Toxicol. 1991 Feb;16(2):275–87.

56.   Zwickl CM, Smith HW, Zimmermann JL, Wierda D. Immunogenicity of biosynthetic human LysPro insulin compared to native-sequence human and purified porcine insulins in rhesus monkeys immunized over a 6-week period. Arzneimittelforschung. 1995 Apr;45(4):524–8.

57.   Food and Drug Administration. Center for Biologics Evaluation and Research. Meeting of the Biological Response Modifiers Advisory Committee. In: Bethesda MD. 1999.

58.   Gunn H. Immunogenicity of recombinant human interleukin-3. Clin Immunol Immunopathol. 1997 Apr;83(1):5–7.

59.   Black KE, Murray J a, David CS. HLA-DQ determines the response to exogenous wheat proteins: a model of gluten sensitivity in transgenic knockout mice. J Immunol. 2002;169(10):5595–600.

60.   Rosloniec EF, Brand DD, Myers LK, Whittington KB, Gumanovskaya M, Zaller DM, et al. An HLA-DR1 transgene confers susceptibility to collagen-induced arthritis elicited with human type II collagen. J Exp Med. 1997;185(6):1113–22.

61.   Madoiwa S, Yamauchi T, Hakamata Y, Kobayashi E, Arai M, Sugo T, et al. Induction of immune tolerance by neonatal intravenous injection of human factor VIII in murine hemophilia A. J Thromb Haemost. 2004;2(5):754–62.

62.   Madoiwa S, Yamauchi T, Kobayashi E, Hakamata Y, Dokai M, Makino N, et al. Induction of factor VIII-specific unresponsiveness by intrathymic factor VIII injection in murine hemophilia A. J Thromb Haemost. 2009;7(5):811–24.

63.   Fishwild DM, O'Donnell SL, Bengoechea T, Hudson D V, Harding F, Bernhard SL, et al. High-avidity human IgG kappa monoclonal antibodies from a novel strain of minilocus transgenic mice. Nat Biotechnol. 1996;14(7):845–51.

64.   Geluk a, Taneja V, van Meijgaarden KE, Zanelli E, Abou-Zeid C, Thole JE, et al. Identification of HLA class II-restricted determinants of Mycobacterium tuberculosis-derived proteins by using HLA-transgenic, class II-deficient mice. Proc Natl Acad Sci U S A. 1998;95(18):10797–802.

65.   Mendez MJ, Green LL, Corvalan JR, Jia XC, Maynard-Currie CE, Yang XD, et al. Functional transplant of megabase human immunoglobulin loci recapitulates human antibody response in mice. Nat Genet. 1997;15(2):146–56.

66.   Neeno T, Krco CJ, Harders J, Baisch J, Cheng S, David CS. HLA-DQ8 transgenic mice lacking endogenous class II molecules respond to house dust allergens: identification of antigenic epitopes. J Immunol. 1996;156(9):3191–5.

67.   Ishikawa F, Yasukawa M, Lyons B, Yoshida S, Miyamoto T, Yoshimoto G, et al. Development of functional human blood and immune systems in NOD/SCID/IL2 receptor {gamma} chain(null) mice. Blood. 2005 Sep;106(5):1565–73.

68.   Traggiai E, Chicha L, Mazzucchelli L, Bronz L, Piffaretti J-C, Lanzavecchia A, et al. Development of a human adaptive immune system in cord blood cell-transplanted mice. Science. 2004;304(5667):104–7.

69.   Chan AC, Carter PJ. Therapeutic antibodies for autoimmunity and inflammation. Nat Rev Immunol. 2010;10(5):301–16.

70.   Getts DR, Getts MT, McCarthy DP, Chastain EML, Miller SD. Have we overestimated the benefit of human(ized) antibodies? mAbs. 2010. p. 682–94.

71.   Scott DW, De Groot AS. Can we prevent immunogenicity of human protein drugs? Ann Rheum Dis. 2010 Jan;69 Suppl 1:i72–6.

72.   Watanabe Y, Takahashi T, Okajima A, Shiokawa M, Ishii N, Katano I, et al. The analysis of the functions of human B and T cells in humanized NOD/shi-scid/gammac(null) (NOG) mice (hu-HSC NOG mice). Int Immunol. 2009;21(7):843–58.

73.   Shultz LD, Brehm M a, Garcia-Martinez JV, Greiner DL. Humanized mice for immune system investigation: progress, promise and challenges. Nat Rev Immunol. 2012;12(11):786–98.

CHAPTER 4

LIGHT OBSCURATION MEASUREMENTS OF HIGHLY VISCOUS SOLUTIONS: SAMPLE PRESSURIZATION OVERCOMES UNDERESTIMATION OF SUBVISIBLE PARTICLE COUNTS

Daniel Weinbuch[1,2], Wim Jiskoot[2] and Andrea Hawe[1]

[1] Coriolis Pharma Research GmbH, Am Klopferspitz 19, 82152 Martinsried-Munich, Germany

[2] Division of Drug Delivery Technology, Cluster BioTherapeutics, Leiden Academic Centre for Drug Research (LACDR), Leiden University, PO Box 9502, 2300 RA Leiden, The Netherlands

Abstract

Light obscuration (LO) is the current standard technique for subvisible particle analysis in the quality control of parenterally administered drugs, including therapeutic proteins. Some of those, however, exhibit high viscosities due to high protein concentrations, which can lead to false results by LO measurements. In this study, we show that elevated sample viscosities, from about 9 cP, lead to an underestimation of subvisible particle concentrations, which is easily overlooked when considering reported data alone. We evaluated a solution to this problem, which is the application of sample pressurization during analysis. The results show that this is an elegant way to restore the reliability of LO analysis of highly viscous products without the necessity of additional sample preparation.

Introduction

Regulatory authorities require all parentally administered drugs/products to be tested for subvisible particulate matter. Light obscuration (LO) is the primary method described by the current pharmacopeias (USP <788> and Ph.Eur. 2.9.19) for the quantification of subvisible particles in parenteral products (1,2). However, for biopharmaceutical products other methods, such as flow imaging microscopy or electric zone sensing, are expected by the authorities as well (3). In light obscuration, a syringe pump draws the sample through the system, where particulate contaminants or impurities block a certain amount of light from a laser beam. The resulting "shadow" is detected by an optical sensor and converted into an equivalent circular diameter. However, for highly viscous products, such as high-concentration protein formulations for subcutaneous administration (4), LO measurements are potentially compromised (5) and a more time-consuming microscopy method has to be used, which is not always applicable to amorphous protein particles (1). High protein concentrations can impede light obscuration measurements because of an increased refractive index of the solution. Herewith the RI difference between proteinaceous particles and solution becomes so small that the particles become "invisible", which has been investigated previously by our group (6). In this study we focused on the influence of high viscosity to show that elevated sample viscosities from about 9 cP lead to an underestimation of subvisible particle concentrations, which is easy to overlook when considering reported data alone. We evaluated a solution to this problem involving the application of sample pressurization during analysis. The results show that this is an elegant way to restore the reliability of LO analysis of highly viscous products, e.g., highly concentrated protein formulations, without necessitating additional sample preparation.

Materials & Methods

Materials

Glycerol (≥ 99%) was purchased from Sigma Aldrich (Steinheim, Germany) and pharmaceutical grade sucrose was provided by Südzucker (Mannheim, Germany). Polyclonal IgG (Hizentra®) was obtained from a local pharmacy. NIST traceable 2-µm polystyrene sizing standards were purchased from Thermo Scientific (Ulm, Germany).

Sample preparation

Glycerol and sucrose solutions were prepared in purified water in the stated concentrations. A highly concentrated protein solution at elevated viscosity (48 cP) was

obtained by upconcentration of polyclonal IgG (Hizentra®) from 200 mg/mL to about 250 mg/mL by using a centrifugal filter unit with a 10 kDa molecular weight cutoff (Millipore, Schwalbach, Germany). Subsequently, all solutions were filtered through a 0.22-µm syringe filter (Millipore, Schwalbach, Germany). Samples were measured with or without the addition of polystyrene sizing standards (2 µm) in a final dilution of 1:10,000.

Light obscuration (LO)

Particle concentrations in a size range between 1 and 200 µm were measured with a PAMAS SBSS (Partikelmess- und Analysesysteme GmbH, Rutesheim, Germany) equipped with an HCB-LD-25/25 sensor, a 1-mL syringe pump, and a pressurizable sample chamber (Figure 1). Four measurements of 0.3 mL with a pre-run volume of 0.2 mL and a fixed flow rate of 10 mL/min were performed following the current draft USP <787> method (5) with or without pressurization of the sample chamber at 4 bar above atmosphere. The mean particle concentration was calculated from the last 3 (out of 4) measurements. Unless stated differently, samples were measured in triplicate and mean and standard deviations were calculated.

Viscosity measurements

A Paar Physica MCR-100 rheometer (Anton Paar GmbH, Ostfildern-Scharnhausen, Germany) equipped with an MK22 cone was used to measure the dynamic viscosity of a 1-mL sample at 20°C every 5 s during a shear rate ramp from 50 to 500 s^{-1} over 17 min with a cone-to-plate gap of 50 µm. All solutions showed Newtonian behavior. Samples were measured in triplicate and mean and standard deviations were calculated.
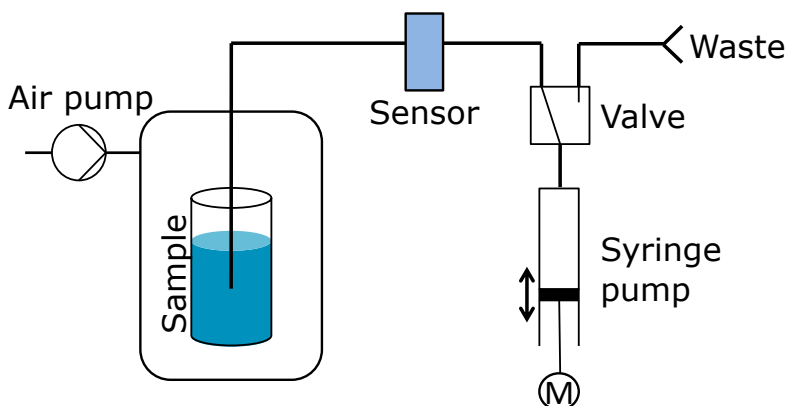

Figure 1: Schematic overview of the PAMAS SBSS light obscuration device

Results and discussion

Filtered solutions of sucrose and glycerol (0, 25, 50 and 75% w/v and v/v, respectively) were used to simulate high-viscosity samples. Analysis by light obscuration at 0 and 4 bar sample pressurization resulted in low background counts (< 100 particles/mL > 1 µm), showing that sample preparation and/or the light obscuration system itself introduce negligible quantities of foreign particulate matter (data not shown). Next, purified water, sucrose, and glycerol solutions were spiked with 2-µm polystyrene sizing standards, resulting in approximately $8x10^4$ particles per milliliter, as measured in purified water at ambient pressure conditions (Figure 2A). Results of the polystyrene sizing standards in purified water, measured under sample pressurization, showed similar particle counts. At increased concentrations of glycerol (> 50% v/v) or sucrose (> 75% w/v), however, particle concentrations apparently decreased when measured at ambient pressure conditions. A similar observation was made when a highly concentrated protein solution (polyclonal IgG at approx. 250 mg/mL) with a viscosity of 48 cP spiked with 2-µm polystyrene sizing standards was measured. Here the determined particle concentration, derived from a single LO measurement, decreased from $8.2x10^4$ particles per ml when measured at 4 bar to $4.3x10^4$ particles per ml when measured without sample pressurization (Figure 2B), showing the relevance of the problem to highly concentrated protein formulations.
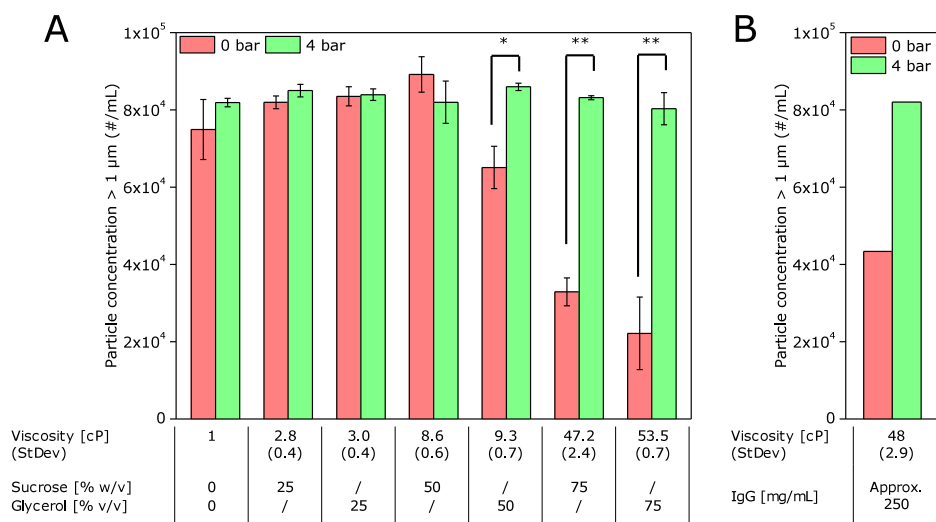

Viscosity [cP] (StDev)	1	2.8 (0.4)	3.0 (0.4)	8.6 (0.6)	9.3 (0.7)	47.2 (2.4)	53.5 (0.7)
Sucrose [% w/v]	0	25	/	50	/	75	/
Glycerol [% v/v]	0	/	25	/	50	/	75

Viscosity [cP] (StDev)	48 (2.9)
IgG [mg/mL]	Approx. 250

Figure 2: Measured particle concentrations by light obscuration, with and without sample pressurization, of A) water and different glycerol and sucrose solutions and B) high concentrated protein solution, all containing a fixed concentration of 2-µm polystyrene sizing standards. Error bars and values in brackets show standard deviations from triplicate particle concentration and viscosity measurements, respectively. *p<0.05, **p<0.005 (based on one-way ANOVA)

The reduction in particle counts can be explained by an intake of air into the syringe pump of the LO system (Figure 3). This air intake was also observed for the same highly concentrated glycerol and sucrose solutions without the addition of sizing standards, however, with no significant effect on the measured particle concentration. This indicates that the air bubbles did not pass the detector, because their high refractive index makes them easily detectable by the system (7). Thus, the air enters the light obscuration system between sensor and syringe pump cell through tubing connections and/or valves, as a result of an under-pressure created by the slow-moving high-viscosity solutions. This results in an overestimated measurement volume and, consequently, an underestimation of particle concentrations. The sample viscosity at which the effect started to occur in our tested system was approximately 9 cP (Figure 2A), a value that can easily be reached in concentrated protein formulations (8).

Figure 3: Fig. 3. Image of the PAMAS SBSS light obscuration syringe pump aspirating A) purified water and B) 75% (w/v) sucrose solution during sample measurement at ambient pressure conditions.

Since the air intake may depend on the state of the system tubing and valves, two other light obscuration systems (type PAMAS SVSS) —one equipped with a 1-mL syringe pump and the other with a 10-mL one— were tested as well. All of the tested systems showed a similar air intake at very comparable viscosity values (results not shown). This indicates that it is a general problem that is not related to one specific PAMAS system. Moreover,

depending on their maintenance state, individual LO systems might leak air at even lower viscosity values.

It is important to realize that the underestimation of particle concentration resulting from air intake may be overlooked when considering reported data alone. The syringe pump needs to be observed by the operator during method development and specifically tested for air intake when samples of increased viscosities are to be analyzed by LO. Alternatively, or in addition, one could follow the method described in this study and verify if counting or sizing standards spiked into water and into the formulation result in a similar increase in particle counts.

The application of light obscuration can, given the requirements of regulatory authorities and current pharmacopeias, only be circumvented by the application of microscopic techniques, which are more labor-intensive and less precise (9). The current draft USP <787>, which is tailored for the analysis of biopharmaceuticals, states that sample dilution with a low viscosity solvent (e.g., purified water) is a possible "last resort" solution. This, however, may have an influence on the composition, distribution or concentration of proteinaceous particles. Another more elegant way to measure high-viscosity solutions without sample dilution is the application of overpressure on the sample side. As shown in Figure 2, the application of 4 bar above atmospheric pressure can restore the reliability of light obscuration measurements for highly viscous solutions with viscosities of up to at least 50 cP.

Conclusions

We have demonstrated that particle concentrations in highly viscous samples, as measured by light obscuration, are potentially underestimated. This is due to an intake of air into the measurement system and consequently a reduced measurement volume. Importantly, this can easily be overlooked by the operator, since blank measurements are not affected, though they should be anticipated prior to the analysis of viscous samples. Sample pressurization is a simple and effective way to overcome this problem even for solutions with viscosities above 50 cP.

Acknowledgements

References

1.   Ph.Eur. 2.9.19. General, particulate contamination: sub-visible particles. In: The European Pharmacopoeia,. 7th ed. 2011.

2.   USP <788>. Particulate Matter in Injections. In: The United States Pharmacopoeia, National Formulary. 2006.

3.   Kirshner LS. Regulatory expectations for analysis of aggregates and particles. In: Colorado Protein Stability Conference. Breckenridge, CO; 2012.

4.   Jezek J, Rides M, Derham B, Moore J, Cerasoli E, Simler R, et al. Viscosity of concentrated therapeutic protein compositions. Adv Drug Deliv Rev. Elsevier B.V.; 2011 Oct;63(13):1107–17.

5.   Demeule B, Messick S, Shire SJ, Liu J. Characterization of particles in protein solutions: reaching the limits of current technologies. AAPS J. 2010 Dec;12(4):708–15.

6.   USP <787>. Subvisible particulate matter in therapeutic protein injections. In: The United States Pharmacopoeia, National Formulary.

7.   Zölls S, Gregoritza M, Tantipolphan R, Wiggenhorn M, Winter G, Friess W, et al. How subvisible particles become invisible-relevance of the refractive index for protein particle analysis. J Pharm Sci. 2013 Mar 5;102(5):1434–46.

8.   Kamerzell TJ, Pace AL, Li M, Danilenko DM, McDowell M, Gokarn YR, et al. Polar solvents decrease the viscosity of high concentration IgG1 solutions through hydrophobic solvation and interaction: formulation and biocompatibility considerations. J Pharm Sci. 2013 Apr;102(4):1182–93.

9.   Cao S, Narhi LO, Jiang Y. Analytical Methods to measue sub-visible particulates. In: Analysis of aggregates and particles in protein pharmaceuticals. Wiley; 2012.

CHAPTER 5

MICRO-FLOW IMAGING AND RESONANT MASS MEASUREMENT (ARCHIMEDES) – COMPLEMENTARY METHODS TO QUANTITATIVELY DIFFERENTIATE PROTEIN PARTICLES AND SILICONE OIL DROPLETS

Daniel Weinbuch[1,2,*], Sarah Zölls[1,3,*], Michael Wiggenhorn[1], Wolfgang Friess[3], Gerhard Winter[3], Wim Jiskoot[2] and Andrea Hawe[1]

[1] Coriolis Pharma Research GmbH, Am Klopferspitz 19, 82152 Martinsried-Munich, Germany

[2] Division of Drug Delivery Technology, Cluster BioTherapeutics, Leiden Academic Centre for Drug Research (LACDR), Leiden University, PO Box 9502, 2300 RA Leiden, The Netherlands

[3] Department of Pharmacy, Pharmaceutical Technology and Biopharmaceutics, Ludwig Maximilian University, Butenandtstr. 5-13, 81377 Munich, Germany

* shared first authors

Abstract

Our study aimed to comparatively evaluate Micro-Flow Imaging (MFI) and the recently introduced technique of resonant mass measurement (Archimedes, RMM) as orthogonal methods for the quantitative differentiation of silicone oil droplets and protein particles. This distinction in the submicron and micron size range is highly relevant for the development of biopharmaceuticals, in particular for products in prefilled syringes. Samples of artificially generated silicone oil droplets and protein particles were quantified individually and in defined mixtures to assess the performance of the two techniques. The built-in MFI software solution proved to be suitable to discriminate between droplets and particles for sizes above 2 µm at moderate droplet/particle ratios (70:30 − 30:70). A customized filter developed specifically for this study greatly improved the results and enabled reliable discrimination also for more extreme mixing ratios (95:5 − 15:85). RMM showed highly accurate discrimination in the size range of about 0.5 to 2 µm independent of the ratio, provided that a sufficient number of particles (> 50 counted particles) were counted. We recommend applying both techniques for a comprehensive analysis of biotherapeutics potentially containing silicone oil droplets and protein particles in the submicron and micron size range.

Introduction

Protein aggregates can be classified according to their size as visible (> 100 µm), micron (1-100 µm), submicron (100 nm-1000 nm) and nanometer particles (< 100 nm) (1). Especially aggregates in the micron and submicron size range raise concerns as they are potentially immunogenic (2,3), could coalesce to form larger particles over time or function as nuclei for further aggregation (4). Even though the United States Pharmacopeia (USP) and the European Pharmacopoeia (Ph. Eur.) currently define concentration limits in parenteral solutions only for particles larger than 10 µm, regulatory authorities increasingly expect quantitative characterization of micron particles from 1 to 10 µm and qualitative characterization of submicron particles from 100 nm to 1000 nm already in early stages of the development phase (5–7). In many cases substantial amounts of particles below 10 µm are often present in formulations that meet the limits of the pharmacopoeias for larger particles (8–10).

In general, particles of all sizes can be proteinaceous or non-proteinaceous. Among the group of non-proteinaceous particles, silicone oil droplets, which are also quantified as particles by routine methods like light obscuration, play a major role. This is especially important for products in prefilled syringes or cartridges, where silicone oil droplets are introduced into the product deriving from the lubrication of the glass barrel and the plunger. In a case study, silicone oil droplets were identified inside the eyes of patients after intravitreal injection, likely originating from the siliconized glass syringes (11). In earlier studies, silicone oil droplets were detected in insulin syringes and associated with loss of insulin efficacy (12,13). Furthermore, silicone oil droplets were present in Interferon products in prefilled syringes (14). Even though silicone oil itself is not necessarily harmful to the patient (15), it has been described to induce aggregation of monoclonal antibodies (16) and various other proteins (17,18), and the formation of protein-silicone oil complexes (18,19), which might potentially be immunogenic (20). From a manufacturing perspective, elevated concentrations of (silicone) oil droplets can indicate problems during the production process, e.g., improper siliconization of syringes or contamination from leaking components during lyophilization. These factors make an analytical differentiation of the total particle load into protein particles and silicone oil droplets necessary.

Among the various techniques for particle analysis (21), scanning electron microscopy coupled with energy dispersive X-ray spectroscopy (SEM-EDX) (22), Fourier-transformed infrared (FTIR) (22), and Raman microscopy (23), asymmetrical flow field flow fractionation (24), electrical sensing zone as well as flow cytometry (25) are in principle able to differentiate silicone oil droplets and protein particles. However, mainly flow

imaging microscopy techniques and the recently introduced resonant mass measurement (RMM) technique are designed for the differentiation of these particles in a higher throughput and without cumbersome sample preparation (e.g. staining or fixation). Micro-Flow Imaging (MFI) has received major attention for the analysis of protein particles (22,26–28) but has also been applied for the identification of silicone oil droplets (29). Silicone oil droplets were successfully differentiated from protein particles on MFI images on the basis of their spherical shape (30) and, more efficiently, by employing a multi-parametric filter (31).

The recently introduced Archimedes system employs the novel principle of RMM for the analysis of submicron and micron particles (32). The sample solution is flushed through a microchannel inside a resonating cantilever (also designated as suspended microchannel resonator (SMR)) which changes its frequency depending on the mass of the particles passing the channel. Importantly, positively buoyant particles (e.g. silicone oil droplets) and negatively buoyant particles (e.g. protein particles) can be clearly discriminated as they increase and decrease the frequency of the cantilever, respectively (33). With a theoretical size range from about 50 nm up to about 6 µm (depending on the sensor and the particle type), RMM bridges the "submicron size gap" (15,34) between on the one hand flow imaging microscopy and light obscuration, which cover the micrometer size range, and on the other hand nanoparticle tracking analysis and dynamic light scattering, which allow analysis in the nanometer size range. Literature on RMM is still very limited. Patel et al. (35) presented a first study on the principle of RMM using various microspheres as well as silicone oil droplets and protein particles for a technical evaluation of the system. Barnard et al. (14) applied RMM to analyze protein particles and silicone oil droplets in marketed Interferon-beta products. However, the accuracy of the differentiation between these two particle types was not investigated in those studies and remains to be elucidated.

The aim of our study was to evaluate MFI and RMM as orthogonal tools for the quantitative discrimination between silicone oil droplets and proteinaceous particles in the micron and submicron range. For this purpose, defined mixtures of silicone oil droplets and protein particles were prepared at various ratios on the basis of the distributions expected in marketed biopharmaceutical products in prefilled syringes. The optical discrimination of silicone oil droplets from protein particles in MFI by (i) the built-in software solution "find similar" and (ii) a new customized data filter developed in this study was compared to the physical discrimination principle of RMM.

Materials & Methods

Materials

Etanercept (Enbrel®, prefilled syringe, lot no. 31576, exp. 12/2008; lot no. 32411, exp. 09/2009), adalimumab (Humira®, prefilled syringe, lot no. 292209A05, exp. 10/2006; lot no. 430989A04, exp. 02/2008), rituximab (MabThera®, vial, lot no. B6073, exp. 12/2013), and infliximab (Remicade®, vial, lot no. 7GD9301402, 7FD8701601, 7RMKA81402, pooled) were donated by local hospitals. Sucrose, mannitol, sodium chloride, trisodium citrate dihydrate and polysorbate 80 were purchased from VWR (Darmstadt, Germany), disodium hydrogenphosphate dihydrate and sodium dihydrogenphosphate dihydrate were purchased from Merck KGaA (Darmstadt, Germany). Silicone oil with a viscosity of 1000 cSt (same viscosity as used in other studies (15,16,25) and as listed in the Ph.Eur. monography for silicone oil as a lubricant (36)), citric acid, and arginine hydrochloride were purchased from Sigma Aldrich (Steinheim, Germany).

Preparation of protein samples

Etanercept solution at a concentration of 5 mg/mL was prepared by dilution of 50 mg/mL etanercept (removed from the prefilled syringe through the needle) in 25 mM phosphate buffer (pH 6.3) containing 100 mM NaCl, 25 mM arginine hydrochloride, and 1% sucrose. Adalimumab solution at a concentration of 5 mg/mL was prepared by dilution of 50 mg/mL adalimumab in 15 mM phosphate/citrate buffer (pH 5.2) containing 105 mM NaCl, 1.2% mannitol, and 0.1% polysorbate 80.

Rituximab solution at a concentration of 1 mg/mL was prepared by dilution of 10 mg/mL rituximab commercial product in 25 mM citrate buffer (pH 6.5) containing 154 mM NaCl and 0.07% polysorbate 80 (formulation buffer). The formulation was filtered using a 0.2-µm polyethersulfone syringe filter (Sartorius, Göttingen, Germany) and kept at 2-8 °C for a maximum of one week. Heat-stressed rituximab was prepared by incubating 1.5 mL of the 1 mg/ml rituximab solution for 30 min at 71 °C in a thermomixer (Eppendorf, Hamburg, Germany). Stir-stressed rituximab was prepared by incubating 3 mL of the 1 mg/ml rituximab solution in a 5R glass vial using a 12 mm Teflon®-coated stir bar at 1000 rpm for 24 hours at room temperature on a magnetic stirrer (Heidolph MR 3001K, Heidolph, Schwabach, Germany). Stressed rituximab at 1 mg/ml (protein particle stock suspension) was stored at 2-8°C until the measurement.

Infliximab solution at a concentration of 1 mg/mL was prepared by dilution of 10 mg/mL infliximab commercial product in 100 mM phosphate buffer (pH 7.2). The formulation was filtered using a 0.2-µm polyethersulfone syringe filter. Heat-stressed infliximab was

prepared by incubating 0.5 mL of the 1 mg/mL infliximab solution for 30 minutes at 60 °C in a thermomixer. Stir-stressed infliximab was prepared by incubating 8 mL of the 1 mg/mL infliximab solution in a 10R glass vial using an 18-mm Teflon®-coated stir bar at 250 rpm for 24 hours at room temperature on a magnetic stirrer (Heidolph MR Hei-Standard).

Preparation of silicone oil emulsion

Pure silicone oil was added to filtered formulation buffer (0.2-µm polyethersulfone syringe filter (Sartorius, Göttingen, Germany)) in a particle-free 15-mL conical tube (VWR, Darmstadt, Germany) to a final concentration of 2% (w/v) to generate a pure emulsion without additives. After vortexing briefly, silicone oil droplet formation was induced by sonication in a water bath (Sonorex, Brandelin, Berlin, Germany) for 10 min. Fresh silicone oil emulsion (silicone oil droplet stock emulsion) was prepared on the day of the measurement and kept at room temperature.

Preparation of individual and mixed samples of silicone oil droplets and protein particles

Silicone oil droplet stock emulsion and/or protein particle stock suspension (heat-stressed rituximab) was diluted in unstressed protein solution or filtered formulation buffer for the preparation of mixed and individual samples. Unless stated otherwise, samples were prepared to a final protein concentration of 0.5 mg/mL. Mixed samples were prepared to cover ratios of silicone oil droplets to protein particles of 95:5 to 15:85 based on particle counts > 1 µm determined by MFI. Individual samples were prepared to contain the same amount of silicone oil droplets and protein particles, respectively, as in the mixed samples and were referred to as the theoretical concentration. The samples were gently mixed with a pipette, kept at room temperature and measured on the day of preparation.

Micro-Flow Imaging

An MFI DPA4100 series A system (ProteinSimple, Santa Clara, California) equipped with a 100-µm flow cell, operated at high magnification (14x) and controlled by the MFI View software version 6.9 was used. The system was flushed with 5 mL purified water at maximum flow rate and flow cell cleanliness was checked between measurements. Unstressed and filtered rituximab or the appropriate formulation buffer was used to perform "optimize illumination" prior to each measurement. Samples of 0.65 mL with a pre-run volume of 0.3 mL were analyzed at a flow rate of 0.1 mL/min (n=3). MVAS version 1.2 was used for data analysis.

Development of a customized filter for MFI

The MVAS software of the MFI system enables the discrimination of particles based on optical parameters of the generated images through the "find similar" operation. For our study, a minimum of 20 particles above 5 μm clearly recognizable as silicone oil droplets was selected for the discrimination. In addition to this, a customized filter was developed specifically for the heat-stressed Rituximab samples of this study. In detail, the new filter was based on four customized size-specific cut-offs for particle parameters of silicone oil droplets provided by MFI (Figure 1), which proved to be suitable to discriminate silicone oil droplets and protein particles. This approach is a modification of previous work by Strehl et al. (31). The four parameters used for our filter were intensity mean (Figure 1A), intensity minimum (Figure 1B), intensity standard deviation (Figure 1C) and aspect ratio (Figure 1D).
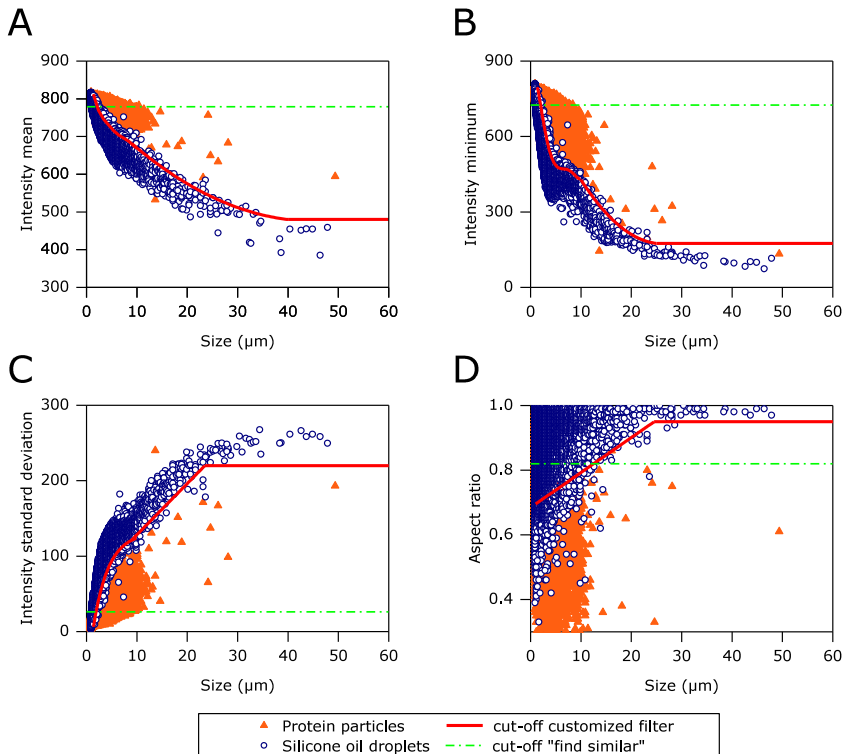

Figure 1 Scatter plots of particle parameters: A) intensity mean, B) intensity minimum, C) intensity standard deviation, and D) aspect ratio for individual samples containing only protein particles (heat-stressed rituximab) or only silicone oil droplets analyzed separately by MFI and merged into one graph per particle parameter. The solid red lines illustrate cutoffs as a function of size, generated by our customized fit for the discrimination between silicone oil droplets and protein particles. The dash-dotted green lines illustrate linear cutoffs used by the MVAS software for the "find similar" operation.

The first three parameters are based on the intensity of the particle image, which is directly proportional to the transparency of the particle (27). The intensity mean describes the mean intensity value over all pixels within one particle; the intensity minimum describes the intensity of the darkest pixel of a particle; and the intensity standard deviation describes differences between higher and lower intensity values within the same particle. The aspect ratio defines the shape of a particle with "1" for an absolutely spherical particle and "0" for a needle with an infinite length. For each of the four particle parameters, the individual distributions for silicone oil droplets and protein particles from heat-stressed rituximab were compared as a function of size. Cut-offs were defined at the mean value of the 95% confidence intervals between the two populations (Figure S1). A polynomial function was automatically fitted to these points from 1 to 11 μm and applied for particles from 1 to 9 μm. Above 11 μm, the number of counts acquired was not sufficient for this statistical approach; therefore, the fit was adjusted manually in this larger size range. The automated and the manual fit were overlapped in the size range from 9 to 11 μm to ensure a smooth transition. Since the silicone oil droplet population was more homogeneous than the protein particle population, the customized filter was set to identify objects as silicone oil droplets only when they fulfilled all four cut-off fit criteria. Particles showing values below the cutoff for intensity mean and minimum (Figure 1A and B) and at the same time above the cutoff for intensity standard deviation and aspect ratio (Figure 1C and D) were marked as silicone oil droplets by the algorithm. Particles fulfilling less than four of these criteria were assigned as non-silicone oil particles, which means in our case protein particles.

Resonant mass measurement

An Archimedes system (Affinity Biosensors, Santa Barbara, California) was equipped with a Hi-Q Micro Sensor and controlled by ParticleLab software version 1.8. The sensor was flushed for 60 s with purified water prior to analysis. Subsequently, possible impurities in the system were removed by two "sneeze" operations (liquid in the sensor is pushed into both directions) and the system was flushed again for 60 s with purified water. The sample solution was then loaded for 45 s. Prior to analysis, the limit of detection (LOD) was determined three times in automatic LOD mode. The mean value was then set fixed for each measurement. Samples of 150 nL were analyzed (n=3) and fresh sample solution was loaded for each of the triplicate measurements.

Size determination of particles by RMM is based on the frequency shift f which is proportional to the buoyant mass M_B and depending on the sensitivity S of the resonator (Equation 1).

$$M_B = \Delta f * S$$

Equation 1

The conversion of buoyant mass M_B into dry mass M (Equation 2) and diameter D (Equation 3) is then based on the density of the particle, $\rho_{particle}$ (1.32 g/mL for protein particles, based on the density of pure protein (37) and the recommendation of the manufacturer; 0.97 g/mL for silicone oil, according to the supplier) and the density of the fluid, ρ_{fluid} (calculated based on the sensor frequency relative to the frequency and the density of water as a reference).

$$M = \frac{M_B}{1 - \rho_{fluid} / \rho_{particle}}$$

Equation 2

$$D = \sqrt[3]{\frac{6M}{\pi\rho_{particle}}}$$

Equation 3

Results and discussion

Silicone oil droplets in prefilled syringes

Expired prefilled syringes of etanercept and adalimumab were available for the study and analyzed in order to gain insight into relevant levels and size distributions of silicone oil droplets in marketed products as a worst case scenario. Four and six years after expiration, respectively, MFI determined for both products about 4×10^5 particles/mL above 1 µm. Based on the images generated by MFI, about 80% of the particles above 5 µm in both products could be identified as silicone oil droplets using the "find similar" operation provided by the MVAS software. RMM determined 3.2×10^6 particles/mL larger than 0.5 µm for etanercept and 2.0×10^6 particles/mL for Adalimumab, of which 51% and 97%, respectively, could be attributed to silicone oil. Three and four years after expiration, RMM determined for both analyzed products lower concentrations of protein particles and of silicone oil droplets when compared to products four and six years after expiration, respectively (Table S1). This implies that total particle concentrations as well as the ratio between silicone oil droplets and protein particles can vary substantially between products, lots and age of the product.

Determination of total particle concentrations (without discrimination)

For the evaluation of MFI and RMM, silicone oil droplets were artificially generated, which appeared similar to those found in etanercept and adalimumab prefilled syringes with respect to their shape, optical properties (Figure 2) and size distribution (Figure S2). The concentrations used in our study (0.003% to 0.025% (w/v) silicone oil) provided droplet concentrations similar to those identified in the expired etanercept and adalimumab prefilled syringes and are in agreement with other studies suggesting the presence of up to 0.03% of silicone oil in prefilled syringes (38,39). A heat-stress method was developed using rituximab as a model for the generation of particles with a similar appearance to protein particles in etanercept prefilled syringes. A stir-stress method was developed for the generation of particles similar to those in adalimumab prefilled syringes (Figure 2). All protein samples showed comparable particle size distributions with the smaller particles representing the largest fraction (Figure S3). Protein particles in concentrations from 1×10^5 to 5×10^5 particles/mL above 1 µm (according to MFI) were combined with silicone oil droplets in concentrations from 1×10^5 to 3×10^5 particles/mL above 1 µm (according to MFI). Using MFI and RMM, several samples with varying concentrations of protein particles and silicone oil droplets were analyzed, both individually and as mixtures at various defined droplet/particle ratios.
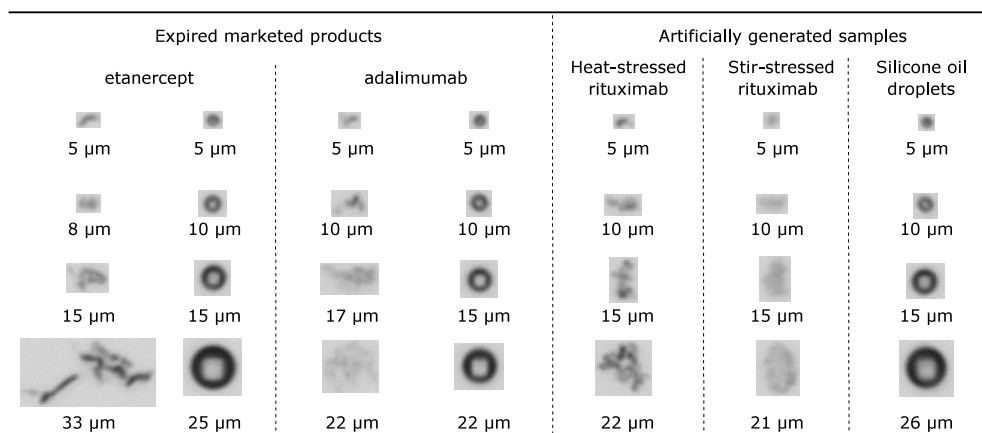

Figure 2: Examples of MFI images of protein particles and silicone oil droplets detected in marketed products and artificially generated samples.

First, the particle concentrations for individual samples containing either only silicone oil droplets or only protein particles were determined by MFI and RMM. One combination is shown as a representative example in Figure 3 for the overlapping measurement size range of both techniques (1-4 µm). Overall, the results indicate that particle counts and size distributions by MFI and RMM are in general agreement. However, certain differences

were observed depending on the type of sample and the ratio of protein particles and silicone oil droplets: For samples containing only silicone oil, RMM detected slightly more droplets of 1 to 4 µm as compared to MFI, while MFI detected more droplets in the size range from 2 to 4 µm (Figure 3A). This trend was reproducible for all silicone oil droplet samples, with an up to twofold higher silicone oil droplet count in the size range of 1 to 4 µm detected by RMM as compared to MFI.

This difference might be due to two major reasons:

(i) Silicone oil droplets of sizes up to 50 µm were identified by MFI, which are much larger than the microchannel diameter of RMM (8 µm). Those particles larger than 8 µm represent only 4% of all silicone oil droplets in the sample detected by MFI by number; however, they contain 72% of the total mass of all silicone oil droplets in the sample detected by MFI (mass was calculated based on droplet counts at the respective diameter and the density of silicone oil of 0.97 g/mL). These observations led us to the hypothesis that larger silicone oil droplets might be fragmented into smaller ones by shear forces inside the microchannels and capillaries of the RMM system. This would result in an increased number of smaller silicone oil droplets in RMM. Our hypothesis was supported by MFI data from a sample containing only silicone oil, which was analyzed before RMM and collected after an RMM measurement. In this case, an increase in silicone oil droplet concentration between 1 and 2 µm with a concomitant decrease above 2 µm was observed when comparing particle concentrations before and after the RMM measurement (Figure S4A). It could be shown that this was clearly an effect of the RMM measurement itself and not of the dilution of the sample during the RMM measurement (Figure S4B). A decreased flow rate during sample analysis might reduce this fragmentation effect but would further increase the already long measurement time of RMM.

(ii) Additionally, small particles near the detection limit of MFI could be "overlooked" by the software, as suggested also by others (40), further enhancing the differences between MFI and RMM for small (1 µm) silicone oil droplet counts.
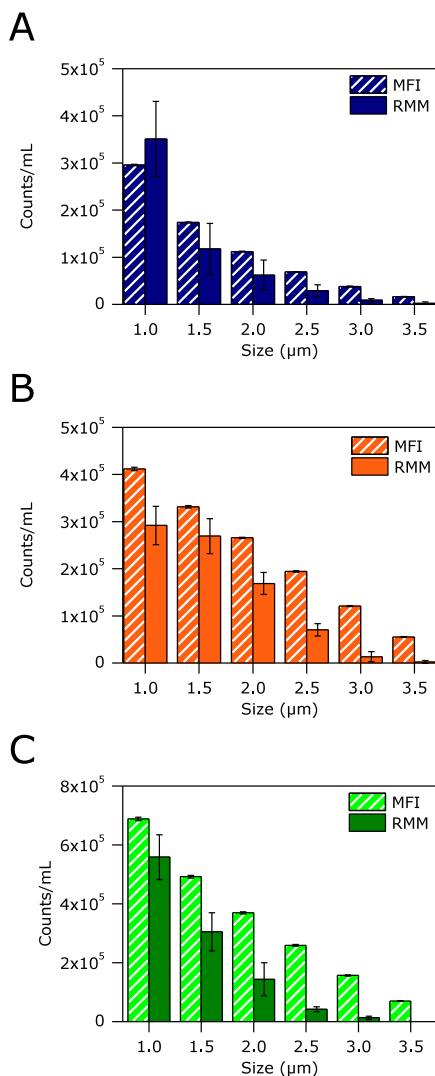
A

B

C

Figure 3: Cumulative counts in the size range of 1–4 µm of A) a sample containing only silicone oil droplets, B) a sample containing only protein particles (heat-stressed rituximab), and C) the corresponding mixture (droplet–particle ratio 40:60 for particles >1 µm based on MFI) as determined by MFI and RMM. Error bars represent standard deviations from triplicate measurements.

In contrast to the results from silicone oil samples, RMM detected consistently less protein particles in individual samples than MFI over the entire 1 to 4 µm size range (Figure 3B). This was also observed in a previous study by our group (41). This difference is suggested to occur for two reasons:

(i) MFI and RMM apply fundamentally different measurement principles (Figure 4): MFI captures 2D microscopic particle images (Figure 4A) and size determination of particles by MFI is performed according to their spatial dimension on the images defined by the outer boundary of the particle. The differentiation of protein particles and silicone oil droplets is based on morphological parameters such as particle shape and transparency. In contrast, RMM detects particles as distinct positive or negative peaks in the frequency trace caused by the physical parameter of particle buoyancy (Figure 4B). However, protein particles may vary in density and contain substantial amounts of liquid (42). This is not included into the size calculation by RMM, causing a potential underestimation of particle sizes in RMM as compared to MFI, which includes liquid inside the particle in the size calculation. This in turn would lead to an apparent shift of the complete particle size distribution in RMM towards smaller particle sizes resulting in lower concentrations detected for the respective size bins in RMM as compared to MFI.

 (ii) As a second reason, the micron-sized capillaries and channels of the RMM sensor are vulnerable to clogging by particles at or above the upper size limit of the system. Even though RMM offers several tools to remove stuck particles, clogging cannot always be avoided. Thus, large stuck particles could hinder other particles from reaching the sensor. This could explain why the concentration discrepancy between RMM and MFI is more pronounced at larger particle sizes. Smaller particles will pass a clogged site more easily, whereas larger particles, although still in the measurement range, are more likely to be excluded from the analysis. Altogether, this will result in lower apparent protein particle concentrations in RMM. A possible solution would be sample preparation for highly aggregated samples, e.g. filtration or centrifugation, which can however potentially change sample properties. In the future, a potential system reconfiguration by the manufacturer could decrease clogging issues.

Total particle concentrations for mixed samples containing both silicone oil droplets and protein particles also revealed slight differences between MFI and RMM for the overlapping size range of 1 to 4 µm (Figure 3C). For moderate ratios (silicone oil droplets/protein particles 40:60 based on MFI shown as a representative sample), RMM detected less particles than MFI, likely due to the underestimation of protein particles as described before. However, in mixed samples of higher silicone oil content (silicone oil droplets/protein particles 80:20 or 95:5 based on MFI) similar concentrations were determined by the two techniques. In those samples, the overestimation of silicone oil droplets by RMM was balanced out by the underestimation of protein particles by RMM leading to similar total particle counts in MFI and RMM. For all samples, RMM showed

higher standard deviations than MFI. This is probably mainly due to the small analyzed volume in RMM (about 0.15 µL) as compared to MFI (about 35 µL).

It was further investigated whether the presence of both silicone oil droplets and protein particles within the same sample influenced the accuracy of MFI or RMM to determine total particle concentrations. For MFI, the concentration determined for mixed samples of silicone oil droplets and protein particles from heat-stressed rituximab matched very closely the sum of the concentrations determined for the corresponding individual samples (Figure S5A). For RMM, the concentration for the mixed sample reasonably matched the sum of the individual samples for the main size classes (Figure S5B). These observations were consistent for different ratios and also for protein particles from stir-stressed rituximab mixed with silicone oil droplets. This justified the use of particle counts of individual samples as the theoretical concentrations for mixed samples.

Discrimination between silicone oil droplets and protein particles

The discrimination between silicone oil droplets and protein particles by MFI and RMM is based on clearly different mechanisms (see above and Figure 4). The optical discrimination by MFI bears the potential risk of false classification due to optically similar silicone oil droplets and protein particles in the lower size range, especially near the detection limit. In contrast, the discrimination by RMM based on the physical parameter of particle buoyancy enables a clear discrimination with minimal risk of false classification. In this case, the difference in density between silicone oil droplets and protein particles is beneficial.

Discrimination between droplets and particles by MFI

In the present paper, the performance of MFI was assessed using the built-in software solution "find similar" and a customized data filter developed specifically for this study. To evaluate the reliability of our customized filter, the following control experiments were performed: the filter was applied on samples containing only silicone oil droplets and the number of objects falsely marked as protein particles was determined and vice versa. Our customized filter marked less than 3% of the counts in the samples containing only silicone oil droplets ($3x10^5$ particles/mL > 1 µm based on MFI) falsely as protein particles (> 2 µm) and less than 8% of the counts in the samples containing only protein particles ($4x10^5$ particles/mL > 1 µm based on MFI) falsely as silicone oil droplets (> 2 µm). These controls illustrate the capability of our filter to properly discriminate protein particles and silicone oil droplets. The requirement that all four criteria of particle parameters need to be fulfilled at the same time is the main difference of our filter compared to the filter

previously developed by Strehl et al. (31), which used the product of four particle parameters as criterion for particle classification. In this case, extreme values in one parameter could shift the product to the side of one particle type although the other three parameters would classify it clearly as the other particle type. Thus, their filter led to errors of 10% to 12% (> 2 µm) for silicone oil droplets classified falsely as protein particles; the error for protein particles classified falsely as silicone oil droplets depended strongly on the type of protein particles and varied between 2% and 42% in their study (31).
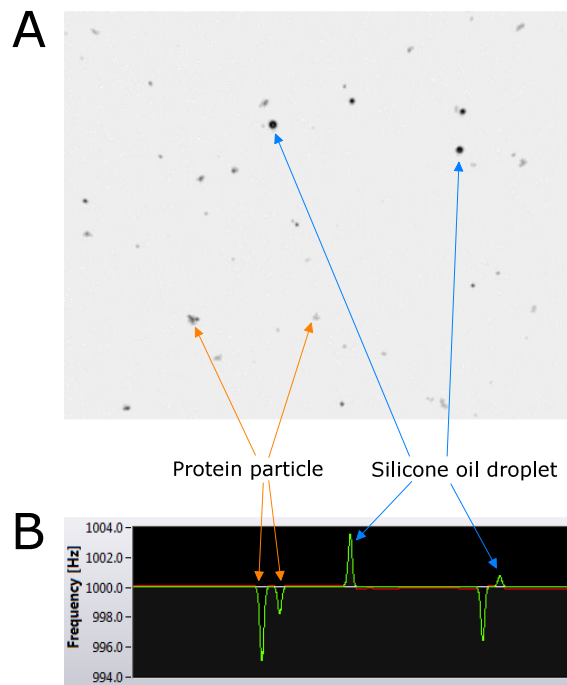

Figure 4: aw data of an exemplary mixed sample containing protein particles (heat-stressed rituximab) and silicone oil droplets from A) MFI (image-based discrimination) and B) RMM (frequency-based discrimination).

In contrast, our filter applies more strict criteria for silicone oil droplet identification as particles fulfilling only three out of four criteria are not marked as silicone oil droplets leading to lower errors as discussed above. However, for protein particles generated from a different monoclonal IgG (infliximab) by heat stress or stir stress the customized filter marked up to 40% (> 2 µm) falsely as silicone oil droplets. This was most likely due to the lower intensity (lower transparency) of particle images of this IgG, which makes a misclassification as silicone oil droplets of similarly low transparency more likely. This is in agreement with the literature, where large variations were also observed by Strehl et al. (31) when their filter was applied to different types of protein particles. The MVAS

software filter could not be tested on these protein samples as it was based on manual selection of silicone oil droplet images which were not present in these pure protein samples.

The "find similar" operation of the MVAS software as well as the customized filter were both used to categorize particles from mixed samples into silicone oil droplets and non-silicone oil particles. Non-silicone oil particles were defined as protein particles in our case. The obtained concentrations were compared to the theoretical concentrations based on the analysis of the individual samples, which were used to assess the accuracy of both methods (Figure 5A, C, and Figure 6). For moderate droplet/particle number ratios from 30:70 to 70:30 based on MFI, both the selection by "find similar" and the customized filter were able to determine the correct concentrations within acceptable deviations for particles > 2 μm. This was observed for samples containing silicone oil droplets and protein particles from heat-stressed Rituximab (Figure 5A exemplarily shows the results for a sample with a droplet/particle ratio of 40:60 based on MFI). For stir-stressed Rituximab (Figure 5C) the customized filter for MFI showed superior discrimination compared to the "find similar" method for particles > 2 μm, even though the customized filter was designed based on heat-stressed Rituximab particles. The even higher intensity of MFI particle images of stir-stressed Rituximab compared to those of heat-stressed Rituximab (Figure 2) likely contributes to this: since three out of four parameters of the customized filter are based on the particle intensity, it facilitates discrimination from the lower intensity silicone oil droplets. Furthermore, the customized filter was superior for samples with more extreme droplet/particle number ratios (see Figure 6A and B for representative examples) and for samples based on original, undiluted Rituximab solution (Figure 6C).

Thus, for particles between 2 μm and 25 μm, the development of a customized filter is useful for an accurate discrimination by MFI. For particles with a size below 2 μm, discrimination by an alternative method is recommended (e.g. RMM, as discussed later) as both "find similar" and the customized filter were not reliably capable of determining the correct concentration. For particles larger than 25 μm, due to usually low particle numbers in this size range, manual classification of the MFI images might be preferred over the built-in software solution or a customized filter. Those particles can usually be identified easily by visual evaluation of the images.
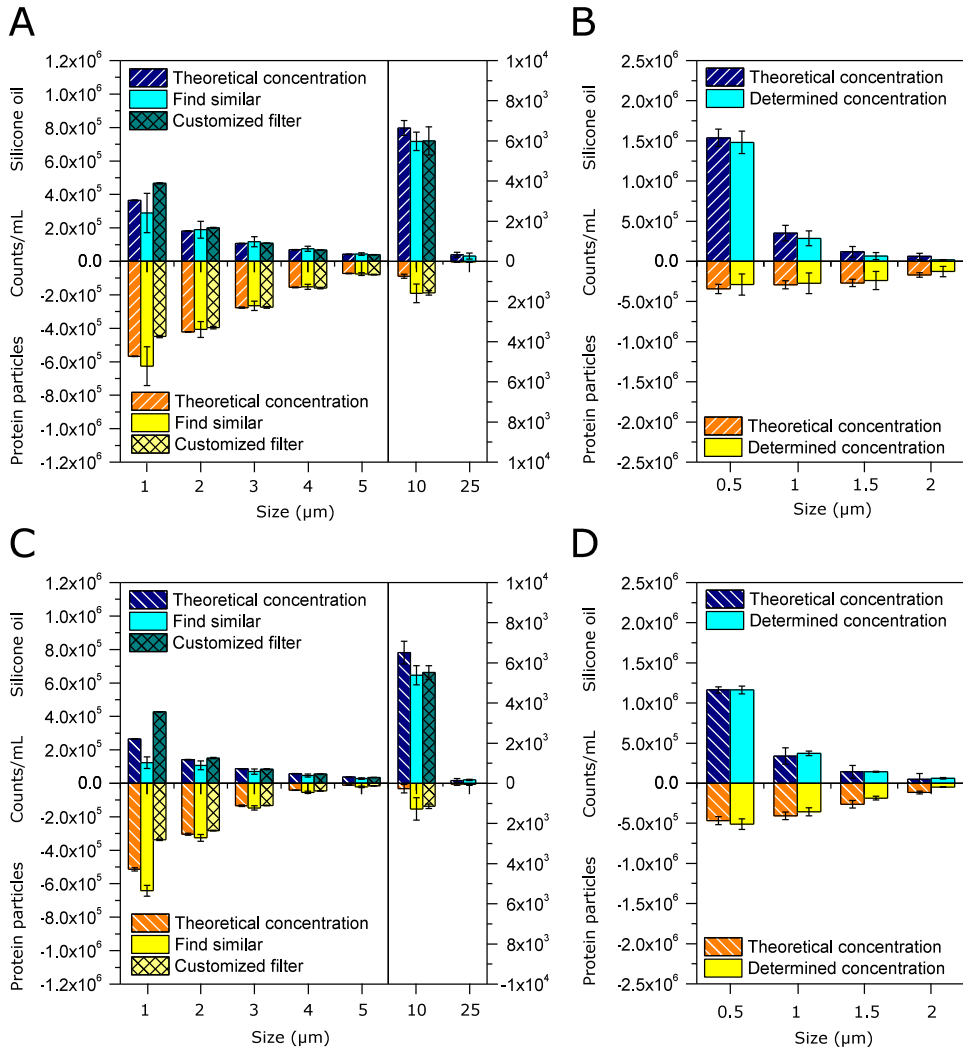
Figure 5: Results from MFI (A and C) or RMM (B and D) for the discrimination between silicone oil droplets and protein particles. Histograms comparing the theoretical concentrations (based on individual samples) and determined concentrations of silicone oil droplets and protein particles (A and B, heat-stressed rituximab; C and D, stir-stressed rituximab) in mixed samples with moderate ratios (droplet–particle ratio 40:60 based on MFI). Error bars represent standard deviations from triplicate measurements.
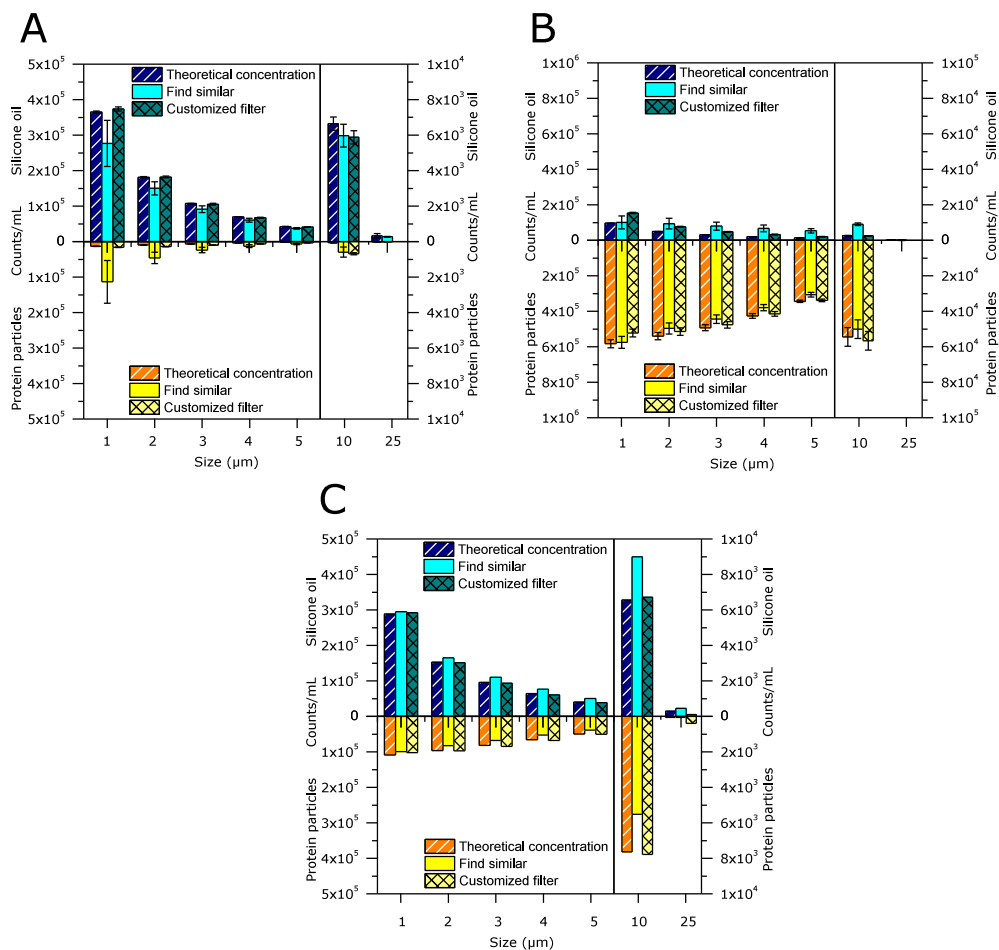
Figure 6: MFI cumulative particle counts comparing theoretical concentrations (based on individual samples) and determined concentrations of silicone oil droplets and protein particles (heat-stressed rituximab) in droplet–particle ratios of A) 95:5 and B) 15:85 in samples containing 0.5 mg/mL rituximab as well as C) 60:40 in a sample containing undiluted rituximab (10 mg/mL). Error bars (A and B) represent standard deviations from triplicate measurements.

Discrimination between droplets and particles by RMM

As described for MFI, RMM was evaluated with respect to an accurate discrimination between silicone oil droplets and protein particles in mixed samples (Figure 5B, D, and Figure 7). For moderate particle/droplet ratios, RMM was consistently able to discriminate particles correctly with small deviations from the theoretical concentrations for heat-stressed (Figure 5B) and stir-stressed rituximab (Figure 5D). Large deviations of 20% or more from the theoretical concentration were only observed if the discrimination was

based on less than 50 counted particles (corresponding in this case to total concentrations (droplets + particles) < $3x10^5$ particles/mL) and thus statistical representation of the sample population was limited. This was for example the case for particles larger than 2 μm (Figure 5B and D). Increasing the analyzed sample volume would compensate for the limited reliability of RMM to quantify low particle concentrations, as also reported by others.[35] However, it needs to be considered that very long measurement times associated with large analyzed volumes could also provoke changes in sample properties. In contrast, fairly high concentrations of protein particles > $2x10^6$ particles/mL caused high standard deviations potentially due to the increased probability of coinciding particles and also blockage of the channel by particles (Figure 7A). However, extreme droplet/particle ratios with high amounts of silicone oil droplets provided moderate standard deviations and also fairly accurate determination of the theoretical concentration (Figure 7B exemplarily displays results for a droplet/particle ratio of 95:5 based on RMM). Those results provide evidence that RMM discrimination is reliable for particles below 2 μm.

Comparison of results for MFI and RMM

For a final evaluation of MFI and RMM regarding the discrimination of silicone oil droplets and protein particles, results for the same sample were compared between the two techniques. For silicone oil droplets and heat-stressed Rituximab (Figure 5A and B, droplet/particle ratio 40:60) as well as stir-stressed Rituximab (Figure 5C and D, droplet/particle ratio 40:60), RMM detected a higher fraction of silicone oil droplets as compared to MFI for the sizes above 1 μm already in the individual samples. This originated foremost from the differences in total concentration determination as discussed earlier: RMM detected in general more silicone oil droplets than MFI, whereas MFI detected in general more protein particles than RMM (see also Figure 3). However, in this size range, RMM results for the mixed samples are considered more reliable as RMM differentiation was shown to be highly accurate (Figure 5B and D). MFI differentiation suffered from low image resolution in the lower size range leading to large deviations for both the "find similar" operation and the customized filter (Figure 5A and C). With increasing particle size, the ratios between MFI and RMM in the individual samples converged and similar ratios for individual samples were obtained for particles > 2 μm (Figure 5A and B show a droplet/particle ratio of 30:70 for particles > 2 μm in individual samples for both MFI and RMM). For mixed samples, the concentration obtained by MFI is suggested to be more reliable for sizes above 2 μm as the discrimination between droplets and particles was highly accurate, especially when the customized filter was applied (Figure 5A and C). RMM analysis of objects with a size above 2 μm was based on small

numbers of counts, questioning the reliability of the determined concentrations (Figure 5B and D) in our study.
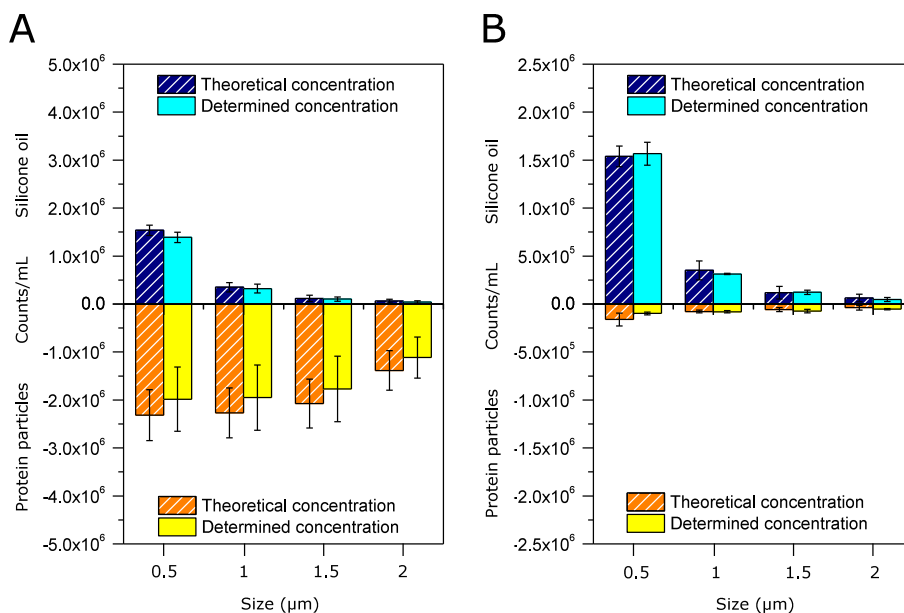

Figure 7: RMM cumulative particle counts comparing theoretical concentrations (based on individual samples) and determined concentrations of silicone oil droplets and protein particles (heat-stressed rituximab) in droplet–particle ratios of A) 40:60 and B) 95:5. Error bars represent standard deviations from triplicate measurements.

Recommendations and conclusions

Table 1 summarizes properties as well as pros and cons during the application of MFI and RMM which were identified in our study. For MFI, the customized filter was shown to provide correct results for moderate and extreme ratios between silicone oil droplets and protein particles. The filter was developed using heat-stressed rituximab particles, but was also found applicable for rituximab particles generated by stir stress and for samples containing rituximab solution in high concentrations (10 mg/mL). In contrast, the application for infliximab particles generated by either heat or stir stress resulted in large errors. These results emphasize the necessity of customizing the filter to each specific protein, the formulation, and the particle type / stress method of interest. Thus, the development of a customized filter for quality control of protein therapeutics in prefilled syringes with comparable manufacturing conditions can be considered reasonable. In contrast, the implementation during formulation development with varying conditions should be critically evaluated case by case. The separation by the MVAS software was

acceptably accurate especially for moderate ratios of silicone oil droplets and protein particles. It could still be applied in those cases, when costs and time for the development of a customized filter would exceed the benefit of a more accurate discrimination. However, the differentiation by "find similar" showed clearly higher standard deviations as compared to the customized filter. This higher variation of the "find similar" operation originated most likely from the underlying sample and operator dependent manual selection of the particle images. For both MFI-based solutions it is important to consider that the separation is based on the identification of silicone oil droplets, whereas the remaining particles, identified only as "non-silicone oil particles", are simply equated with protein particles by the operator.

Table 1: Summarizing comparison of MFI and RMM for the analysis of silicone oil droplets and protein particles.

	MFI (MFI4100, HighMag Settings)	RMM (Archimedes, Micro Sensor)
Properties of the techniques		
Principle	Flow imaging microscopy with digital image analysis. Sizing based on optical particle boundary.	Mass determination by quantification of frequency shift. Sizing based on particle density
Size range	1-70 µm	0.3-4 µm
Differentiation of protein particles and silicone oil droplets	Based on morphological parameters (shape, transparency...) of particle images. Differentiation may be time-consuming (esp. development of customized filter).	Based on particle buoyancy (density). Differentiation during the measurement without additional time consumption.
Concentration range	Up to 1×10^6 particles/mL (coincidence not indicated by the system)	3×10^5 to 1×10^7 particles/mL (coincidence indicated by the system)
Reproducibility	Higher reproducibility	Lower reproducibility (due to lower analyzed volume)
Status of the technique	Established R&D and cGMP technique	Novel R&D technique
Pros and Cons during application		
Protein particles	Clear visualization of larger particles.	Clogging by larger particles possible.
Silicone oil droplets	Detection of larger droplets without fragmentation.	Fragmentation of larger droplets possible.
Samples containing protein particles and silicone oil droplets	2-10 µm: good differentiation by built-in software filter or (preferably) customized filter. > 10 µm: easy identification by optical evaluation of particle images.	0.5-2 µm: unambiguous differentiation due to physical detection principle.
Complexes of protein particles and silicone oil droplets	Potential identification of larger complexes (> about 5-10 µm).	Potential misclassification, miscalculation of particle size or no detection.
More than one particle type of higher density (e.g. protein and rubber, steel, glass)	Potential differentiation according to visual appearance (refractive index or shape).	No differentiation possible.

For RMM, the discrimination was very accurate for different types of protein particles and different ratios as long as sufficiently high numbers of particles were detected. The high accuracy of RMM is due to the straightforward categorization of particles and droplets according to buoyant mass. This makes RMM a very robust technique for exactly this task. It needs to be considered that RMM can only discriminate one type of positively buoyant from one type of negatively buoyant particles. Thus, if a sample contains protein particles as well as other particles of higher density than the buffer, e.g., particles shed from filling pumps or rubber stoppers, RMM is not able to discriminate them. Here, methods such as SEM-EDS, FT-IR or Raman microscopy (43) could be used as orthogonal methods to further identify these "non-silicone oil" particles. Furthermore, complexes consisting of both protein and silicone oil can pose a challenge for the technique of RMM: The reported size of those complexes may be incorrect due to the simultaneous influence of both material densities on the density of the complex. As a worst case the complexes might be missed entirely as the higher density of protein is compensated by the lower density of silicone oil, eliminating a clear density difference between particle and formulation. Those complexes might be detectable by MFI (given that they are large enough) as shown for an IgG particle containing silicone oil (22). In our study, only very few of those complexes were observed in MFI, because protein particles and silicone oil droplets were prepared separately to avoid interactions of protein and silicone oil during the particle formation process.

Taken together, the robust detection principle of RMM has brought significant benefit to the field of protein product characterization, especially for the discrimination of silicone oil droplets and protein particles. RMM differentiation is recommended for particles below 2 µm, provided that sufficient particle quantities are detected. MFI differentiation is recommended above 2 µm, preferably using a customized filter. In order to cover a size range as broad as possible, both techniques should be applied in parallel for a comprehensive analysis of samples potentially containing silicone oil droplets and protein particles in the size range from 500 nm to 70 µm.

References

1. Narhi LO, Schmit J, Bechtold-Peters K, Sharma D. Classification of protein aggregates. J Pharm Sci. 2012 Feb;101(2):493–8.

2. Carpenter J, Cherney B, Lubinecki A, Ma S, Marszal E, Mire-Sluis A, et al. Meeting report on protein particles and immunogenicity of therapeutic proteins: filling in the gaps in risk evaluation and mitigation. Biologicals. 2010 Sep;38(5):602–11.

3. Rosenberg AS. Effects of protein aggregates: an immunologic perspective. AAPS J. 2006 Jan;8(3):E501–7.

4. Chi EY, Krishnan S, Randolph TW, Carpenter JF. Physical stability of proteins in aqueous solution: mechanism and driving forces in nonnative protein aggregation. Pharm Res. 2003 Sep;20(9):1325–36.

5. USP <788>. Particulate Matter in Injections. In: The United States Pharmacopoeia, National Formulary. 2009.

6. Ph.Eur. 2.9.19. General, particulate contamination: sub-visible particles. In: The European Pharmacopoeia,. 7th ed. 2011.

7. Kirshner LS. Regulatory expectations for analysis of aggregates and particles. In: Colorado Protein Stability Conference. Breckenridge, CO; 2012.

8. Kerwin BA, Akers MJ, Apostol I, Moore-Einsel C, Etter JE, Hess E, et al. Acute and long-term stability studies of deoxy hemoglobin and characterization of ascorbate-induced modifications. J Pharm Sci. 1999 Jan;88(1):79–88.

9. Hawe A, Friess W. Stabilization of a hydrophobic recombinant cytokine by human serum albumin. J Pharm Sci. 2007 Nov;96(11):2987–99.

10. Tyagi AK, Randolph TW, Dong A, Maloney KM, Hitscherich C, Carpenter JF. IgG particle formation during filling pump operation: A case study of heterogeneous nucleation on stainless steel nanoparticles. J Pharm Sci. 2009;98(1):94–104.

11. Freund KB, Laud K, Eandi CM, Spaide RF. Silicone oil droplets following intravitreal injection. Retina. 26(6):701–3.

12. Chantelau E, Berger M. Pollution of insulin with silicone oil, a hazard of disposable plastic syringes. Lancet. 1985;325(8443):1459.

13. Chantelau E, Berger M, Bohlken B. Silicone oil released from disposable insulin syringes. Diabetes Care. 1986;9(6):672–3.

14. Barnard JG, Babcock K, Carpenter JF. Characterization and quantitation of aggregates and particles in interferon-β products: Potential links between product quality attributes and immunogenicity. J Pharm Sci. 2013;102(3):915–28.

15. Felsovalyi F, Janvier S, Jouffray S, Soukiassian H, Mangiagalli P. Silicone-oil-based subvisible particles: Their detection, interactions, and regulation in prefilled container closure systems for biopharmaceuticals. J Pharm Sci. 2012;101(12):4569–83.

16. Thirumangalathu R, Krishnan S, Ricci MS, Brems DN, Randolph TW, Carpenter JF. Silicone oil - and agitation-induced aggregation of a monoclonal antibody in aqueous solution. J Pharm Sci. 2009 Sep;98(9):3167–81.

17. Jones LS, Kaufmann A, Middaugh CR. Silicone oil induced aggregation of proteins. J Pharm Sci. 2005 Apr;94(4):918–27.

18. Ludwig DB, Carpenter JF, Hamel J-B, Randolph TW. Protein adsorption and excipient effects on kinetic stability of silicone oil emulsions. J Pharm Sci. 2010 Apr;99(4):1721–33.

19. Britt KA, Schwartz DK, Wurth C, Mahler HC, Carpenter JF, Randolph TW. Excipient effects on humanized monoclonal antibody interactions with silicone oil emulsions. J Pharm Sci. 2012 Sep 16;101(12):4419–32.

20. Kossovsky N, Heggers JP, Robson MC. Experimental demonstration of the immunogenicity of silicone-protein complexes. J Biomed Mater Res. 1987 Sep;21(9):1125–33.

21. Zölls S, Tantipolphan R, Wiggenhorn M, Winter G, Jiskoot W, Friess W, et al. Particles in therapeutic protein formulations, Part 1: overview of analytical methods. J Pharm Sci. 2012 Mar;101(3):914–35.

22. Wuchner K, Büchler J, Spycher R, Dalmonte P, Volkin DB. Development of a microflow digital imaging assay to characterize protein particulates during storage of a high concentration IgG1 monoclonal antibody formulation. J Pharm Sci. 2010 Aug;99(8):3343–61.

23. Lankers M, Munhall J, Valet O. Differentiation between foreign particulate matter and silicone oil induced protein aggregation in drug solutions by automated Raman spectroscopy. Microsc Microanal. 2008 Aug 3;14(S2):1612–3.

24. Fraunhofer W, Winter G. The use of asymmetrical flow field-flow fractionation in pharmaceutics and biopharmaceutics. Eur J Pharm Biopharm. 2004 Sep;58(2):369–83.

25. Ludwig DB, Trotter JT, Gabrielson JP, Carpenter JF, Randolph TW. Flow cytometry: a promising technique for the study of silicone oil-induced particulate formation in protein formulations. Anal Biochem. 2011 Mar 15;410(2):191–9.

26. Sharma DK, King D, Oma P, Merchant C. Micro-flow imaging: flow microscopy applied to sub-visible particulate analysis in protein formulations. AAPS J. 2010 Sep;12(3):455–64.

27. Sharma DK, Oma P, Pollo MJ, Sukumar M. Quantification and characterization of subvisible proteinaceous particles in opalescent mAb formulations using micro-flow imaging. J Pharm Sci. 2010 Jun;99(6):2628–42.

28. Demeule B, Messick S, Shire SJ, Liu J. Characterization of particles in protein solutions: reaching the limits of current technologies. AAPS J. 2010 Dec;12(4):708–15.

29. Liu L, Ammar DA, Ross LA, Mandava N, Kahook MY, Carpenter JF. Silicone oil microdroplets and protein aggregates in repackaged bevacizumab and ranibizumab: effects of long-term storage and product mishandling. Invest Ophthalmol Vis Sci. 2011 Feb;52(2):1023–34.

30. Sharma D, Oma P, Krishnan S. Silicone Microdroplets in Protein Formulations - Detection and Enumeration. Pharm Technol. 2009;33(4):74–9.

31. Strehl R, Rombach-Riegraf V, Diez M, Egodage K, Bluemel M, Jeschke M, et al. Discrimination between silicone oil droplets and protein aggregates in biopharmaceuticals: a novel multiparametric image filter for sub-visible particles in microflow imaging analysis. Pharm Res. 2012 Feb;29(2):594–602.

32. Burg TP, Godin M, Knudsen SM, Shen W, Carlson G, Foster JS, et al. Weighing of biomolecules, single cells and single nanoparticles in fluid. Nature. 2007 Apr 26;446(7139):1066–9.

33. Dextras P, Burg TP, Manalis SR. Integrated measurement of the mass and surface charge of discrete microparticles using a suspended microchannel resonator. Anal Chem. 2009 Jun 1;81(11):4517–23.

34. Rosenberg AS, Verthelyi D, Cherney BW. Managing uncertainty: A perspective on risk pertaining to product quality attributes as they bear on immunogenicity of therapeutic proteins. J Pharm Sci. 2012;101(10):3560–7.

35. Patel AR, Lau D, Liu J. Quantification and Characterization of Micrometer and Submicrometer Subvisible Particles in Protein Therapeutics by Use of a Suspended Microchannel Resonator. Anal Chem. 2012 Jul 13;84(15):6833–40.

36. Ph.Eur. 3.1.8. Silicone oil used as a lubricant. In: The European Pharmacopoeia,. 7th ed. 2010.

37. Fischer H, Polikarpov I, Craievich AF. Average protein density is a molecular-weight-dependent function. Protein Sci. 2004 Oct;13(10):2825–8.

38. Majumdar S, Ford BM, Mar KD, Sullivan VJ, Ulrich RG, D'souza AJM. Evaluation of the effect of syringe surfaces on protein formulations. J Pharm Sci. 2011 Jul;100(7):2563–73.

39. Chantelau E. Silicone oil contamination of insulin. Diabet Med. 1989 Apr;6(3):278.

40. Pedersen JS. Statistical evaluation of MFI dataset quality for high-throughput analysis. In: Protein Simple User Meeting, Basle, Switzerland. 2012.

41. Zölls S, Gregoritza M, Tantipolphan R, Wiggenhorn M, Winter G, Friess W, et al. How subvisible particles become invisible-relevance of the refractive index for protein particle analysis. J Pharm Sci. 2013 Mar 5;102(5):1434–46.

42. Ripple DC, Wayment JR, Carrier MJ. Standards for the Optical Detection of Protein Particles. Am Pharm Rev. 2011;(4):90–6.

43. Cao X, Masatani P, Torraca G, Wen ZQ. Identification of a mixed microparticle by combined microspectroscopic techniques: A real forensic case study in the biopharmaceutical industry. Appl Spectrosc. 2010;64(8):895–900.

Supplementary information

Table S1: Total particle and silicone oil droplet concentrations of expired marketed products in prefilled syringes determined by RMM.

Product	Total particle concentration (> 0.5 µm)	Identified as silicone oil droplets (> 0.5 µm)
etanercept		
lot 32411, exp.09/2009	1.50×10^6	1.46×10^6
lot 31576, exp.12/2008	3.25×10^6	1.68×10^6
adalimumab		
lot 430989A04, exp.02/2008	1.74×10^6	1.61×10^6
lot 292209A05, exp.10/2006	2.01×10^6	1.94×10^6
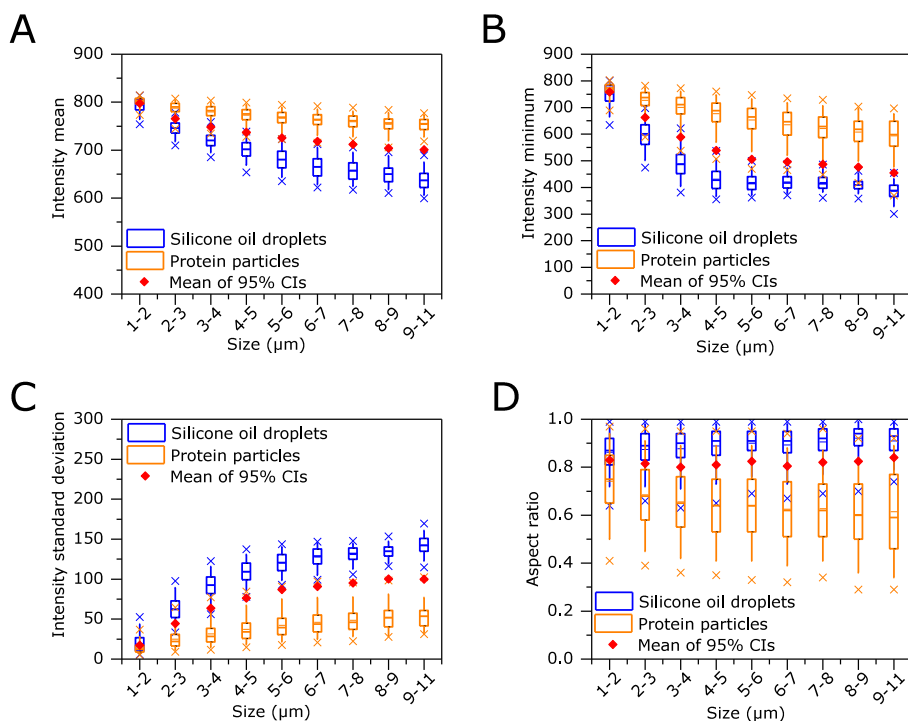
Figure S1: Distribution of the MFI particle parameters A) intensity mean, B) intensity minimum, C) intensity standard deviation and D) aspect ratio for individual samples of silicone oil droplets and protein particles (heat-stressed Rituximab). Box plots show 25/75% (box) and 5/95% percentiles (whisker) as well as minimum and maximum values (X). The mean values of the 95% confidence intervals (CI) were used as a basis to fit the function for the customized filter.
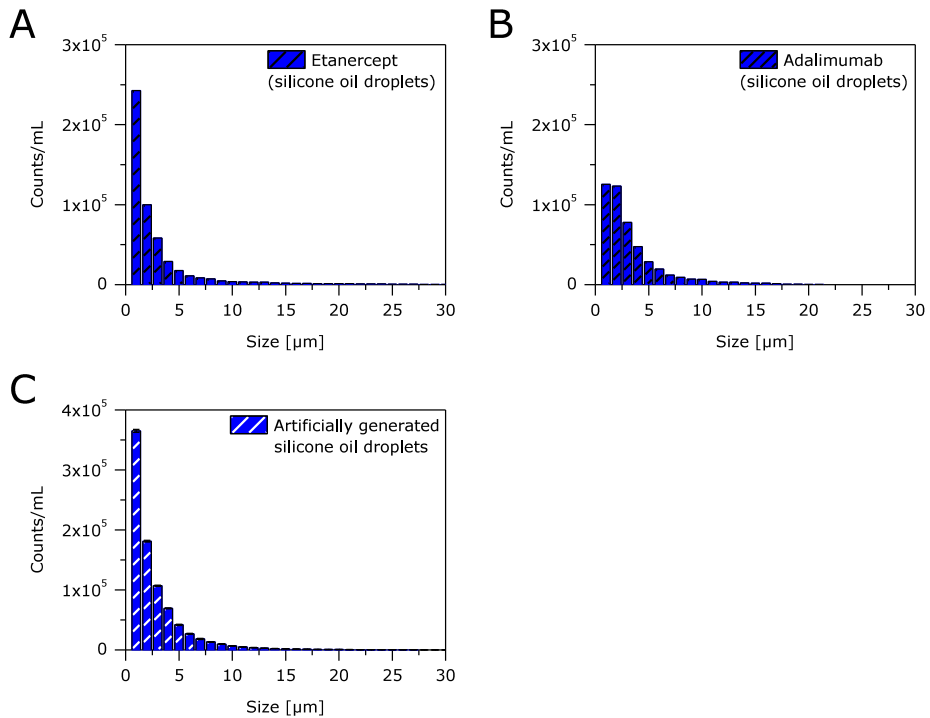
Figure S2: Cumulative size distributions of silicone oil droplets determined by MFI and identified by the "find similar" operation in A) Etanercept prefilled syringes, B) Adalimumab prefilled syringes, C) a sample containing only artificially generated silicone oil droplets. Error bars represent standard deviations from triplicate measurements.
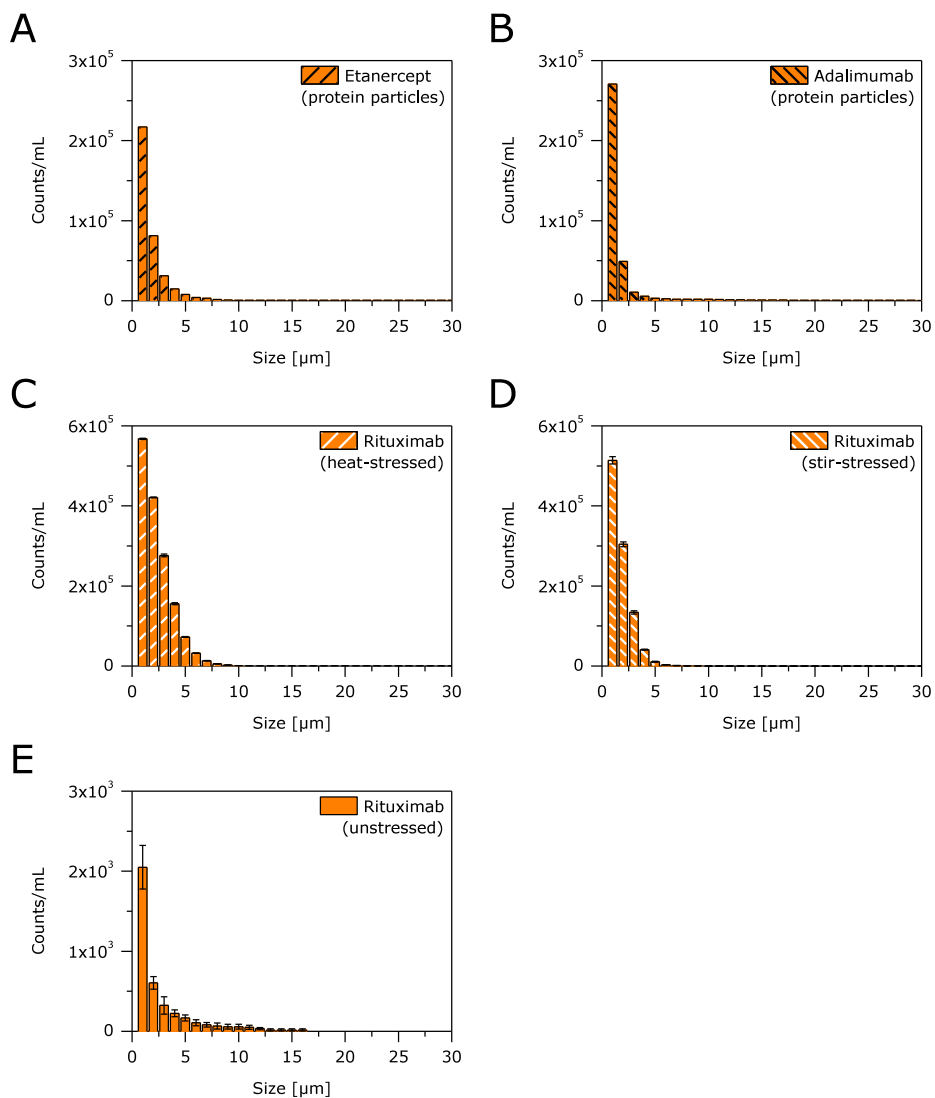
Figure S3: Cumulative size distributions of protein particles determined by MFI and identified by the "find similar" operation for silicone oil droplets (protein particles are identified as the inverse population) in A) Etanercept prefilled syringes, B) Adalimumab prefilled syringes, C) heat-stressed Rituximab, D) stir-stressed Rituximab, E) unstressed Rituximab. Error bars represent standard deviations from triplicate measurements.
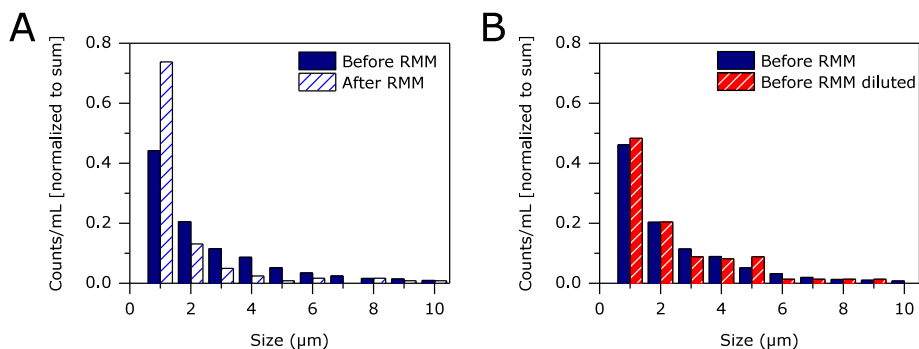
Figure S4: Differential size distribution of a sample containing only silicone oil droplets (0.04% (w/v)) analyzed by MFI, A) before RMM and collected after RMM analysis and B) before and after dilution according to the dilution factor 218 of the sample during RMM analysis. Counts were normalized to the total particle count.
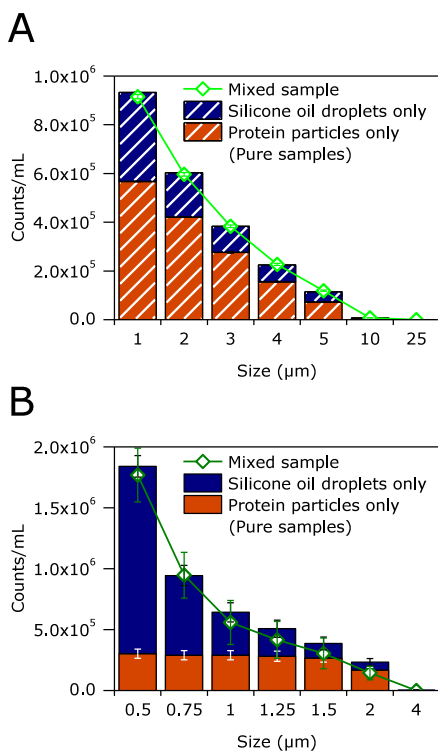

Figure S5: Cumulative counts in individual samples of silicone oil droplets and protein particles (heat-stressed Rituximab) and the corresponding mixture analyzed by A) MFI and B) RMM. Error bars represent standard deviations from triplicate measurements.

CHAPTER 6

FLOW IMAGING MICROSCOPY FOR PROTEIN PARTICLE ANALYSIS – A COMPARATIVE EVALUATION OF FOUR DIFFERENT ANALYTICAL INSTRUMENTS

Sarah Zölls[1,2]*, Daniel Weinbuch[1,3]*, Michael Wiggenhorn[1], Gerhard Winter[2], Wolfgang Friess[2], Wim Jiskoot[3], Andrea Hawe[1]

[1] Coriolis Pharma Research GmbH, Am Klopferspitz 19, 82152 Martinsried-Munich, Germany

[2] Ludwig Maximilian University, Department of Pharmacy, Pharmaceutical Technology and Biopharmaceutics, Butenandtstr. 5-13, 81377 Munich, Germany

[3] Division of Drug Delivery Technology, Cluster BioTherapeutics, Leiden Academic Centre for Drug Research (LACDR), Leiden University, PO Box 9502, 2300 RA Leiden, The Netherlands

[3] Sterile Product and Analytical Development, Merck Research Laboratories, Kenilworth, NJ USA

* shared first authors

Abstract

Flow imaging microscopy was introduced as a technique for protein particle analysis a few years ago and has strongly gained in importance ever since. The aim of the present study was a comparative evaluation of four of the most relevant flow imaging microscopy systems for biopharmaceuticals on the market: MFI4100, MFI5200, FlowCAM VS1, and FlowCAM PV. Polystyrene standards, particles generated from therapeutic monoclonal antibodies, and silicone oil droplets were analyzed by all systems. The performance was critically assessed regarding quantification, characterization, image quality, differentiation of protein particles and silicone oil droplets, and handling of the systems. The FlowCAM systems, especially the FlowCAM VS1, showed high resolution images. The FlowCAM PV system provided the most precise quantification of particles of therapeutic monoclonal antibodies, also under impaired optical conditions by an increased refractive index of the formulation. Furthermore, the most accurate differentiation of protein particles and silicone oil droplets could be achieved with this instrument. The MFI systems provided excellent size and count accuracy (evaluated with polystyrene standards), especially the MFI5200 system. This instrument also showed very good performance for protein particles, also in case of an increased refractive index of the formulation. Both MFI systems were easier to use and appeared more standardized regarding measurement and data analysis as compared to the FlowCAM systems. Our study shows that the selection of the appropriate flow imaging microscopy system depends strongly on the main output parameters of interest and it is recommended to decide based on the intended application

Introduction

Protein aggregates and particles are important quality attributes of therapeutic protein formulations (1–3). Especially micron sized aggregates (subvisible protein particles) (4) are considered as critical due to their potential risk of enhancing an immunogenic response (5). Quantification of (not necessarily proteinaceous) subvisible particles larger than 10 µm and 25 µm in parenterals is required by the pharmacopoeias, and is commonly performed using light obscuration (LO) techniques (6,7). For therapeutic protein products regulatory agencies increasingly ask for quantification and characterization of particles with a size below 10 µm by an orthogonal approach (8,9). Furthermore, the availability of an increasing number of emerging techniques (10,11) extends the spectrum of particle analysis tools and enables a more detailed characterization of the particles counted. These factors inspired the development of a new educational chapter USP<1787> entitled "Measurement of Subvisible Particulate Matter in Therapeutic Protein Injections" (12). It is currently being discussed whether this chapter should include particle analysis starting already from 2 µm as well as the use of additional techniques, such as flow imaging microscopy. Flow imaging microscopy has already been used extensively in research and development (13–19) and more recently also for quality control/routine testing (own experiences). However, it needs to be considered that the calculation of particle size depends on the underlying measurement principle and may differ between LO and flow imaging microscopy. Moreover, comparison of results is influenced by the type of diameter selected for data evaluation and the algorithm that the instrument is using.

Flow imaging microscopy uses a CCD camera with high magnification to capture images of the sample solution passing through a thin flow cell. The flow cell is illuminated and particles with a different refractive index (RI) than the solution decrease the light intensity compared to the background and can be detected on the captured images (20,21). Particle size and count information is then generated based on image analysis. Besides quantification, the digital particle images allow for subsequent morphological characterization including size, shape and optical parameters. This, however, requires sufficiently high image quality to draw reliable conclusions (21). A prominent application example is the differentiation of silicone oil droplets and protein particles in prefilled syringes and cartridges. For this approach, flow imaging microscopy has been successfully applied in several studies (22–24). In general, flow imaging microscopy tends to be more sensitive than LO for small transparent protein particles and therefore usually detects higher particle numbers (13,15,25). An increased RI of the formulation, leading to a decreased RI difference between particles and formulation, can impede a correct

detection of protein particles by light-based techniques. Compared to LO, MFI was shown to be slightly more robust against such a decreased RI difference (13,26).

There are several flow imaging microscopy instruments available on the market provided by different suppliers. Those are, for example, Sysmex Flow Particle Image Analyzer (FPIA) 3000 by Malvern Instruments (Worcestershire, UK), various Occhio Flowcell systems by Occhio (Angleur, Belgium), the MicroFlow Particle Sizing System by JM Canty (Buffalo, New York), several Micro-Flow Imaging (MFI) systems by Protein Simple (Santa Clara, California), and various Flow Cytometer And Microscope (FlowCAM) systems by Fluid Imaging (Yarmouth, Maine). In this study, MFI and FlowCAM systems with different settings were evaluated (Table 1). Both systems are often used for the analysis of subvisible particles in research and development and partly also for routine testing in a QC environment. A short general article about the handling of MFI and FlowCAM is available (27), but no comprehensive report about a direct comparison of the four systems has been published until now.

Here we present the first study thoroughly challenging four of the most relevant flow imaging microscopy systems for biopharmaceuticals on the market: MFI4100 and MFI5200 as well as FlowCAM VS1 and FlowCAM PV. By that we want to provide a basis for the increasing use of such systems in QC and support industry and authorities in their efforts towards new standards in the field of subvisible particle characterization.

Materials & Methods

Materials

Infliximab (Remicade®, lots no. 7GD9301402, 7FD8701601, 7RMKA81402, pooled) and rituximab (MabThera®, lot no. B6082) were provided by local hospitals. Polystyrene particle standards were purchased from Duke Scientific (through Thermo Scientific, Fremont, California) and diluted in water for analysis.

Sucrose, sodium hydroxide, di-sodium hydrogenphosphate dehydrate, and sodium dihydrogenphosphate dihydrate were purchased from Merck KGaA (Darmstadt, Germany). Sodium chloride, sodium citrate dehydrate, and polysorbate 80 were from VWR (Darmstadt, Germany). Silicone oil with a viscosity of 1000 cSt (as listed in the Ph.Eur. monography for silicone oil as a lubricant (24)) was purchased from Sigma Aldrich (Steinheim, Germany). The water used in this study was highly purified water (Advantage A10 purification system, Millipore, Newark, New Jersey).

Sucrose solutions were prepared by dilution (w/w) of a 70% (w/w) solution, filtered using a 0.2-µm cellulose acetate syringe filter (Minisart®, Sartorius Stedim Biotech, Aubagne, France) and air bubbles were removed by centrifugation for 5 minutes at 7,000 g (Centrifuge 5810R, Eppendorf, Hamburg, Germany) prior to use.

Preparation of protein samples

Rituximab solution at a concentration of 1 mg/mL was prepared by dilution of 10 mg/mL rituximab commercial product in 25 mM citrate buffer (pH 6.5) containing 154 mM NaCl and 0.07% polysorbate 80 (formulation buffer). The formulation was filtered using a 0.2 µm polyethersulfone syringe filter (Sartorius, Göttingen, Germany) and kept at 2-8°C for a maximum of one week. Heat-stressed rituximab was prepared by incubating 1.5 mL of the 1 mg/ml rituximab solution for 30 min at 71 °C in a thermomixer (Eppendorf, Hamburg, Germany). Stressed rituximab at 1 mg/mL (protein particles stock suspension) was stored at 2-8°C until the measurement.

Infliximab solution at a concentration of 1 mg/mL was prepared by dilution of 10 mg/mL infliximab commercial product in 100 mM phosphate buffer (pH 7.2). The formulation was filtered through a 0.2-µm polyethersulfone syringe filter. Stir-stressed infliximab was prepared by incubating 8 mL of the 1 mg/mL infliximab solution in a 10R glass vial using a 18-mm Teflon®-coated stir bar at 250 rpm for 24 hours at room temperature on a magnetic stirrer (MR Hei-Standard, Heidolph, Schwabach, Germany).

For analysis of protein samples, stressed protein solution was diluted in the appropriate buffer (filtered through a 0.22-µm cellulose acetate/nitrate membrane filter, MF-Millipore®, Millipore), sucrose solution or water.

Preparation of silicone oil emulsion

Silicone oil was added to filtered formulation buffer in a particle-free 15-mL conical tube to a final concentration of 2% (w/v) to generate an emulsion without additives. After vortexing briefly, silicone oil droplet formation was induced by sonication in a water bath (Sonorex, Brandelin, Berlin, Germany) for 10 min. Fresh silicone oil emulsion (silicone oil droplet stock emulsion) was prepared on the day of the measurement and kept at room temperature.

Table 1: Overview of Technical Parameters and Settings of the Systems Evaluated in this Study

Parameter	Effect on	MFI4100	MFI5200	FlowCAM VS1	FlowCAM PV
Magnification (combination of camera and lens magnification)	Image resolution	14x	5x	200x	100x
Flow cell depth (depth of field)	Sample volume / flow rate Measurement time	100 µm	100 µm	50 µm	80 µm
Focus adjustment	Size accuracy	By screw driver (supported by software)	By screw driver (supported by software)	By turning knob (evaluated optically)[a]	By manufacturer (not adjustable by user)
Size range	-	0.75 – 70 µm	1 – 70 µm	2 – 50 µm[b]	2 – 80 µm[b]
Flow rate	Sampling efficiency, measurement duration	Fixed (0.1 mL/min)	Fixed (0.17 mL/min)	Adjustable (0.005-200 mL/min)[c], (0.07 mL/min in this study)	Adjustable (0.005-20 mL/min)[c], (0.04 mL/min in this study)
Image capture rate	Statistical relevance of the data	Fixed to maximize efficiency and to minimize image overlaps	Fixed to maximize efficiency and to minimize image overlaps	Adjustable (1-22 frames/second) (20 frames/second in this study)	Adjustable (1-22 frames/second) (21 frames/second in this study)
Sampling efficiency	Statistical relevance of the data	Fixed (5-8%)	Fixed (80-85%)	Adjustable (5-8% in this study)	Adjustable (80-85% in this study)
CFR21 part 11 compatibility	GMP suitability	No	Yes	No	Yes

[a] support by software available in the newest generation of the FlowCAM VS1 according to the manufacturer;
[b] official size range as indicated by the manufacturer, lower size limit could be extended to 1 µm in this study;
[c] depending on the syringe size

Preparation of individual and mixed samples of silicone oil droplets and protein particles

Silicone oil droplet stock emulsion and/or protein particles stock suspension was diluted in unstressed protein solution or filtered formulation buffer for the preparation of mixed and individual samples. Mixed samples were prepared in a number ratio of 10:90 based on particle counts > 2 µm determined by MFI4100. Individual samples were prepared to contain the same number of silicone oil droplets and protein particles, respectively, as in the mixed samples and are referred to as the theoretical concentration. All samples were prepared to a final protein concentration of 0.5 mg/mL rituximab. The samples were gently mixed with a pipette, kept at room temperature and measured on the day of preparation.

Refractive index determination

Refractive indices of sucrose solutions were determined using an Abbé refractometer (Carl Zeiss, Oberkochen, Germany). Measurements were performed in triplicate at a wavelength of 589 nm at room temperature and the mean value was calculated.

Light obscuration (LO)

Polystyrene standards were analyzed by light obscuration using a PAMAS SVSS-C (Partikelmess- und Analysesysteme, Rutesheim, Germany) equipped with an HCB-LD-25/25 sensor in order to obtain a reference value for linearity evaluation with polystyrene standards of MFI4100, MFI5200, FlowCAM VS1, and FlowCAM PV. Samples were diluted to a concentration of approx. 10^3 particles/mL as a reference point for the flow imaging microscopy instruments. Three measurements of a volume of 0.3 mL for each sample were performed with a pre-run volume of 0.5 mL at a fixed fill rate, emptying rate and rinse rate of 10 mL/min and the mean particle concentration per mL was reported by the system. Samples were measured in triplicate and mean and standard deviation were calculated.

Micro-Flow Imaging

MFI4100

An MFI4100 system (ProteinSimple) equipped with a 100-µm flow cell, operated at high magnification (14x) and controlled by the MFI View software version 6.9 was used. The system was flushed with 5 mL purified water at maximum flow rate and flow cell cleanliness was checked visually between measurements. Water, the appropriate sucrose solution, filtered unstressed rituximab formulation (0.5 mg/mL) or the appropriate formulation buffer was used to perform "optimize illumination" prior to each

measurement to ensure correct thresholding of the MFI system. Samples of 0.65 mL with a pre-run volume of 0.3 mL were analyzed at a flow rate of 0.1 mL/min and a fixed camera rate (not adjustable by the user) leading to a sampling efficiency of about 5-8%. Samples were measured in triplicate and mean and standard deviation were calculated.

MFI5200

An MFI5200 system (ProteinSimple) equipped with a 100-µm flow cell and controlled by the MFI View System Software (MVSS) version 2-R2.6.1.20.1915 was used. The system was flushed with 10 mL purified water at maximum flow rate and flow cell cleanliness was checked visually between measurements. "Optimize illumination" prior to each measurement was done comparably to MFI4100. Samples of 0.5 mL with a pre-run volume of 0.2 mL were analyzed at a flow rate of 0.17 mL/min and a fixed camera rate (not adjustable by the user) leading to a sampling efficiency of about 80-85%. Samples were measured in triplicate and mean and standard deviation were calculated.

Particle data analysis MFI

For both systems, MFI View Analysis Suite (MVAS) version 1.2 was used for data analysis. Particles stuck to the flow cell wall were only counted once and edge particles were excluded from analysis. Particle size was evaluated as the diameter of a circle with the same projected area as the particle (designated as ECD, equivalent circular diameter, in the MFI software). For the discrimination of silicone oil droplets and protein particles, a minimum of 20 particles (MFI4100) or 50 particles (MFI5200) above 5 µm clearly recognizable as silicone oil droplets was selected for the "find similar" operation in the MVAS software.

FlowCAM analysis

FlowCAM VS1

A FlowCAM VS1 Benchtop B3 system (Fluid Imaging Technologies) was equipped with a 50 µm single-use cell, a 20x magnification lens and controlled by the VisualSpreadsheet software version 3.1.10. A new 50-µm multi-use flow cell was recently introduced, but was not available at the time of the study. The system was flushed with 1 mL purified water at a flow rate of 0.5 mL/min and flow cell cleanliness was checked visually. 0.5 mL sample solution with a pre-run volume of 0.5 mL (primed manually into the flow cell) was analyzed with a flow rate of 0.07 mL/min and a camera rate of 20 frames/s leading to a sampling efficiency of about 5-8%. Only dark pixels were selected for particle size determination at the preset default threshold value of 20. Particle size was evaluated as the diameter of a circle with the same projected area as the particle (designated as ABD, area based diameter, in the FlowCAM software). For the discrimination of silicone oil

droplets and protein particles, a filter can be developed and the parameters can be saved in the software. However, to ensure comparability with the MFI systems and to represent the analysis of a single sample as good as possible, the selection of silicone oil droplets in this study was performed on a sample-by-sample basis. A minimum of 20 particles above 5 µm clearly recognizable as silicone oil droplets was selected for the "find similar as selected" function. Samples were measured in triplicate and mean and standard deviation were calculated.

FlowCAM PV

A FlowCAM PV-100 Benchtop system (Fluid Imaging Technologies) was equipped with a 80-µm multi-use cell, a 10x magnification lens and controlled by the VisualSpreadsheet software version 3.4.2. The system was flushed with 5x1 mL purified water by the flushing function in the software and flow cell cleanliness was accepted if less 10 particles were counted in 0.02 mL of water in the "autoimage mode (no save)". 0.5 mL sample solution with a pre-run volume of 0.2 mL (primed manually into the flow cell) was analyzed with a flow rate of 0.04 mL/min and a camera rate of 21 frames/s leading to a sampling efficiency of about 80-85%. Dark and light pixels were selected for particle size determination at the preset default threshold value of 30. Particle size was evaluated as the diameter of a circle with the same projected area as the particle (designated as ABD, area based diameter, in the FlowCAM software). For the discrimination of silicone oil droplets and protein particles through the "find similar" operation, a minimum of 100 particles above 5 µm clearly recognizable as silicone oil droplets was selected to generate a library. The complete particle population was filtered by the "find similar as library" function. The resulting particle population was sorted by filter score and particles with filter scores of 0 to 5 (with 0 describing images which the highest match to the images in the library) were defined as silicone oil droplets. This procedure was necessary as the software was not able to perform the same "find similar as selected function" as applied for the FlowCAM VS1 which was probably due to the clearly higher number of particles images by the FlowCAM PV. Samples were measured in triplicate and mean and standard deviation were calculated.

Performance evaluation

Critical performance parameters (e.g. image quality, size accuracy, and several other factors as described below) were ranked relatively within the evaluated systems. The system with the strongest performance for one specific parameter was scored as "4" (++++), the system with the weakest performance in this parameter was scored as "1" (+). In detail, the performance was quantified as follows: The image quality parameters were

evaluated by eye. Polystyrene sizing and counting performance was judged with respect to the specifications by the manufacturer (NIST-traceable), linearity was evaluated based on the deviation from the theoretical concentration expected from the dilution factor and the linearity of the obtained concentrations (assessed by the R^2 value). For the robustness towards RI influences, the relative decrease in the measured protein particle concentration in formulations with a higher RI was used for the ranking. The differentiation of silicone oil droplets and protein particles was evaluated based on the match with the theoretical concentration within the system (based on individual samples) and the standard deviation, defined as precision. The rating of handling parameters was based on the personal judgment of the authors.

Results and discussion

Count and size performance with polystyrene standards

The four systems MFI4100, MFI5200, FlowCAM VS1, and FlowCAM PV were first evaluated regarding their size and count performance with monodisperse certified polystyrene standards. All systems determined the correct concentration of a 5 µm polystyrene count standard with 3000 ± 300 particles/mL > 3 µm (Table 2).

Concentration linearity was evaluated with different dilutions of 5-µm polystyrene size standards over a wide range from about $4x10^2$ to $8x10^6$ particles/mL. The obtained concentrations for particles > 3 µm (as specified for the 5-µm count standard) were compared to the theoretical concentration as determined by LO in the low concentration range (4056 particles/mL for the second highest dilution) and calculated for the higher concentrations (Figure 1). All systems showed good overall linearity, but underestimated the particle number at high concentrations (Figure 1A) probably due to coincidence of particles, meaning that two particles which are located very closely next to or behind each other are detected as one particle. For the highest concentration of theoretically $8x10^6$ particles/mL, a measurement was only possible with the MFI4100 and FlowCAM VS1. MFI5200 and FlowCAM PV were not able to handle such high particle concentrations as the measurements were automatically aborted at $1x10^6$ and $5x10^5$ captured particles, respectively. This is due to a software setting limiting the number of captured particles to 500,000 per analysis to ensure proper data handling. The limit can be increased, but this would slow down data processing by the software. For the sample with a theoretical concentration of $4x10^6$ particles/mL, MFI4100, MFI5200, and FlowCAM VS1 underestimated the particle concentration by less than 10%, whereas the FlowCAM PV system detected 25% less particles than actually expected. In the medium concentration

range of theoretically $4x10^3$ to $1x10^6$ particles/mL, all systems showed good results (Figure 1B and C). Whereas the FlowCAM systems slightly underestimated the concentration, the MFI4100 system overestimated the concentration in the case of theoretically $4x10^5$ particles/mL. The MFI5200 system constantly showed deviations from the theoretical concentration of less than 2%. For the lowest concentration of theoretically 406 particles/mL, MFI4100, MFI5200 and FlowCAM PV showed large deviations of 11-28% and only the FlowCAM VS1 system detected the theoretical concentration within 1% (Figure 1C). All systems showed large relative standard deviations in the low concentration range below $4x10^3$ particles/mL (8% for MFI5200, 18% and more for the other systems).

Size accuracy was evaluated with monodisperse polystyrene size standards of 2, 5, and 10 µm. Overall, the MFI systems rendered images of poorer resolution, but better size accuracy as compared with the FlowCAM systems evaluated in this study (Table 2 and Figure 2). The MFI4100 system underestimated the size of the 2 µm polystyrene standards due to resolution limitations for those small particles, but showed satisfying size accuracy for 5 µm and 10 µm as well as a narrow distribution for all sizes (Figure 2A). MFI5200 was the only system that determined all sizes accurately and with a high precision (Figure 2B). The images of size standards obtained by the MFI systems appeared rather blurry, but comparable in size and optical appearance, leading to the observed good size accuracy and precision. In contrast, the images obtained by the FlowCAM systems showed high resolution and sharpness, but also a large variability in size and optical appearance. Especially the FlowCAM VS1 system showed clear deviations from the correct size (Table 2) and also a broad size distribution with apparently more than one population per analyzed size standard (Figure 2C). This is particularly striking for the 10 µm polystyrene standard, for which two apparent populations around 10 µm and 12 µm were detected. The 10 µm peak particles appear to be captured in focus, whereas the 12 µm peak particles appear out of focus as indicated by the concentrical rings. Although the FlowCAM software VisualSpreadsheet is theoretically able to exclude out-of-focus particles, this was not performed as it would compromise the accuracy of the particle concentration and does therefore not represent a suitable option for real protein sample analysis. The FlowCAM PV rendered images of slightly lower resolution, but in return better size homogeneity leading to better size accuracy and precision (Figure 2D). For a mixed sample of 2 µm, 5 µm, and 10 µm polystyrene size standards, the described differences in image quality and homogeneity led to a better separation between the sizes in the MFI systems as compared with the FlowCAM systems (Figure 2A-D, lower panels). The underlying reasons for the differing image quality and homogeneity are assumed to be (i) the magnification and (ii) the depth of focus (Table 1). Furthermore, the threshold value in the

FlowCAM systems influences the size accuracy as there is always a trade-off between size accuracy and image fragmentation.

Image properties

As discussed above, differences in the image properties and especially in the image homogeneity lead to divergences in size determination. Furthermore, the image quality is a crucial parameter for morphological analysis and for a reliable discrimination of different particle types, e.g. proteinaceous vs. non-proteinaceous particles. Therefore, we compared images of polystyrene standards, artificially generated silicone oil droplets, and protein particles (heat-stressed rituximab) (Figure 3). In general, images provided by the FlowCAM systems appeared sharper and of higher resolution than images captured by the MFI systems. This is mainly due to the smaller focus area and higher magnification of the FlowCAM optics. Thus, many morphological details were already visible on particles as small as 5 µm in size, especially for the FlowCAM VS1 system. However, the small focus area caused particles of the same type to appear optically different, which could be well observed on images for polystyrene standards and silicone oil droplets. Dark particles with a bright halo as well as bright particles with a dark edge and several nuances in between were detected within one sample. For protein particles, images captured by the FlowCAM systems appeared more uniform regarding the optical contrast than for polystyrene standards and silicone oil droplets. The MFI4100 system provided comparable images of protein particles. In contrast the images captured by the MFI5200 system appeared more variable, presumably due to its larger view window which results in different illumination of particles depending on their location within the view window. For protein particles, this can lead to a high diversity in the optical appearance due to diffraction patterns within those heterogeneous particles (21). However, it is difficult to judge which instrument displays the real heterogeneity of protein particles as this is not known. The difference in sharpness and resolution between MFI systems and FlowCAM systems was particularly obvious for protein particles with sizes of about 5 µm and 10 µm. Here, FlowCAM images provide more morphological details, whereas MFI images appear rather blurry. Furthermore, the MFI systems capture only pixels of the particle which are darker than the background. In contrast, the FlowCAM systems use a different background calibration procedure allowing the additional depiction of pixels brighter than the background which probably result from specific diffraction patterns (21). This contributes to the enhanced visibility of morphological details but also leads to the heterogeneity in FlowCAM images. Within the brands, the MFI4100 and FlowCAM VS1 captured better images than the MFI5200 and FlowCAM PV.
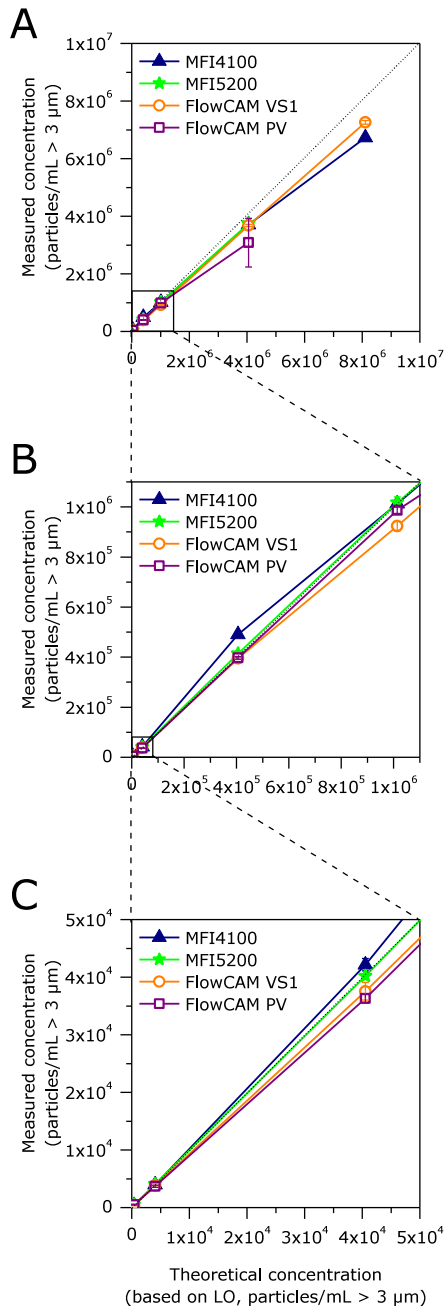
Figure 1: Linearity of particle concentration measurements by MFI4100, MFI5200, FlowCAM VS1, and FlowCAM PV. 5 µm PS standards measured at various dilutions. The theoretical concentrations are based on the counts of the second highest dilution obtained by LO (result: 4056 particles/mL). A) Full concentration range, B) zoom into medium concentrations, C) zoom into low concentrations. Error bars represent standard deviations from triplicate measurements.

Table 2: Results of polystyrene standard measurements with MFI4100, MFI5200, FlowCAM VS1, and FlowCAM PV.

Standard type	Specifications	MFI4100	MFI5200	FlowCAM VS1	FlowCAM PV
5 µm count standard	3000 ± 300 part./mL (> 3 µm)[a]	2906 ± 324 part./mL[c]	3203 ± 116 part./mL[c]	2779 ± 162 part./mL[c]	2974 ± 184 part./mL[c]
2 µm size standard	1.999 ± 0.020 µm[b]	1.74 ± 0.28 µm[d]	1.95 ± 0.35 µm[d]	3.20 ± 1.39 µm[d]	2.38 ± 0.90 µm[d]
5 µm size standard	4.993 ± 0.040 µm[b]	5.10 ± 0.80 µm[d]	5.12 ± 0.57 µm[d]	5.94 ± 1.61 µm[d]	4.66 ± 1.52 µm[d]
10 µm size standard	10.00 ± 0.08 µm[b]	10.56 ± 1.22 µm[d]	10.16 ± 1.16 µm[d]	10.71 ± 2.41 µm[d]	9.66 ± 1.43 µm[d]

[a] Based on light obscuration
[b] Based on microscopy
[c] Standard deviation from three measurements
[d] Full peak width at half of the maximum height

An additional cause of image variability in the FlowCAM systems for polystyrene standards and silicone oil droplets might be the illumination of the flow cell. While the background of an MFI flow cell appears uniformly grey (Supporting information, Figure S1A and B), the background of a FlowCAM flow cell seems to be less evenly illuminated, especially for the FlowCAM VS1 system (Supporting information, Figure S1C and D). This can affect the overall brightness of an image depending on where within the flow cell it was captured. According to the manufacturer, this feature is currently under development for the FlowCAM systems.
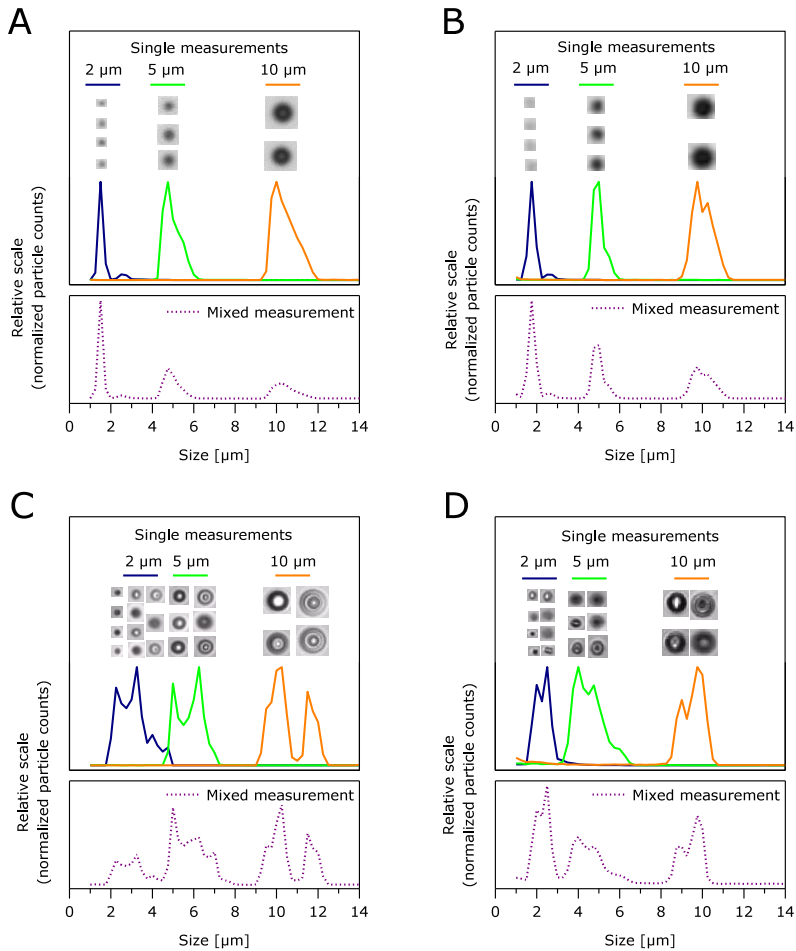
Figure 2: Size accuracy and precision of 2 μm, 5 μm and 10 μm PS size standards measured separately (upper panels) and as a mix (lower panels) by A) MFI4100, B) MFI5200, C) FlowCAM VS1, and D) FlowCAM PV. Representative images are shown above the corresponding peak of the size distribution.

Quantification of protein particles

Because the captured particle images form the basis for particle analysis, a potential correlation between image quality and detected particle numbers was investigated. To this end, protein particles were generated by heating a rituximab formulation and analyzed by the four systems. Due to the time-shifted availability of the FlowCAM systems, the exact same sample could not be analyzed in parallel by all four systems. Instead, one sample was analyzed in parallel by the MFI4100 and FlowCAM VS1 (Figure 4A). Another sample, prepared later under the same conditions, was analyzed in parallel by the MFI5200 and FlowCAM PV as well as by MFI4100 for comparison (Figure 4B). Thus, the

difference in the cumulative size distribution between Figure 4A and 4B can be attributed to the variability in the sample preparation. System-dependent differences can only be evaluated within Figure 4A or within Figure 4B. Although the image resolution for particles below 2 µm was poor and the official lower size limit of the FlowCAM systems is 2 µm, counting of particles could be performed for particles > 1 µm with satisfying data quality for all systems. This has been shown before for the MFI4100 system (26). For the same sample, the FlowCAM VS1 system detected more particles below 3 µm but fewer particles above 3 µm, particularly above 10 µm, as compared with the MFI4100 system.

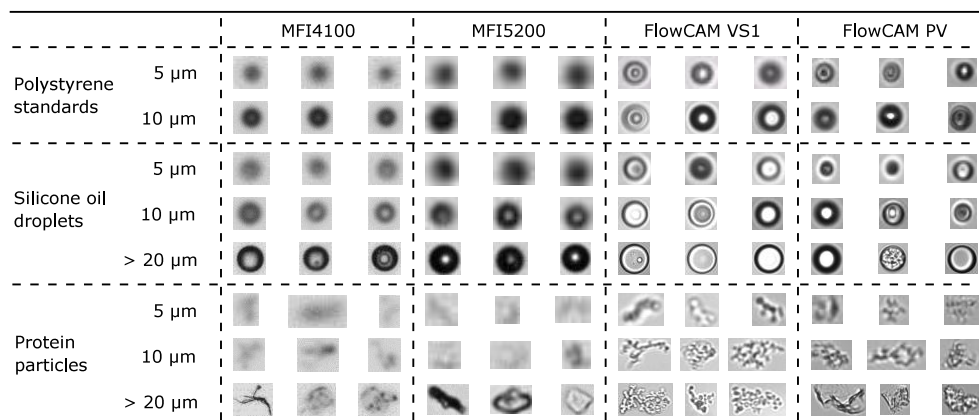|		MFI4100	MFI5200	FlowCAM VS1	FlowCAM PV
Polystyrene standards	5 µm				
	10 µm				
Silicone oil droplets	5 µm				
	10 µm				
	> 20 µm				
Protein particles	5 µm				
	10 µm				
	> 20 µm				

Figure 3: Representative images of polystyrene standards, silicone oil droplets and protein particles (heat-stressed rituximab) of different particle sizes scaled to the same image size.

A possible reason for this might be image fragmentation which was observed for the FlowCAM VS1 when using the setting "only dark particles" (Figure 5). It seems that bright parts of particles were detected as the particle boundary by the software. This effect was observed for particles larger than 10 µm. Although image fragmentation might also have occurred for smaller particles it could not be confirmed by optical evaluation of the images due to resolution limitations. Changing the settings to "dark & light" might have decreased this effect but, as discussed earlier, failed to provide the correct size for polystyrene size standards and was therefore not chosen. This shows again that the user has to accept a certain trade-off between good size accuracy and robustness against image fragmentation for the FlowCAM systems. On the one hand, this brings along certain user-dependency and data variability and there is no optimal setting for all purposes. On the other hand, those many adjustable settings in the FlowCAM systems enable the handling of a specific problem. In contrast, the MFI systems require the trust of the user in the predefined settings which cannot be changed. For the other systems evaluated in this study image fragmentation was not observed for the same samples. However, for an IgG-containing

sample from a different study image fragmentation was observed for the MFI4100 system (data not shown due to confidentiality).
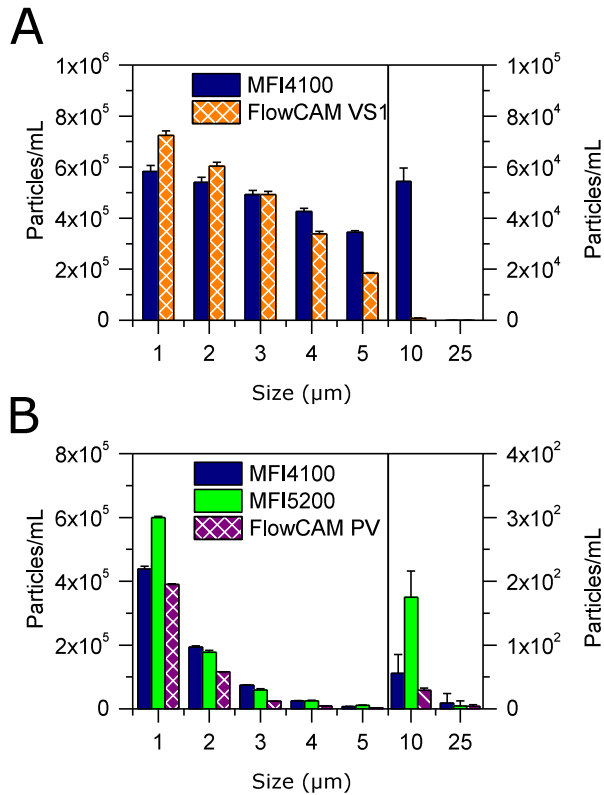

Figure 4: Cumulative particle counts for protein particles of heat-stressed rituximab analyzed by A) MFI4100 and FlowCAM VS1 and B) MFI4100, MFI5200, and FlowCAM PV. Error bars represent standard deviations from triplicate measurements.

For the second sample analyzed, MFI5200 and FlowCAM PV detected similar size distributions with slightly less particles detected by the FlowCAM PV system (Figure 4B). Clearly more small particles larger than 1 µm were detected by the MFI5200 system, pointing on the one hand towards a better sensitivity for small transparent particles, on the other hand potentially also towards undetected image fragmentation. For the FlowCAM PV system it needs to be considered that the official size range of this system starts only at 2 µm and was extended consciously in this study. For total particle concentrations larger than 2 µm, similar concentrations were detected by all three systems. The difference for particles larger than 10 µm is probably due to the low total number in this size range causing higher standard deviations. In general, the MFI5200 and

FlowCAM PV showed lower standard deviations for total particle counts larger than 1 µm as compared with the MFI4100 and FlowCAM VS1, as could be expected from the differences in the analyzed volume.

It was shown earlier that light-based quantification of protein particles is influenced by the RI of both, particles and surrounding formulation and that this effect is partly system dependent (26). Therefore, the robustness of MFI4100, MFI5200, and FlowCAM PV towards RI influences was determined by quantifying protein particles larger than 1 µm (stir-stressed infliximab) in the same concentration in formulations of increasing RI, adjusted by addition of sucrose (Figure 6). The FlowCAM VS1 system was not available at the time of these experiments. Particle concentrations obtained by MFI4100 were rather sensitive to an increase in RI of the formulation. In 20% sucrose (RI 1.36), 80% of the original particle concentration was still detected whereas in 50% sucrose (RI 1.42), only 25% could be detected. MFI5200 and FlowCAM PV were both more robust towards RI influences: in 20% sucrose, 93% and 89% of the original particle concentration, respectively, were still detected and in 50% sucrose the apparent concentration decreased only to 54% and 69% with MFI5200 and FlowCAM PV, respectively. The reason for the superior performance of MFI5200 and FlowCAM PV is potentially connected to optimized optical settings of these newer systems. Two different control experiments in a previous study have shown that the particle concentration was not affected directly by the high sucrose concentration, e.g. by dissolution or generation of particles (26). Instead, the decreased RI difference between particles and surrounding formulation reduced the apparent particle concentration. The RI of a 20% sucrose solution (1.36) represents pharmaceutically relevant conditions, e.g. at high protein concentration or a combination of excipients such as sucrose and high protein concentration (26).
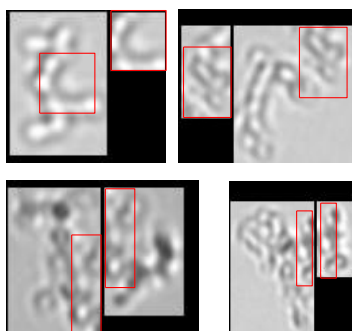

Figure 5: Images of protein particles around 10 µm (heat-stressed rituximab) captured by the FlowCAM VS1 system. Red boxes indicate overlapping or doubly imaged regions in two separate images due to image fragmentation.

Differentiation of silicone oil droplets and protein particles

A major advantage of flow imaging microscopy as compared with other analytical techniques for subvisible particles, e.g. LO or electrical sensing zone analysis, is the possibility to characterize particles based on images (10). Parameters such as shape and transparency can be used to differentiate between different particle types by mathematical filters (22,23). In this context, the discrimination of silicone oil droplets and protein particles is especially relevant due to the increasing application of prefilled syringes. Similar to a previous study protein particles (heat-stressed rituximab) and silicone oil droplets were generated to represent particles and droplets in marketed products (22). The samples were analyzed by MFI4100, MFI5200, FlowCAM VS1, and FlowCAM PV as individual samples (to obtain the theoretical concentration within the same system) and in controlled mixtures. The "find similar" algorithm in the respective software was used to differentiate between silicone oil droplets and protein particles. Due to the time-shifted availability of the FlowCAM systems, the exact same sample could not be analyzed in parallel by all four systems. Instead, one group of samples was analyzed in parallel by the MFI4100 and FlowCAM VS1 (Figure 7A and C). Another group of samples which was prepared later under the same conditions was analyzed in parallel by the MFI5200 and FlowCAM PV (Figure 7B and D). The concentration was adjusted in such a way that similar total particle counts larger than 1 µm were obtained for both groups of samples with the MFI4100 as the bridging instrument. However, the relative size distribution for protein particles differed clearly between the two sample groups. Thus, the differentiation performance was evaluated within the systems, but not between the systems. The evaluation was based on the match of the detected concentration (in mixed samples) and the theoretical concentration (in individual samples) within each system. The theoretical concentration may differ from system to system and is only valid for the mixed samples analyzed by the same system. Although an optical discrimination of silicone oil droplets and protein particles based on the particle images, which is the basis for the "find similar" operation, was only reasonable for particles of 5 µm and larger, the "find similar" function of the software was able to differentiate particles down to 2 µm.

The FlowCAM PV system showed the best match with the theoretical concentration, thus the best differentiation of silicone oil droplets and protein particles (Figure 7D). The MFI5200 and FlowCAM PV (Figure 7B and D) showed a higher precision than the MFI4100 and FlowCAM VS1 (Figure 7A and C). Overall, the FlowCAM systems (Figure 7C and D) showed better differentiation accuracy than the MFI systems (Figure 7A and B), probably due to the higher image quality. However, the differences were rather small and results might depend on the specific sample properties. In conclusion, all systems proved to be

suitable for the differentiation of silicone oil droplets and protein particles from 2 to 10 μm. For particles below 2 μm, alternative techniques such as resonant mass measurement (RMM) can be beneficial (22). For particles larger 10 μm, it is recommended independently of the system to differentiate particles by optical evaluation of the images rather than by applying the "find similar" function. This approach is feasible due to the clear images and usually low particle counts in this size range.
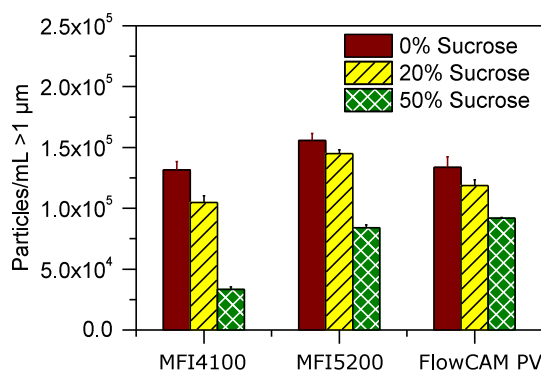

Figure 6: Total particle counts for protein particles of stir-stressed infliximab for fixed particle concentrations in sucrose solutions of varying concentration and thus RI. Error bars represent standard deviations from triplicate measurements.

Handling of the systems

Concerning the hardware, MFI systems only allow the adjustment of the sample volume. This ensures standardized, user-independent measurements and repeatable results, but requires full trust in the settings predefined by the manufacturer, which cannot be customized to specific needs or samples. In contrast, the FlowCAM systems allow changes in optical settings (e.g. threshold, shutter and gain) or technical settings (flow rate, image capture rate) offering customization of the analysis to specific needs for experienced users, but impede comparability between samples analyzed by different operators, at different times or even by different instruments of the same type.

The exchange of a flow cell, which requires the adjustment of the focus as a critical parameter for image-based particle analysis, is straightforward and unambiguous for the MFI systems. For the FlowCAM systems, especially the FlowCAM VS1, this process was found to be cumbersome but this is currently being improved by the manufacturer. Furthermore, the MFI systems use a peristaltic pump enabling high flow rates and large volumes which is useful for an efficient cleaning step, but the flow rate needs to be calibrated regularly. The FlowCAM systems for small volumes (as applicable for protein samples) are typically equipped with a syringe pump, which does not require calibration

by the user, but is restricted in volume and speed limited by the flow cell diameter. Thus, cleaning cycles with FlowCAM need to be performed several times with low volume and flow rate, especially in case of small syringe sizes.
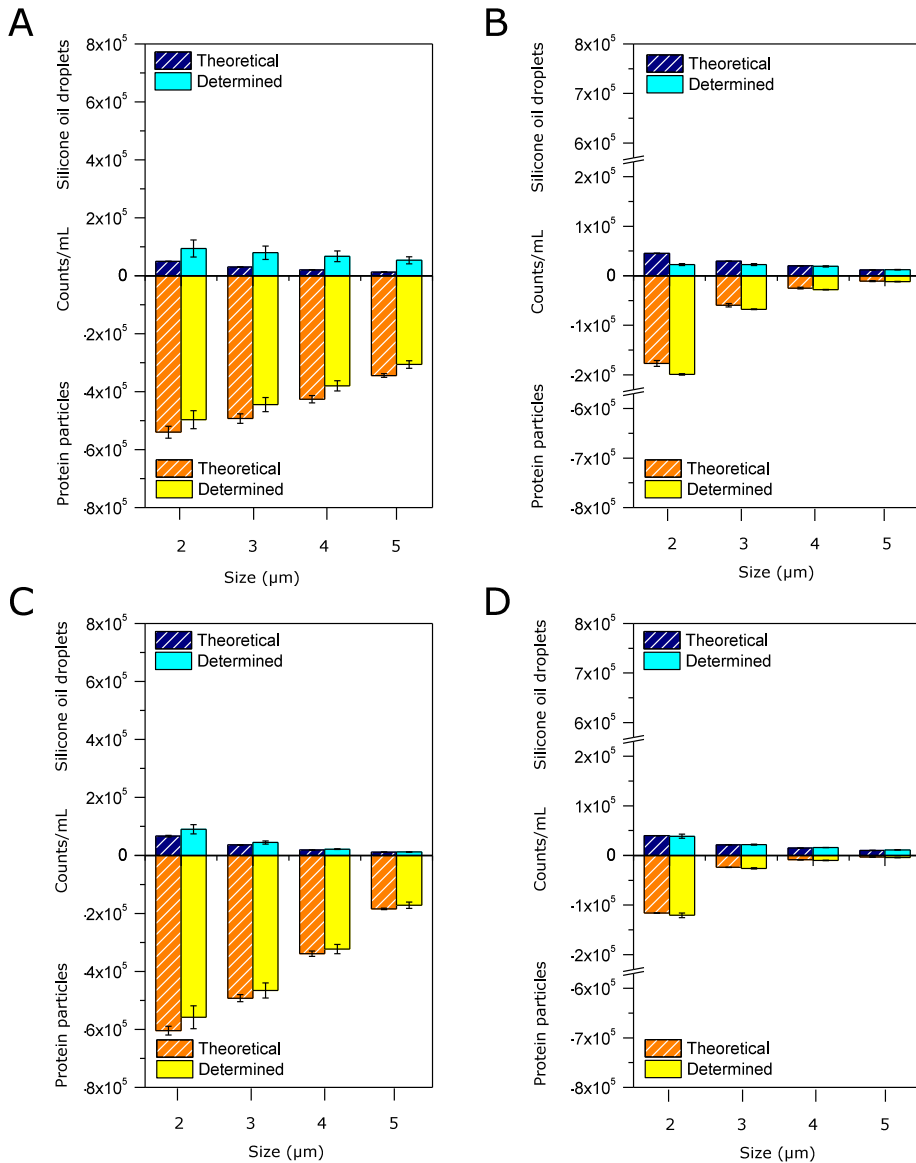
Figure 7: Cumulative particle counts comparing theoretical concentrations (based on individual samples measured with the corresponding instrument) and determined concentrations (mixed samples) of artificially generated silicone oil droplets and protein particles (heat-stressed rituximab) in a droplet/particle ratio of 10:90 (based on particle counts > 2 μm with MFI4100). A) MFI4100, B) MFI5200, C) FlowCAM VS1, D) FlowCAM PV. Error bars represent standard deviations from triplicate measurements.

127

Concerning the software, the MFI systems use different software types for the measurement (MFI View software for MFI4100, MVSS for MFI5200) and the data analysis (MVAS), whereas the FlowCAM systems apply the same software for both steps (VisualSpreadsheet). While the latter allows the analysis of the particle population, regarding size distribution and cropped images, already during the measurement as a real time analysis, this data becomes available only after the measurement for the MFI systems. However, the MVAS software includes an essential function to "remove stuck particles" (particles stuck to the flow cell wall which would otherwise be counted on every image they were captured on). This option is not yet available for VisualSpreadsheet but is currently under development. In both software solutions, particle data can be exported in many different ways and the raw data of every single particle (e.g. shape or transparency values) is available. MVAS enables export of single particle images, whereas VisualSpreadsheet offers collages of particle images. Regarding the differentiation of silicone oil droplets and protein particles, the analysis of a single sample is simpler in MVAS, while VisualSpreadsheet enables the generation of libraries from selected particles, which can be used to build a filter for future samples. In addition, VisualSpreadsheet offers the possibility to sort the resulting population of similar particles by "filter score", i.e. by similarity to the selected particles. Taken together, MFI systems are more standardized, whereas FlowCAM systems are designed for more flexibility for the user, concerning both hardware and software.

Conclusions

Our study showed that the selection of the appropriate flow imaging microscopy system depends strongly on the main output parameters of interest and the intended application. Each system shows its strengths and weaknesses in different aspects (Table 3). We categorized the four systems evaluated in this study based on the technical data and the results obtained in this study into high-resolution systems (MFI4100 and FlowCAM VS1, because of higher image quality, but lower sampling efficiency) and high-efficiency systems (MFI5200 and FlowCAM PV, because of slightly lower image quality, but higher sampling efficiency as compared to the corresponding system from the same manufacturer). The best images were obtained by the FlowCAM VS1 system, which was seen as the best system among the high-resolution instruments. The best performance regarding particle counting accuracy and precision was achieved by the MFI5200 system, which appeared to be the preferred system among the high-efficiency instruments. The MFI4100 and the FlowCAM PV system were observed as all-round systems which might be a good compromise between the other two systems that are more biased towards particle counting (MFI5200) or particle imaging (FlowCAM VS1).

Table 3: Results of polystyrene standard measurements with MFI4100, MFI5200, FlowCAM VS1, and FlowCAM PV.

Parameter		MFI4100	MFI5200	FlowCAM VS1	FlowCAM PV
Image properties	Resolution	++	+	++++	+++
	Contrast within the particle	+	++	++++	+++
	Image consistency (standards)	++++	++++	+	+
Polystyrene size	Accuracy	+++	++++	+	++
	Precision	+++	++++	+	++
Polystyrene count	Accuracy	+++	++	+	++++
	Precision	+	++++	+++	++
	Linearity	++	++++	++++	+
Protein Particle quantification	Precision	+	+++	+	++++
	Robustness against RI influences	++	+++	n.a.	++++
Differentiation of silicone oil droplets and protein particles	Match with the theoretical concentration	+	++	+++	++++
	Precision	+	+++	++	++++
Handling	Hardware	+++	++++	+	++
	Software for measurement	++++	+++	+	++
	Software for data analysis	++++		+++	

+++ + = strongest performance;

+++ = second strongest performance;

++ = third strongest performance;

+ = weakest performance; all criteria were judged only relatively among the evaluated systems.

Acknowledgements

References

1. Carpenter JF, Randolph TW, Jiskoot W, Crommelin DJA, Middaugh CR, Winter G, et al. Overlooking subvisible particles in therapeutic protein products: gaps that may compromise product quality. J Pharm Sci. 2009 Apr;98(4):1201–5.

2. Carpenter J, Cherney B, Lubinecki A, Ma S, Marszal E, Mire-Sluis A, et al. Meeting report on protein particles and immunogenicity of therapeutic proteins: filling in the gaps in risk evaluation and mitigation. Biologicals. 2010 Sep;38(5):602–11.

3. Hawe A, Wiggenhorn M, van de Weert M, Garbe JHO, Mahler H-C, Jiskoot W. Forced degradation of therapeutic proteins. J Pharm Sci. 2012 Mar;101(3):895–913.

4. Narhi LO, Schmit J, Bechtold-Peters K, Sharma D. Classification of protein aggregates. J Pharm Sci. 2012 Feb;101(2):493–8.

5. Rosenberg AS. Effects of protein aggregates: an immunologic perspective. AAPS J. 2006 Jan;8(3):E501–7.

6. Ph.Eur. 2.9.19. General, particulate contamination: sub-visible particles. In: The European Pharmacopoeia,. 7th ed. 2011.

7. USP <788>. Particulate Matter in Injections. In: The United States Pharmacopoeia, National Formulary. 2009.

8. Kirshner LS. Regulatory expectations for analysis of aggregates and particles. In: Colorado Protein Stability Conference. Breckenridge, CO; 2012.

9. Guidance for Industry: Immunogenicity Assessment for Therapeutic Protein Products. Biotechnol Law Rep. 2013 Jun;32(3):172–85.

10. Zölls S, Tantipolphan R, Wiggenhorn M, Winter G, Jiskoot W, Friess W, et al. Particles in therapeutic protein formulations, Part 1: overview of analytical methods. J Pharm Sci. 2012 Mar;101(3):914–35.

11. Burg TP, Godin M, Knudsen SM, Shen W, Carlson G, Foster JS, et al. Weighing of biomolecules, single cells and single nanoparticles in fluid. Nature. 2007 Apr 26;446(7139):1066–9.

12. Narhi LO. AAPS update on USP expert committee for Sub visible particle analysis. Newsletter of the AAPS Aggregation and Biological Relevance Focus Group. 2012;3(2).

13. Demeule B, Messick S, Shire SJ, Liu J. Characterization of particles in protein solutions: reaching the limits of current technologies. AAPS J. 2010 Dec;12(4):708–15.

14. Sharma DK, Oma P, Pollo MJ, Sukumar M. Quantification and characterization of subvisible proteinaceous particles in opalescent mAb formulations using micro-flow imaging. J Pharm Sci. 2010 Jun;99(6):2628–42.

15.   Wuchner K, Büchler J, Spycher R, Dalmonte P, Volkin DB. Development of a microflow digital imaging assay to characterize protein particulates during storage of a high concentration IgG1 monoclonal antibody formulation. J Pharm Sci. 2010 Aug;99(8):3343–61.

16.   Joubert MK, Luo Q, Nashed-Samuel Y, Wypych J, Narhi LO. Classification and characterization of therapeutic antibody aggregates. J Biol Chem. 2011;286(28):25118–33.

17.   Barnard JG, Babcock K, Carpenter JF. Characterization and quantitation of aggregates and particles in interferon-β products: Potential links between product quality attributes and immunogenicity. J Pharm Sci. 2013;102(3):915–28.

18.   Barnard JG, Singh S, Randolph TW, Carpenter JF. Subvisible particle counting provides a sensitive method of detecting and quantifying aggregation of monoclonal antibody caused by freeze-thawing: Insights into the roles of particles in the protein aggregation pathway. J Pharm Sci. 2011;100(2):492–503.

19.   Patel AR, Lau D, Liu J. Quantification and Characterization of Micrometer and Submicrometer Subvisible Particles in Protein Therapeutics by Use of a Suspended Microchannel Resonator. Anal Chem. 2012 Jul 13;84(15):6833–40.

20.   Sharma DK, King D, Oma P, Merchant C. Micro-flow imaging: flow microscopy applied to sub-visible particulate analysis in protein formulations. AAPS J. 2010 Sep;12(3):455–64.

21.   Brown L. Characterizing Biologics Using Dynamic Imaging Particle Analysis. Suppl to BioPharm Int. 2011;August:4–9.

22.   Weinbuch D, Zölls S, Wiggenhorn M, Friess W, Winter G, Jiskoot W, et al. Micro-flow imaging and resonant mass measurement (archimedes) - complementary methods to quantitatively differentiate protein particles and silicone oil droplets. J Pharm Sci. 2013;102(7):2152–65.

23.   Strehl R, Rombach-Riegraf V, Diez M, Egodage K, Bluemel M, Jeschke M, et al. Discrimination between silicone oil droplets and protein aggregates in biopharmaceuticals: a novel multiparametric image filter for sub-visible particles in microflow imaging analysis. Pharm Res. 2012 Feb;29(2):594–602.

24.   Sharma D, Oma P, Krishnan S. Silicone Microdroplets in Protein Formulations - Detection and Enumeration. Pharm Technol. 2009;33(4):74–9.

25.   Huang C-T, Sharma D, Oma P, Krishnamurthy R. Quantitation of protein particles in parenteral solutions using micro-flow imaging. J Pharm Sci. 2009 Sep;98(9):3058–71.

26.   Zölls S, Gregoritza M, Tantipolphan R, Wiggenhorn M, Winter G, Friess W, et al. How subvisible particles become invisible-relevance of the refractive index for protein particle analysis. J Pharm Sci. 2013 Mar 5;102(5):1434–46.

27.   Wilson GA, Manning MC. Flow imaging: Moving toward best practices for subvisible particle quantitation in protein products. J Pharm Sci. 2013;102(3):1133–4.
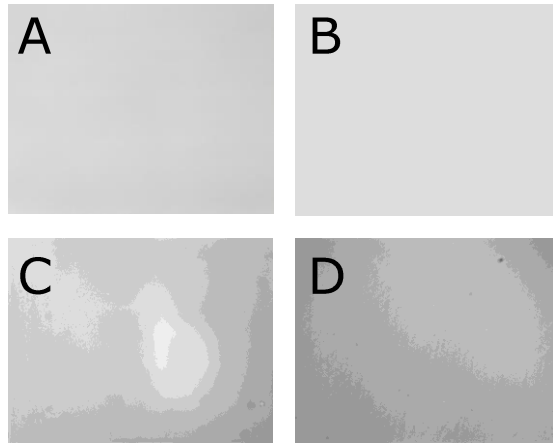
Supplementary information

Figure S1: Images of a clean flow cell (purged with water) in A) MFI4100, B) MFI5200, C) FlowCAM VS1, and D) FlowCAM PV.

CHAPTER 7

NANOPARTICULATE IMPURITIES IN PHARMACEUTICAL-GRADE SUGARS AND THEIR INTERFERENCE WITH LIGHT SCATTERING-BASED ANALYSIS OF PROTEIN FORMULATIONS

Daniel Weinbuch[1,2], Jason K. Cheung[3], Jurgen Ketelaars[4], Vasco Filipe[5], Andrea Hawe[1], John den Engelsman[4], Wim Jiskoot[1,2]

[1] Coriolis Pharma Research GmbH, Am Klopferspitz 19, 82152 Martinsried-Munich, Germany

[2] Division of Drug Delivery Technology, Cluster BioTherapeutics, Leiden Academic Centre for Drug Research (LACDR), Leiden University, PO Box 9502, 2300 RA Leiden, The Netherlands

[3] Sterile Product and Analytical Development, Merck Research Laboratories, Kenilworth, NJ USA

[4] Analytical Development and Validation, Biologics Manufacturing Sciences and Commercialisation, Merck Manufacturing Division, MSD, 5342 CC Oss, The Netherlands

[5] Analytical Department, Adocia, 69003 Lyon, France

Abstract

Purpose. In the present study we investigated the root-cause of an interference signal (100-200 nm) of sugar-containing solutions in dynamic light scattering (DLS) and nanoparticle tracking analysis (NTA) and its consequences for the analysis of particles in biopharmaceutical drug products.

Methods. Different sugars as well as sucrose of various purity grades, suppliers and lots were analyzed by DLS and NTA before and (only for sucrose) after treatment by ultrafiltration and diafiltration. Furthermore, Fourier transform infrared (FTIR) microscopy, scanning electron microscopy coupled energy-dispersive X-ray spectroscopy (SEM-EDX), and fluorescence spectroscopy were employed.

Results. The intensity of the interference signal differed between sugar types, sucrose of various purity grades, suppliers, and batches of the same supplier. The interference signal could be successfully eliminated from a sucrose solution by ultrafiltration (0.02 μm pore size). Nanoparticles, apparently composed of dextrans, ash components and aromatic colorants that were not completely removed during the sugar refinement process, were found responsible for the interference and were successfully purified from sucrose solutions.

Conclusions. The interference signal of sugar-containing solutions in DLS and NTA is due to the presence of nanoparticulate impurities. The nanoparticles present in sucrose were identified as agglomerates of various impurities originating from raw materials.

Introduction

The safety and efficacy of a therapeutic protein depends in part on its chemical and physical stability. Degradation, such as aggregation, of a therapeutic protein can reduce the availability of the protein's active form, can negatively affect its pharmacokinetic properties and might cause adverse effects, such as unwanted immunogenicity (1–3). To enhance the chemical and physical stability of a protein therapeutic, biopharmaceutical drug products contain a combination of specific formulation additives to ensure the chemical and physical stability of the therapeutic protein.

Among the many known excipients sugars, in particular sucrose and trehalose are employed, because they are preferentially excluded from the protein's surface, thus, increasing the free energy of the system and thereby promoting conformational stability (4–6). Examples of sugar-containing products on the market are amongst others Enbrel®, Avastin® and Stelara®. Sugars are also extensively used for lyophilized protein formulations as cryoprotectors and lyoprotectors, e.g., Herceptin®, Serostim® and Remicade (7). As with all reagents that are approved for the use in pharmaceutical drug products, testing procedures and purity criteria of sugars are defined and regulated by the respective pharmacopeias.

Throughout the development of a therapeutic protein and its respective drug product, particle analysis is performed to assess product quality and protein stability. This practice has received increasing attention during the past few years and dynamic light scattering (DLS) became a commonly applied tool for this task in various phases of development, e.g., formulation screening, real-time or accelerated stability studies, and forced degradation studies. The value of DLS analysis comes from its wide size range it covers (from about a nanometer to several micrometers), the fast and easy performance, and its high sensitivity towards larger species, such as protein aggregates and particles (8,9). Despite its advantages, however, the analysis can be disturbed by the presence of certain excipients, which scatter light in the relevant size range, such as polysorbate micelles or sugar molecules. Sugar molecules have, according to the literature, a size of about 0.5 and 1 nm for mono- and disaccharides, respectively (10). Interestingly, however, a second signal appearing at around 100-200 nm was consistently found when sugar-containing formulations were analyzed by DLS. In 2007, Kaszuba *et al.* explained the presence of this second signal as to be "probably due to collective diffusion of the sucrose molecules" (11). Ever since, academic and industrial researchers have referred to this signal as the intrinsic phenomenon of sugar interference with DLS. Importantly, this interference marks a big challenge for DLS when analyzing biopharmaceutical drug products, because of difficulties in assessing the formation of aggregates and particles in presence of a permanent signal at

100-200 nm. It further impairs the ability to compare the stability of a protein formulated with different sugars or varying sugar content, e.g., during formulation development. Surprisingly and despite all these issues, the origin of this interference was never truly investigated.

Therefore, the present study was designed to understand the root-cause of the sugar interference with DLS, and its consequences for the analysis of particles in biopharmaceutical drug products. While all tested sugars (sucrose, trehalose, fructose, maltose and galactose) exhibit an interference phenomenon, we show on the example of sucrose that the interference is caused by the presence of actual nanoparticles, which dramatically differ in amount, but less so in size, between suppliers and between batches of the same supplier. A detailed characterization of these particles identified them as impurities originating from raw materials that are not completely removed during the refinement process. The quantities of nanoparticles present in pharmaceutical-grade sucrose were found to be up to 10^9 particles per gram, while the product still can fulfill all requirements set by the current U.S. and European pharmacopeias.

Materials & Methods

Materials

Lysozyme was purchased from Fluka (Buchs, Germany) and a humanized monoclonal antibody of isotype IgG1 (12) was used to model a therapeutic protein. Sucrose was purchased from Sigma (Taufkirchen, Germany), Merck (Darmstadt, Germany), Caelo (Hilden, Germany), VWR (Bruchsal, Germany), and donated by Südzucker (Mannheim, Germany). PVDF syringe filters with a pore size of 0.2 and 0.1 µm were obtained from Millipore (Schwalback, Germany), Anotop syringe filters with a pore size of 0.02 µm were obtained from GE Life Science (Freiburg, Germany).

Sample preparation

All saccharides were dissolved in Milli-Q® water (Millipore) at stated concentrations in percent weight per volume (% w/v). Protein (IgG or lysozyme) was dissolved in a 7% sucrose solution to achieve the desired concentrations. If not stated differently, all solutions were filtered through a 0.2-µm PVDF syringe filter.

Diafiltration

A Minimate II Tangential Flow Filtration (TFF) system (Pall, Crailsheim, Germany) equipped with a 30 kDa TFF capsule (Pall) was used to perform diafiltration on 700 mL of an aqueous

sucrose G solution (50% w/v). Diafiltration against Milli-Q® water was performed until the permeate volume reached 14 times the feed volume. The last filtrate volume was analyzed by DLS and did not show any residual sucrose peaks. The residual sucrose monomer concentration after diafiltration c_{DF} was calculated as 0.3 mg/L, according to Equation 1:

$$c_{DF} = c_I \cdot e^{-N}$$
Equation 1

where c_I is the initial sucrose monomer concentration, N the number of diavolumes, and where no retention of the sucrose monomer by the TFF membrane is assumed. Subsequently, the retenate was concentrated by first using TFF and then 10-kDa centrifugal filter-units (Amicon Ultra 15, Millipore) to a final volume of ca. 0.8 mL. As a control, Milli-Q® water without the addition of sucrose was treated the same way.

Dynamic light scattering (DLS)

DLS measurements were performed with a Zetasizer Nano ZS system (Malvern, Herrenberg, Germany) equipped with a 633 nm He-Ne laser. The scattered light was detected by using non-invasive backscatter detection at an angle of 173°. A sample volume of 500 µL was analyzed in single-use polystyrene semi-micro cuvettes with a path length of 10 mm (Brand, Wertheim, Germany). The Dispersion Technology Software version 6.01 was used for data collection and analysis. If not stated differently, the measurements were made with an automatic attenuator and a controlled temperature of 25 °C. The intensity size distribution, Z-average diameter, derived count rate, and polydispersity index were calculated from the autocorrelation function obtained in 'general purpose mode'. Each sample was measured in triplicate.

Nanoparticle tracking analysis (NTA)

NTA was performed with a NanoSight LM20 (NanoSight, Amesbury, UK). The instrument was equipped with a 405 nm blue laser, a sample chamber and a Viton fluoroelastomer O-ring. If sample dilution was necessary to achieve an optimal concentration for NTA, Milli-Q® water was used as a diluent and all results were calculated back to the original concentration. Samples were loaded into the sample chamber by using a 1-mL syringe and a pre-run volume of 0.5 mL. Samples were analyzed in triplicate at a stopped flow, while 0.1 mL was flushed through the chamber between each repetition. The NTA 2.3 software was used for capturing and analyzing the data. Movements of the particles in the samples were recorded as videos for 60 s, while the shutter and gain settings of the camera were set automatically by the software for an optimal particle resolution.

UV-spectroscopy

UV-spectroscopy was performed in UV-transparent 96-well plates (Corning Incorporation, NY, USA) by using a Tecan Safire^2 plate reader (Tecan Austria GmbH, Grödig, Austria). For each data point, 200 µL of sample was measured in triplicate, each measurement being an average of 20 reads.

Fluorescence spectroscopy

Fluorescence spectroscopy was performed in black 96-well plates (Corning Incorporation, NY, USA) by using a Tecan Safire^2 plate reader (Tecan Austria GmbH, Grödig, Austria). Excitation and emission of a 200-µL sample were 3D-scanned in triplicate, each measurement being an average of 20 reads from 250 − 460 nm and 290 − 600 nm, respectively.

Scanning electron microscopy coupled energy-dispersive X-ray spectroscopy (SEM-EDX)

SEM-EDX measurements were performed with a Jeol JSM-6500F instrument (Jeol, Tokyo, Japan) equipped with a silicon drift detector (Oxford Instruments, Abingdon, U.K.). For preparation 90 µL of each sample was dried under vacuum and at room temperature on top of a sterile plastic coverslip (Nunc Thermo Scientific, Schwerte, Germany), which was fixed onto a SEM-sample holder with an electrically conducting double-sided tape (Plano, Wetzlar, Germany). A self-sticking copper band (Plano) was used to electrically connect the sample surface to the sample holder base. The sample surface was then carbon-coated by using a Bal-Tec MED-020 carbon evaporator (Bal-Tec, Wetzlar, Germany).

Fourier transform infrared microscopy (FTIR)

FTIR measurements were performed on dried samples with a Bruker Hyperion 3000 FTIR microscope equipped with an attenuated total reflection (ATR) objective (Bruker Optics, Ettlingen, Germany) operated by the Bruker Opus 6.5 software. Samples were dried and prepared as described for SEM-EDX analysis, but without the application of a copper band and without carbon coating.

Results

Various sucrose products (Table 1) were analyzed as 10% solutions by DLS and all showed two distinct peaks in the intensity-weighted size distribution (Figure 1A). The position of the first peak correlates to the literature value for the hydrodynamic diameter of a sucrose molecule in water of 0.98 nm (10). The second peak showed its intensity

maximum at ca. 100 to 200 nm for all samples except sucrose C, for which the peak appeared at about 1900 nm. The relative intensity area under the curve (AUC) of this signal varied considerably between samples, ranging from 8.3% for sucrose C to 60.3% for sucrose A, while differences were observed between purity grades, suppliers, and also between batches of the same supplier (Table 1). Also in NTA, a signal at about 100-200 nm was detected with little variation in size distribution but high variations in particle concentration between products (Figure 1B and Table 1). Furthermore, an increase in concentration of sucrose A in water resulted in a linear increase in nanoparticle concentration determined by NTA, while a water control did not show any particles (Figure 1C). Furthermore, the size distribution did not change with increasing sucrose concentration. Additionally, triplicate sample preparations analyzed by DLS and NTA showed high repeatability (data not shown).

IgG and lysozyme formulated at various concentrations in 7% sucrose A solutions were analyzed by DLS. At an IgG concentration of 0.1 mg/mL, the signal from the sucrose molecule (1 nm), the IgG (14 nm) and the 100-200 nm signal were visible (Figure 1D, upper panel). At 1 mg/mL, the 100-200 nm signal disappeared and at 5 mg/mL also the sucrose signal (1 nm) vanished, leaving only the signal from the IgG. For lysozyme (Figure 1D, lower panel), the 100-200 nm signal was detected in presence of all tested protein concentrations (0.1-5 mg/mL), while the signal of the sucrose molecule and lysozyme likely overlapped at about 1-2 nm because of the poor resolution of DLS (13).

Solutions of sucrose B were filtered through filters with decreasing pore size and subsequently analyzed by DLS and NTA (Figure 2A and B). Filtering the solutions through a 0.1-μm filter had a small effect on the size, and little to no effect on the intensity of the 100-200 nm signal. However, filtration through a 0.02-μm filter decreased the signal in both DLS and NTA to background levels and the signal did not reappear after incubation of the filtered sample for 4 days at 25°C (T1). Moreover, it was possible to eliminate the signal from the sucrose monomer peak in a sucrose G solution by using diafiltration (Figure 2C). The purified retentate (before concentrating) maintained a stable size distribution and nanoparticle concentration when incubated at 25°C for 4 days, as determined by DLS and NTA (Figure 2D).

Table 1: Sucrose products used in this study and DLS and NTA results of (10% w/v) sucrose in solution. Numbers show mean values of triplicate measurements

	Supplier	Grade	Lot	DLS					NTA			
				Z-Average (d. nm)	PDF[c]	Derived count rate	Peak 1 (nm)	Peak 2 (nm)	Concentration (10^8/mL)	D10 (nm)	D50 (nm)	D90 (nm)
Sucrose A	Sigma	ACS[a]	SLBD1571V	13.7	0.95	247	0.9	133	27.9	94	158	246
Sucrose B	Sigma	Ph.Eur.[b]	SZBC012V	4.3	0.35	160	0.9	134	7.1	82	131	238
Sucrose C	Merck	Ph.Eur.	K42570987144	1.3	0.12	147	1.0	1899	0.7	96	160	312
Sucrose D	Merck	Ph.Eur.	K3868287934	2.4	0.2	151	0.9	216	2.8	91	147	276
Sucrose E	Südzucker	Ph.Eur.	L115310600	15.4	0.24	161	0.9	188	3.0	95	161	267
Sucrose F	Caelo	Ph.Eur.	12241808	4.2	0.34	157	0.9	139	4.9	81	122	206
Sucrose G	VWR	Ph.Eur.	13C190006	10	0.58	182	1.1	202	27.9	94	153	237

[a] Purity meets or exceeds the standards of the American Chemical Society
[b] Purity meets or exceeds the requirements of the current European Pharmacopeia
[c] Polydispersity index

Upon concentration of the diafiltrated sucrose G retentate containing the nanoparticle fraction, the sample developed a brownish-yellow color and showed an increase in UV$_{420nm}$ absorbance from 0.03 to 0.18 AU. A water control treated the same way as the sucrose G sample showed no particles by DLS and NTA and had an unchanged UV$_{420nm}$ absorbance of 0.02 AU after concentration. Intrinsic fluorescence of the concentrated sample was analyzed to help identifying potential colorants. The fluorescence intensity landscape is shown in Figure 3. Two distinct patterns of maximum fluorescence intensity could be identified in the sample, pattern 1 at ca. 280/390 nm ($\lambda_{Ex}/\lambda_{Em}$) and pattern 2 at ca. 340/420 nm. The water control treated equally did not show any intrinsic florescence (data not shown).
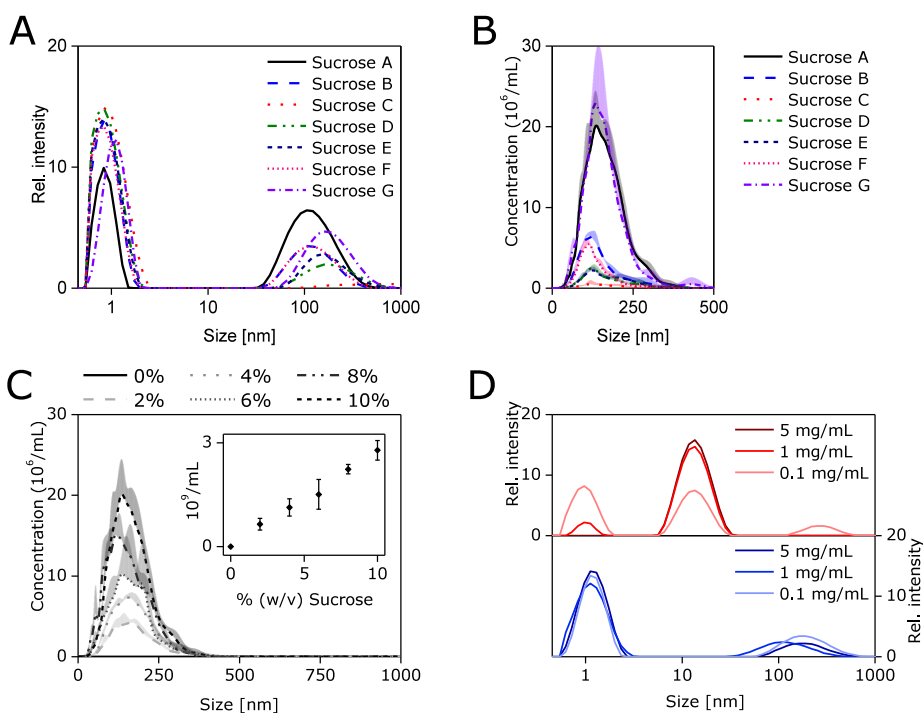

Figure 1: A) Intensity-weighted size distribution by DLS and B) particle size distribution by NTA obtained for different sugars in aqueous solution at 10%. C) Total particle concentration (insert) and particle size distribution obtained by NTA for sucrose A solution from 0 to 10%. D) Intensity-weighted size distribution by DLS for 7% sucrose A solutions containing increasing concentrations of IgG (upper panel) and lysozyme (lower panel). Shown are mean values (A-D) plus standard deviations (B and D) obtained from triplicate measurements.

When the concentrated particle suspension, derived from sucrose G, was vacuum-dried, a thin and compact film layer formed, which did not show any particulate structures by SEM analysis. Rather, the film layer swelled and subsequently ruptured upon extended exposure to the SEM beam, suggesting water entrapment and thus potentially

hygroscopic behavior (Figure S1). No particulate matter was visible by SEM on a vacuum-dried 0.02-µm filter after passing through the concentrated nanoparticle suspension (data not shown). Analysis of the film layer by EDX, however, revealed the presence of several minerals and metals. Signals from silicium, aluminum, calcium, and magnesium were detected, as well as small amounts of phosphor, sulfur, potassium, and iron (Figure 4). The control sample, water processed equally, showed small amounts of silicium and calcium. Carbon, oxygen, and hydrogen signals were also detected, but are method derived and cannot be attributed to the sample.
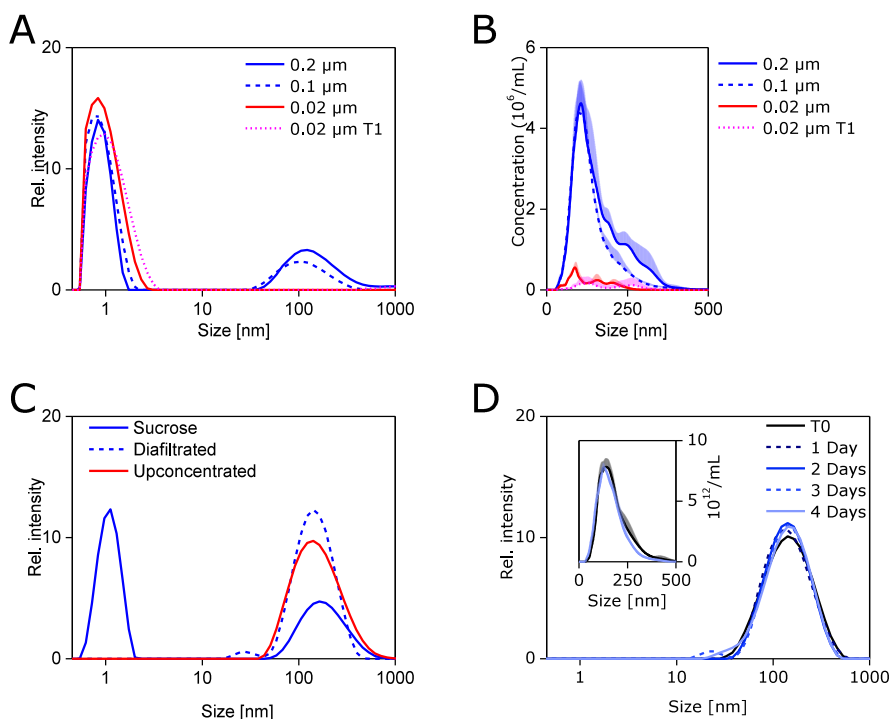

Figure 2: A) Intensity-weighted size distribution by DLS and B) particle size distribution by NTA obtained for sucrose B solutions (10%) after filtration (stated pore size) and storage for 4 days at 25 °C (T1). C) Intensity-weighted size distribution of a 10% sucrose G solution before and after diafiltration and subsequent upconcentration as determined by DLS. D) Intensity-weighted size distribution by DLS and particle size distribution by NTA (insert) of a diafiltrated 10% sucrose G solution stored at 25 °C.

FTIR microscopy was performed on the vacuum-dried sample to detect and identify potential organic material (Figure 5). An FTIR spectrum was obtained that, when compared with the S.T. Japan-Europe GmbH library from 2009, matched closest the spectra of high-molecular-weight dextran (40 kDa, entry# 2130) and cross-linked dextran (Sephadex® G-50, 1.5 – 30 kDa, entry# 8096), with a hit quality of 626 and 620, respectively, with 1,000 being a perfect match. Unprocessed sucrose G powder provided

an FTIR spectrum that matched that of powdered sucrose (entry# 9772), with a hit quality of 959.

Discussion

The interference of sugar-containing solutions with DLS analysis has been observed previously and manifests itself through an additional signal at ca. 100-200 nm, besides the signal at about 1 nm originating from the sugar monomer (11,14). In our study, we found this second signal in solutions of a variety of different sugars (trehalose, fructose, maltose and galactose, data not shown) and different sucrose products (Figure 1A), confirming these previous observations. The 100-200 nm signal in DLS could mistakenly be interpreted as an aggregate peak and mask the formation/presence of protein aggregates. Although this signal will disappear at higher protein concentrations, it should be noted that several antibody drugs are formulated with a sugar at protein concentrations between 1-5 mg/mL (15), where the interference signal will likely show up (Figure 1D). Moreover, blinatumomab, recently approved by the FDA, is formulated at a concentration as low as 12.5 µg/mL and several other protein therapeutics, such as epoetins (16) and cytokines (17), are formulated at similarly low concentrations. Furthermore, during early-stage formulation development, proteins are often used at low concentrations because of limited amounts of material available.
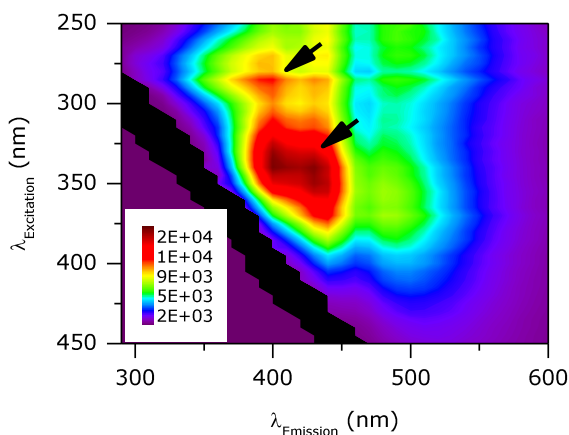
Figure 3: Fluorescence intensity landscape of suspended nanoparticles isolated from sucrose G. The arrows indicate areas of fluorescence maxima. The black area showed strong light scattering and was excluded from the analysis.

Up to now, the interference was suggested to be an intrinsic phenomenon coming from the sugar molecules themselves. However, if the 100-200 nm signal was indeed an intrinsic phenomenon caused by the sugar molecules, one would expect the interference

to be the same for solutions of the same sugar concentration. In contrast, our results could demonstrate high variability of this interference for sucrose across purity grades, suppliers, and also across batches of the same supplier. Further, one batch supplied by Merck (sucrose C) showed this signal to a barely detectable, very low extent and the signal also deviated in size from that of the other products (Table 1). Altogether, this indicates that the interference is caused by particulate matter rather than by monomeric sucrose molecules.

Besides DLS, also NTA detected particles at 100-200 nm showing high variability in particle concentration between the different sucrose products (Figure 1B). Furthermore, the particle concentrations determined by NTA correlate, in relative terms, well with the polydispersity index and the derived count rate determined by DLS using a fixed attenuator (Table 1). Thus, the particles detected by NTA are likely the same as those causing the signal in DLS. It should be noted that sucrose, lysozyme and IgG monomers are below the lower size limit of NTA (18). However, they are detected by DLS, but their signal can in some cases, when a large protein such as an IgG is formulated at high concentration, decrease or even disappear in DLS analysis (Figure 1D). Profound evidence that the presence of suspended particles is responsible for the interference signal comes from the results shown in Figure 2A and B, where this signal in DLS and NTA disappeared after ultrafiltration (0.02 µm). The signal did not re-emerge from the remaining sucrose molecules in solution over the observed time frame of 4 days, suggesting an origin other than an intrinsic phenomenon of the sucrose molecules. After purification by diafiltration, the nanoparticles likely responsible for the interference did not dissolve or further agglomerate to larger particles, at least not readily, when stored in water, supporting the theory of the presence of stable and potentially foreign particulates (Figure 2D).

Following the indication that the nanoparticles might be partially or fully composed of impurities or contaminants, a detailed chemical analysis of the nanoparticles was attempted. No particle like structures could be visualized by SEM analysis of a vacuum-dried particle suspension, because the sample preparation resulted in the formation of a film layer. However, the presence of inorganic elements was determined in this layer by the SEM coupled EDX analysis (Figure 4). The combination of detected elements closely matches the description of an inorganic contaminant called ash, which is a combination of chlorides, sulfates, phosphates, silicates and minerals including calcium, potassium, magnesium and aluminum, mostly present as salts or oxides, as well as clay and sand (19). Ash can enter the sugar cane or beet during growth from the soil, water and added fertilizers, but can also be introduced to the unprocessed sugar by external matter such as dirt or trash. Ash therefore commonly contaminates the unprocessed cane or beet juice,

however, to various degrees and with slight differences in composition depending on the producer. Even though ash is largely cleared off by current refinement processes, an effective removal of ash components in refined white sugar products is still challenging for the sugar industry (20).
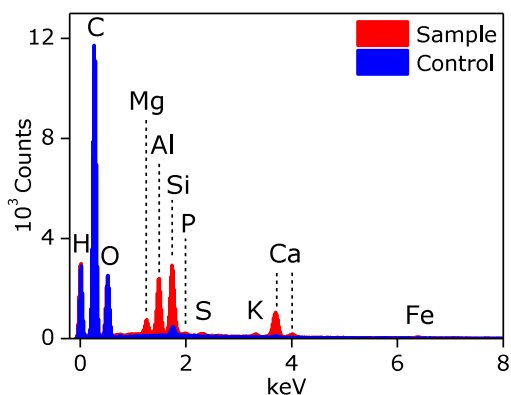

Figure 4: EDX spectrum of vacuum dried nanoparticle isolated from sucrose G (sample) against a water control treated the same way (control). Element analysis was performed against internal standards of the SEM-EDX system.

In the dried particle suspension, we could also detect dextran structures by ATR-FTIR microscopy (Figure 5A). The data suggest that dextran is present as cross-linked fibers, likely responsible for the formation of the hygroscopic film layer upon drying the particles. Dextran is a well-known impurity in the sugar industry, produced due to enzymatic deterioration by *Leuconostoc* bacteria, which mainly enter the sugar cane or beet during harvesting, cutting and grinding, but can also be introduced in later production steps (21). The dextran content in the unprocessed cane or beet juice, however, can vary significantly between different producers, depending amongst others on the delay time between cutting and milling, the harvesting method, the refinement process, and the overall hygiene (22). Importantly, investigations have shown that dextran is not completely removed by current sugar refinement processes (23,24).

It should be noted that both, ash and dextran, are essential components of molasses, a side product of sugar refinement giving brown sugar its distinct color. U.S. and European pharmacopeias require a color test and also UV absorbance data at 420 nm to specifically test pharmaceutical-grade sucrose for molasses remains. As described in the results section, we observed a brownish-yellow color and an increased UV absorbance at 420 nm after concentrating the nanoparticle impurities. The nanoparticle impurities further possessed fluorescence activity in two distinct regions (Figure 3). Diverse amounts of

fluorescent impurities of different compositions have been found in various sugar products by other research groups (20,25–29). According to these studies, the observed fluorescence patterns are caused by a combination of various fluorophores, two of which have close similarities with tryptophan and tyrosine and could be responsible for the fluorescence pattern 1 at ca. 280/390 nm (25–27). Other fluorophores were identified as catechols formed by base-catalyzed sugar degradation and again other are suggested being Maillard reaction polymers, all of which could be potential contributors to the fluorescence pattern 2 (28,29). Fluorescent impurities can be found in various sugar products, however, in different compositions and quantities.
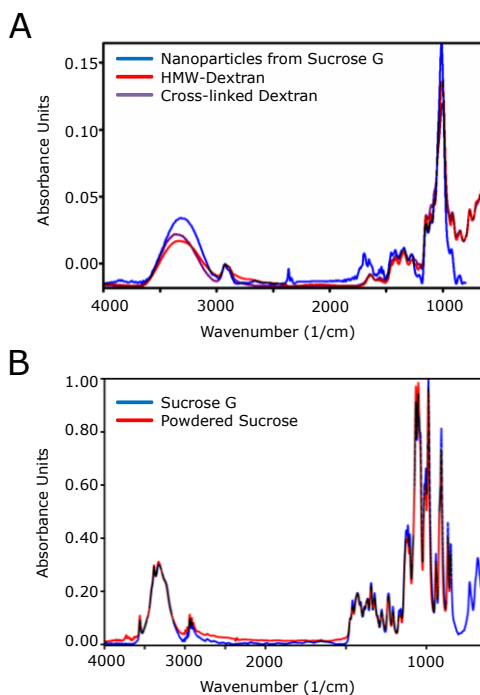

Figure 5: FTIR spectra recorded by FTIR microscopy overlaid with the best fitting entries of the S.T. Japan Europe GmbH database from 2009. A) Recorded spectrum of vacuum dried nanoparticles isolated from sucrose G (blue) overlaid with the entries of high-molecular-weight (red) and cross-linked dextran (violet). B) Recorded spectrum of unprocessed sucrose G (blue) overlaid with the entry of powdered sucrose (red).

Dextran impurities found in sucrose occur in a wide molecular-weight-range from a few kDa to several MDa (21,22), while the ash components detected by EDX and the components suggested by fluorescence spectroscopy are likely much smaller in size. Interestingly, all of those were found in the same particle population with a consistent size of 100-200 nm. Thus, two questions arise from there: i) How do the various impurities come together to form particles and ii) why do these particles occur in such a defined size

distribution, even across various producers? A potential answer to these questions lies in the sugar refinery process itself, particularly in the carbonation or phosphatation step. Here, calcium carbonate or calcium phosphate, respectively, is formed, which co-precipitates with high-molecular-weight components and suspended solids (20). During this step, agglomeration of dextran and other impurities and contaminants could lead to the formation of suspended nanometer sized particles. After the precipitation, the sugar juice is usually clarified by filtration where the membrane's cutoff might be responsible for the defined size distribution of the nanoparticle impurities.

While the exact particle formation process is still rather speculative, it is worth discussing potential ways to deal with nanoparticle impurities in sugars. On the one hand, this could be attempted analytically. For measurements performed by DLS, however, it is not possible to mathematically calculate or subtract the contribution of the nanoparticle impurities from the signal. For measurements performed by NTA, a simple subtraction of the particle counts in the placebo buffer from the particle counts in the sample is possible. Nevertheless, it needs to be noted that the concentration of nanoparticle impurities at pharmaceutically relevant sucrose concentrations can exceed protein particle concentrations even in degraded samples by several orders of magnitude, making simple buffer subtraction statistically meaningless. On the other hand, a pharmaceutical manufacturer could get rid of the nanoparticles through the filtration of sucrose solutions using small pore size filters (e.g., 0.02-µm pores) with commonly available systems for production scale ultrafiltration. It would also be beneficial to improve the sugar refinement processes in order to reduce the amount of impurities in the final sugar product, as has been suggested by various research groups (19–23,30). To ensure effectiveness, however, it would then require monographs to include a test for nanoparticulate impurities in pharmaceutical-grade sugar products.

Conclusions

In this study we demonstrated that sugar, even in pharmaceutical-grade quality, can contain up to 10^{10} nanoparticles per gram in the 100-200 nm range, which can limit the use of techniques for subvisible particle analysis, such as DLS and NTA. The number of nanoparticles can vary significantly between suppliers, as well as between production batches. This makes it very challenging to compare aggregation states of proteins in sugar-containing formulations by DLS and NTA, especially during formulation development. Our results indicate that the nanoparticles found in sucrose are agglomerates of a variety of impurities (dextrans, ash, and aromatic colorants) that were not entirely removed during refinement processes. Importantly, the presence of these nanoparticulate impurities is not

taken into consideration by pharmacopeial quality criteria. Furthermore, the nanoparticle impurities cannot be removed by common sterile filtration using a 0.22-µm pore size filter. However, ultrafiltration could be an effective way to clear the nanoparticles from sucrose solutions. Whether the particles observed in sugars other than sucrose are composed similarly and whether or not these impurities have an impact on a protein's overall stability is currently unknown and is the subject of ongoing follow-up studies.

References

1. Ratanji KD, Derrick JP, Dearman RJ, Kimber I. Immunogenicity of therapeutic proteins: Influence of aggregation. J Immunotoxicol. 2013 Aug 6;6901(2012):1–11.

2. Sauerborn M, Brinks V, Jiskoot W, Schellekens H. Immunological mechanism underlying the immune response to recombinant human protein therapeutics. Trends Pharmacol Sci. 2010 Feb;31(2):53–9.

3. Schellekens H. Immunologic mechanisms of EPO-associated pure red cell aplasia. Best Pract Res Clin. 2005;18(3):473–80.

4. Rowe RC, Sheskey PJ, Cook WG, Fenton ME, Association AP. Handbook of Pharmaceutical Excipients. 7th ed. London: Pharmaceutical Press; 2012.

5. Lee JC, Timasheff SN. The stabilization of proteins by sucrose. J Biol Chem. 1981 Jul 25;256(14):7193–201.

6. Arakawa T, Timasheff SN. Stabilization of protein structure by sugars. Biochemistry. 1982 Dec 7;21(25):6536–44.

7. Schwegman JJ, Hardwick L, Akers M. Practical Formulation and Process Development of Freeze-Dried Products. Pharm Dev Technol. 2005 May 1;10(2):151–73.

8. Nobbmann U, Connah M, Fish B, Varley P, Gee C, Mulot S, et al. Dynamic light scattering as a relative tool for assessing the molecular integrity and stability of monoclonal antibodies. Biotechnol Genet Eng Rev. 2007 Jan;24(1):117–28.

9. Berne BJ, Pecora R. Dynamic Light Scattering: With Applications to Chemistry, Biology, and Physics. New York, NY: Dover Publications; 2000.

10. Mathlouthi M, Reiser P. Sucrose: Properties and Applications. New York, NY: Springer; 1995.

11. Kaszuba M, McKnight D, Connah MT, McNeil-Watson FK, Nobbmann U. Measuring sub nanometre sizes using dynamic light scattering. J Nanoparticle Res. 2007 Oct 26;10(5):823–9.

12. Filipe V, Jiskoot W, Basmeleh AH, Halim A, Schellekens H, Brinks V. Immunogenicity of different stressed IgG monoclonal antibody formulations in immune tolerant transgenic mice. MAbs. 2012;4(6):740–52.

13. Den Engelsman J, Garidel P, Smulders R, Koll H, Smith B, Bassarab S, et al. Strategies for the assessment of protein aggregates in pharmaceutical biotech product development. Pharm Res. 2011 Apr;28(4):920–33.

14. Hawe A, Hulse WL, Jiskoot W, Forbes RT. Taylor dispersion analysis compared to dynamic light scattering for the size analysis of therapeutic peptides and proteins and their aggregates. Pharm Res. 2011 Sep;28(9):2302–10.

15. Uchiyama S. Liquid formulation for antibody drugs. Biochim Biophys Acta. 2014 Nov;1844(11):2041–52.

16.   Brinks V, Hawe A, Basmeleh AHH, Joachin-Rodriguez L, Haselberg R, Somsen GW, et al. Quality of original and biosimilar epoetin products. Pharm Res. 2011 Feb;28(2):386–93.

17.   Lipiäinen T, Peltoniemi M, Sarkhel S, Yrjönen T, Vuorela H, Urtti A, et al. Formulation and stability of cytokine therapeutics. J Pharm Sci. 2015 Dec 9;104(2):307–26.

18.   Filipe V, Hawe A, Jiskoot W. Critical evaluation of Nanoparticle Tracking Analysis (NTA) by NanoSight for the measurement of nanoparticles and protein aggregates. Pharm Res. 2010 May;27(5):796–810.

19.   Hogarth D, Allsopp P, Hogarth M. Manual of Cane Growing. Indooroopilly, Australia: Bureau of Sugar Experiment Stations; 2000.

20.   Chou CC. Handbook of Sugar Refining: A Manual for the Design and Operation of Sugar Refining Facilities. New York, NY: Wiley; 2000.

21.   Promraksa A. Dissertation: Reduction of Dextran Contamination in Raw Sugar Production. Suranaree University of Technology, Nakhon Ratchasima, Thailand; 2008.

22.   Chen JCP, Chou CC. Cane Sugar Handbook: A Manual for Cane Sugar Manufacturers and Their Chemists. New York, NY: Wiley; 1993.

23.   Rauh JS, Cuddihy JA, Falgout RN. Analyzing dextran in the sugar industry: A review of dextran in the factory and a new analytical technique. In: XXVII Conference West Indies Sugar Technology. Port of Spain, Trinidad: Sugar Association of the Caribbean; 2001.

24.   Chou CC, Wnukowski M. Dextran problems in sugar refining: A critical laboratory evaluation. In: Technical Session on Cane Sugar Refining Research. Los Angeles, CA: Science and Education Administration; 1980.

25.   Baunsgaard D, Nørgaard L, Godshall M a. Fluorescence of raw cane sugars evaluated by chemometrics. J Agric Food Chem. 2000 Oct;48(10):4955–62.

26.   Orzel J, Daszykowski M, Walczak B. Controlling sugar quality on the basis of fluorescence fingerprints using robust calibration. Chemom Intell Lab Syst. 2012 Jan;110(1):89–96.

27.   Baunsgaard D, Nørgaard L, Godshall M a. Specific screening for color precursors and colorants in beet and cane sugar liquors in relation to model colorants using spectrofluorometry evaluated by HPLC and multiway data analysis. J Agric Food Chem. 2001 Apr;49(4):1687–94.

28.   Kato H, Mizushima M, Kurata T, Fujimaki M. The formation of Alkyl-p-benzoquinones and Catechols through Base-catalyzed Degradation of Sucrose. Agric Biol Chem. 1973;37(11):2677–8.

29.   Baunsgaard D. Dissertation: Analysis of color impurities in sugar processing using fluorescence spectroscopy and chemometrics. The Royal Veterinary and Agricultural University, Frederiksberg, Denmark; 2000.

30.   Flood C, Flood AE. Removal of color from the sugar manufacturing process by membrane treatment. Suranaree J Sci Technol. 2006;13(4):331–42.

Supplementary information
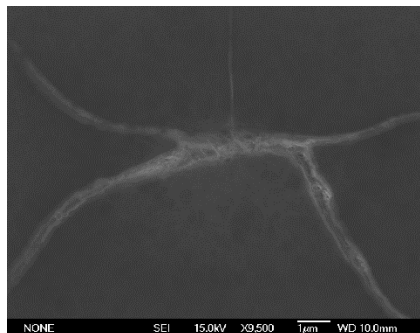
Figure 6: SEM image of vacuum dried nanoparticles isolated from sucrose G, showing a thin and compact film layer that ruptured under the heat of the SEM beam.

CHAPTER 8

NANOPARTICULATE IMPURITIES IN PHARMACEUTICAL-GRADE SUCROSE ARE A POTENTIAL THREAT TO PROTEIN STABILITY

Daniel Weinbuch[1,2], Mark Fogg[3], Mitchel Ruigrok[1,2], Wim Jiskoot[1,2] and Andrea Hawe[1]

[1] Coriolis Pharma Research GmbH, Am Klopferspitz 19, 82152 Martinsried-Munich, Germany

[2] Division of Drug Delivery Technology, Cluster BioTherapeutics, Leiden Academic Centre for Drug Research (LACDR), Leiden University, PO Box 9502, 2300 RA Leiden, The Netherlands

[3] Antitope Ltd, Babraham Research Campus, Babraham Cambridge CB22 3AT, UK

Abstract

Purpose. To investigate the effect of nanoparticulate impurities, recently discovered to be present in pharmaceutical-grade sugars, on the stability of monoclonal antibodies (mAbs).

Methods. Nanoparticulate impurities (NPIs) were first purified from pharmaceutical-grade sucrose and subsequently spiked into trastuzumab, rituximab, infliximab, and cetuximab formulations. The stability of the mAbs as a function of storage time, temperature, and NPI concentration was assessed by visual inspection, flow-imaging microscopy, nanoparticle tracking analysis, size-exclusion chromatography, capillary isoelectric focusing, and intrinsic differential scanning fluorimetry. Furthermore, NPIs were characterized by Laser Doppler electrophoresis and the Glucatell® assay to determine the zeta-potential and the (1-3)-β-glucan content, respectively.

Results. NPIs negatively affected the stability of all mAbs, albeit it to different extents. After spiking with NPIs, trastuzumab mainly showed the formation of high numbers of μm-sized particles and turbidity, rituximab and cetuximab contained high numbers of nm-sized particles, while infliximab formed nm- and μm-sized particles, and showed turbidity. Low molecular weight species were observed for rituximab and infliximab, whereas high molecular weight species were detected for cetuximab only. Furthermore, the stability of trastuzumab and infliximab was affected directly after spiking NPIs. In contrast, degradation of rituximab and cetuximab was observed only after 14 weeks at elevated temperatures. Moreover, the stability of rituximab and infliximab was affected by NPI concentrations that are potentially present in final drug products. The stability of trastuzumab, however, was only affected at elevated NPI concentrations. Lastly, NPIs were shown to contain a high content of (1-3)-β-glucan, which is an immune-modulating molecule.

Conclusions. The presence of NPIs in (bio-)pharmaceutical formulations poses a threat to the stability of mAbs. Additionally, NPIs may have unwanted immunological consequences when present in therapeutic protein products.

Introduction

Formulation development is one of the building blocks assuring the efficacy and safety of a drug product throughout the intended therapy. One of the main goals during formulation development of (bio-)pharmaceutical drug products is to stabilize the functional state of the active pharmaceutical ingredient and to minimize various kinds of degradation that can occur during manufacturing, storage, handling and administration to patients (1,2). During the development of a final drug product, the presence of aggregates and particles, which are considered to be a critical quality attribute, is a major challenge formulation developers are currently facing. Aggregates and particles are ubiquitous in (bio-)pharmaceutical drug products and can occur in sizes ranging from a few nanometer to visible precipitates (3,4). Even though many techniques are available today for the analysis of aggregates and particles, the enormous size range of interest and the large variety of particle compositions and origins complicate their characterization (5,6).

By classification, particles can be of extrinsic, intrinsic or inherent origin (6). Extrinsic particles are materials that are unrelated to the drug product, package, or process (e.g., clothing fragments and hairs), whereas intrinsic particles are non-proteinaceous materials, which are related to the manufacturing or packaging process (e.g., silicon oil droplets). In contrast, inherent particles originate from the drug product, either the protein itself or formulation components. The presence of (inherent) proteinaceous particles has continuously been linked to a decreased drug efficacy and to increased side effects, including life-threatening immunological reactions in patients (7–10).

Recently, our group has discovered a new type of inherent particle, with a size-range between about 100 – 200 nm, that is present in various pharmaceutical-grade sugars such as sucrose, trehalose, fructose, maltose, and galactose (11). Sugars, in particular sucrose and trehalose, are commonly employed as excipients, because they are preferentially excluded from the protein surface, thus increasing the free energy of the system and thereby promoting conformational stability (12–14). Examples of sugar-containing products on the market are Enbrel®, Avastin® and Stelara®. Sugars are also extensively used for lyophilized protein formulations as cryoprotectors and lyoprotectors (e.g., in Herceptin®, Serostim®, and Remicade) (15).

With respect to pharmaceutical-grade sucrose, it has been shown that these nanoparticulate impurities (NPI) dramatically differ in amount, but less so in size, between suppliers and between batches of the same supplier (11). Nonetheless, the presence of NPIs in protein formulations is mostly troubling for other reasons. First, NPIs interfere with light-scattering based analytical techniques, such as dynamic light scattering (DLS) and

nanoparticle tracking analysis (NTA). This complicates the analysis of protein aggregation. Second, NPIs cannot be removed by common sterile filtration through a 0.22-µm pore size filter. Third, the presence of NPIs is currently not taken into consideration by pharmacopeial quality criteria and the effect of NPIs on the stability of therapeutic proteins is unknown.

Therefore, the present study was designed to clarify if NPIs do affect the stability of a therapeutic proteins. With the results presented here, it was shown that NPIs have a negative effect, albeit to different extents, on the stability of several currently marketed monoclonal antibodies (mAbs), namely trastuzumab, rituximab, cetuximab, and infliximab. Furthermore, our data suggests that besides the destabilizing effects, which appeared to be protein specific, NPIs possess inherent immune-modulatory properties and thereby bear the potential to have unwanted immunological consequences when present in therapeutic protein products.

Materials & Methods

Materials

Herceptin® (trastuzumab), MabThera® (rituximab), Remicade® (infliximab), and Erbitux® (cetuximab) were donated by local hospitals. All drug products had exceeded their expiry date. Pharmaceutical-grade sucrose (Ph.Eur.) was purchased from VWR BDH Prolabo® (Bruchsal, Germany) and Südzucker (Mannheim, Germany). Hisitidine-HCl, trehalose, sodium citrate, sodium chloride, sodium dihydrogen phosphate, di-sodium hydrogen phosphate, and citric acid were purchased from Merck (Darmstadt, Germany). Polysorbate 20 and 80, and glycine was purchased from Sigma (Taufkirchen, Germany). Histidine was purchased from Amresco (Solon, OH, USA). PVDF syringe and membrane filters with a pore size of 0.2 µm were obtained from Millipore (Schwalbach, Germany).

Purification of nanoparticulate impurities from sucrose

Nanoparticulate impurities (NPIs) were purified from sucrose (VWR) as described earlier (11). Briefly, sucrose powder was dissolved in Milli-Q® water at a maximum of 50 % (w/v). Concentration of particles and diafiltration against Milli-Q® water to remove sucrose were performed by using a Minimate II Tangential Flow Filtration (TFF) System (Pall, Crailsheim, Germany) equipped with a 30-kDa TFF capsule (Pall) until a diafiltration volume of at least 14 times the sample volume was achieved. The retenate was then filtered through a PVDF syringe filter with a pore size of 0.2 µm and further concentrated by using 10-kDa

centrifugal filter units (Amicon Ultra 15, Millipore). The final sample contained $7x10^{11}$ particles/mL in a size range of about 100-200 nm (based on NTA).

Milli-Q® water without the addition of sucrose was treated the same way as the sucrose solution, using identical volumes and preparation times. The so obtained sample is further named "Control".

Protein formulations

Trastuzumab, rituximab, infliximab, and cetuximab were diluted to a monoclonal antibody (mAb) concentration of 2 mg/mL using following formulation buffers. Trastuzumab: 2.4 mM histidine-HCl, 2.1 mM histidine, 52.9 mM trehalose, and 0.009% polysorbates 20 at pH 6.0. Rituximab: 25 mM citrate buffer, 9 g/L sodium chloride, and 0.7g/L polysorbates 80 at pH 6.5. Infliximab: 5 mM phosphate buffer, 50g/L sucrose (Südzucker), and 0.005% polysorbate 80 at pH 7.2. Cetuximab: 10 mM citric acid buffer, 100 mM sodium chloride, 100 mM glycine, and 0.01% polysorbates 80 at pH 5.5. All formulation buffers were filtered through a PVDF syringe filter with a pore size of 0.2 µm.

Stability study

Trastuzumab, rituximab, infliximab, and cetuximab, as well as their corresponding formulation buffer, were spiked with NPIs to a final concentration of $3.5x10^{10}$ particles/mL (based on NTA) or spiked with an equivalent volume of Control. All samples were then transferred to sterile 2R vials (fill volume 1 mL) and each aliquot (N=1) was measured at least one day after preparation (T0), after 2 (T2w), 8 (T8w), and 14 weeks (T14w) of storage at 2-8, 25 or 40 °C. Sample handling was performed under laminar airflow conditions.

NPI concentration-dependent study

The NPIs were diluted with Control in four 10-fold serial dilution steps. Trastuzumab, rituximab, and infliximab, as well as their corresponding formulation buffer, were then spiked with the diluted NPIs to achieve final NPI concentrations of $3.5x10^{10}$, $3.5x10^{9}$, $3.5x10^{8}$, and $3.5x10^{7}$ particles/mL (based on NTA). Additionally, samples spiked with an equivalent volume of Control were prepared (shown as 0 particles/mL in the results). All samples were prepared in triplicate (N=3) and transferred to sterile 2R vials (fill volume 1 mL) and stored at 40°C for one week. Sample handling was performed under laminar airflow conditions.

Visual inspection

For visual inspection, the vials were tested for the presence or absence of visible particles or turbidity under gentle, manual, radial agitation for 5 seconds in front of a white background and for 5 seconds in front of a black background according to the European Pharmacopoeia (16). Two trained examiners performed the inspection independently.

Micro-flow imaging (MFI)

An MFI5200 system (ProteinSimple, Santa Clara, CA, USA) equipped with a 100-µm flow cell and controlled by the MFI View System Software (MVSS) version 2-R2.6.1.20.1915 was used. The system was flushed with 10 mL purified water at maximum flow rate and flow cell cleanliness was checked visually between measurements. The respective formulation buffer / blank was used to perform illumination optimization prior to each measurement. Samples of 0.5 mL with a pre-run volume of 0.2 mL were analyzed at a flow rate of 0.17 mL/min and a fixed camera rate (not adjustable by the user) leading to a sampling efficiency of about 80–85%.

Nanoparticle tracking analysis (NTA)

NTA was performed with a NanoSight LM20 (NanoSight, Amesbury, UK). The instrument was equipped with a 405 nm blue laser, a sample chamber and a Viton fluoroelastomer O-ring. If sample dilution was necessary to achieve an optimal concentration for NTA, Milli-Q® water was used as a diluent and all results were calculated back to the original concentration. Samples were loaded into the sample chamber by using a 1-mL syringe and a pre-run volume of 0.5 mL. Samples were analyzed in triplicate at a stopped flow, while 0.1 mL was flushed through the chamber between each repetition. The NTA 2.3 software was used for capturing and analyzing the data. Movements of the particles in the samples were recorded as videos for 60 s, while the shutter and gain settings of the camera were set to maximum for an increased particle resolution in the lower size limit.

Size-exclusion chromatography (SEC)

A TSK Gel 4000 SWXL column (300 mm × 7.8 mm) (Tosoh Bioscience, Montgomeryville, PA, USA) and an Agilent 1200 high-performance liquid chromatography system (Agilent Technologies, Palo Alto, CA, USA) coupled to an ultraviolet (UV) detector set at 280 nm was employed for SEC analysis. The mobile phase was composed of 100 mM sodium phosphate, 100 mM sodium sulfate at a pH of 7.0. The flow rate was set to 0.6 mL/min. Samples were centrifuged at 10,000 g for 3 min, kept at 2-8 °C and injected in duplicates of each 25 µL. The sample recovery was calculated as the total peak area relative to the

Control-spiked sample at T0. Peaks with a retention time above 20 min were buffer related and not considered. The monomer peak retention time was at 17.5 min. Peaks with a shorter retention time than the monomer were regarded as high molecular weight (HMW) species. In contrast, peaks with a longer retention time than the monomer were regarded as low molecular weight (LMW) species. Contents of monomer, HMW- and LMW species are given as percentages relative to the total sample recovery.

Capillary isoelectric focusing (cIEF)

Imaged cIEF was conducted on an iCE280 instrument (Convergent Bioscience, Toronto, Canada) equipped with a fluorocarbon-coated cartridge (ProteinSimple) and coupled with a PrinCE Microinjector (Convergent Bioscience) set to room temperature. The UV detector was set to 280 nm. The anode and cathode reservoir were filled with 0.08 M phosphoric acid and 0.1 M sodium hydroxide, respectively (both in 0.1 % methylcellulose, electrolyte kit, ProteinSimple). Samples were prepared and mixed to achieve a final concentration of 0.2 mg/mL protein, 4 M urea (Sigma, Taufkirchen, Germany), 0.35 % (w/v) methylcellulose (ProteinSimple), 4 % (v/v) carrier ampholytes pH 3-10 (GE Healthcare, Little Chalfont, Buckinghamshire, UK), and each 0.5 % (v/v) pI marker 5.85 and 9.77. After a centrifugation step (10,000 g for 3 min), the supernatant was analyzed in duplicates by using a pre-focusing step of 1500 V for 1 min and a focusing step of 3000 V for 6 min. The performance of the system was checked on the day of analysis by using a hemoglobin standard (iCE280 System Suitability Kit, ProteinSimple) according to the recommendations of the manufacturer. The instrument was controlled using the software version 2.3.6, while the recorded electropherograms were analyzed by the software ChromPerfect (Version 5.5.6).

Intrinsic differential scanning fluorimetry (nDSF)

Samples were diluted to a mAb concentration of 2 mg/mL by using their corresponding formulation buffer. The mAbs, as well as their corresponding formulation buffer, were spiked with NPIs to a final concentration of 3.5×10^{10} p/mL or an equivalent volume of Control. All samples were prepared in triplicates (N=3), immediately transferred to High Sensitivity Capillaries (NanoTemper) and the unfolding characteristics from $20-95\,°C$ were analyzed using a Prometheus NT.48 (NanoTemper Technologies, Munich, Germany). The heat ramp was set to 1 °C/min using a laser power of 20%. The PR.Control software version 1.12.3 was used for system control, data acquisition and analysis.

(1-3)-β-glucan detection

An NPI sample (7×10^{11} particles/mL, based on NTA), its 10-kDa filtrate (obtained from the last upconcentration step during the purification process) and the Control were diluted with endotoxin free water in four 10-fold serial dilution steps under aseptic and particle free conditions. The (1-3)-β-glucan levels were measured by using a Glucatell® Kit (Cape Cod,East Falmout, MA, USA), according to the instructions of the manufacturer. This assay is a modified endotoxin assay, where the factor C is deactivated. By that, the assay only gives a signal in presence of (1-3)-β-glucans. In brief, the reagent-sample mixture was placed in a microplate-heating block at 37 °C for the recommended time. A volume of 50 µL from each of the three diazo reagents was added to the mixture to stop the reaction. The absorbance at 545 nm was measured and (1-3)-β-glucan concentration in pg/mL was calculated based on a standard curve.

Laser Doppler electrophoresis (LDE)

NPIs at a concentration of 5×10^{11} p/mL (based on NTA) were buffered at pH 7.4 (1 mM phosphate buffer) or at pH 3.0 (1 mM citrate buffer). After transferring 1000 µL sample into a folded capillary cell (Malvern), the zeta-potential was measured by laser Doppler electrophoresis (LDE) by using a Zetasizer Nano ZS (Malvern Instruments, Worcestershire, UK). Each measurement was the average of 3 zeta-potential measurements consisting of 100 sub runs. Zetasizer software version 7.03 was used for system control and data acquisition.

Results

NPI characterization

The NPIs were purified from pharmaceutical grade sucrose and upconcentrated to around 7×10^{11} particles/mL, as determined by NTA. Their size distribution was between around 100-200 nm and monomodal, as observed in our previous study (11). The Control sample showed particle numbers below the quantification limit of NTA. We additionally characterized the NPIs by LDE analysis, which determined their zeta potential as -13.4 (±1.6) and -8.0 (±0.3) mV at pH 7.4 and 3.0, respectively.

Additionally, the NPIs gave a strong signal in the Glucatell® assay testing for (1-3)-β-glucan (Figure 1). The NPIs 10-kDa filtrate also showed a signal in this assay, however, with a more than one order of magnitude lower intensity. The Control sample showed only a tiny signal and only when tested without dilution. Based on the signals and the corresponding

dilution factors, the NPIs sample (7×10^{11} p/mL) contained 750 ng/mL (1-3)-β-glucan, the 10-kDa filtrate 25 ng/mL, and the Control 0.013 ng/mL.
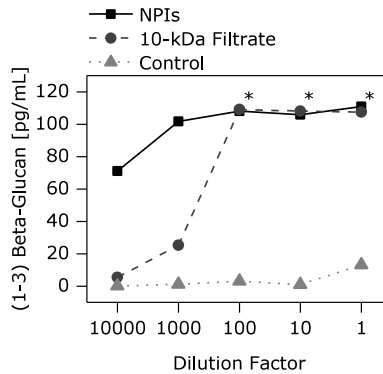

Figure 1: Results of (1-3) β-glucan determination for NPIs, its 10-kDa filtrate and the Control. Data points marked with * exceeded the assay limit.

Stability study using elevated NPI concentration

A stability study was performed with four mAbs (trastuzumab, rituximab, infliximab, and cetuximab) spiked with NPIs at a concentration of 3.5×10^{10} particles/mL, around 10x the concentration potentially present in a marketed drug product (11), or with an equivalent volume of Control.
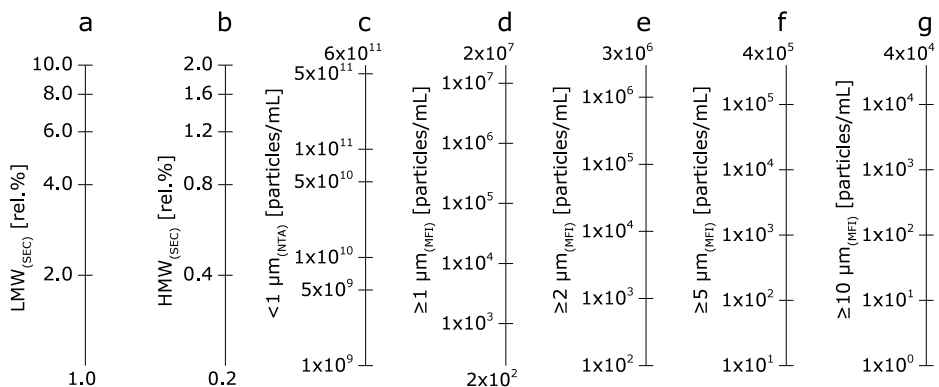
Figure 2: Axis details of radar plots shown in Figure 3. The a- and b-axis show the LMW and HMW content in relative percentage determined by SEC, respectively. The c-axis shows the particle concentration in particles/mL determined by NTA. The d-, e-, f- and g-axis show the cumulative particle concentration above 1, 2, 5 and 10 μm by MFI, respectively. All axes are shown in logarithmic scale with the lowest value in the center and the highest value on the outside of the radar plots in Figure 3.
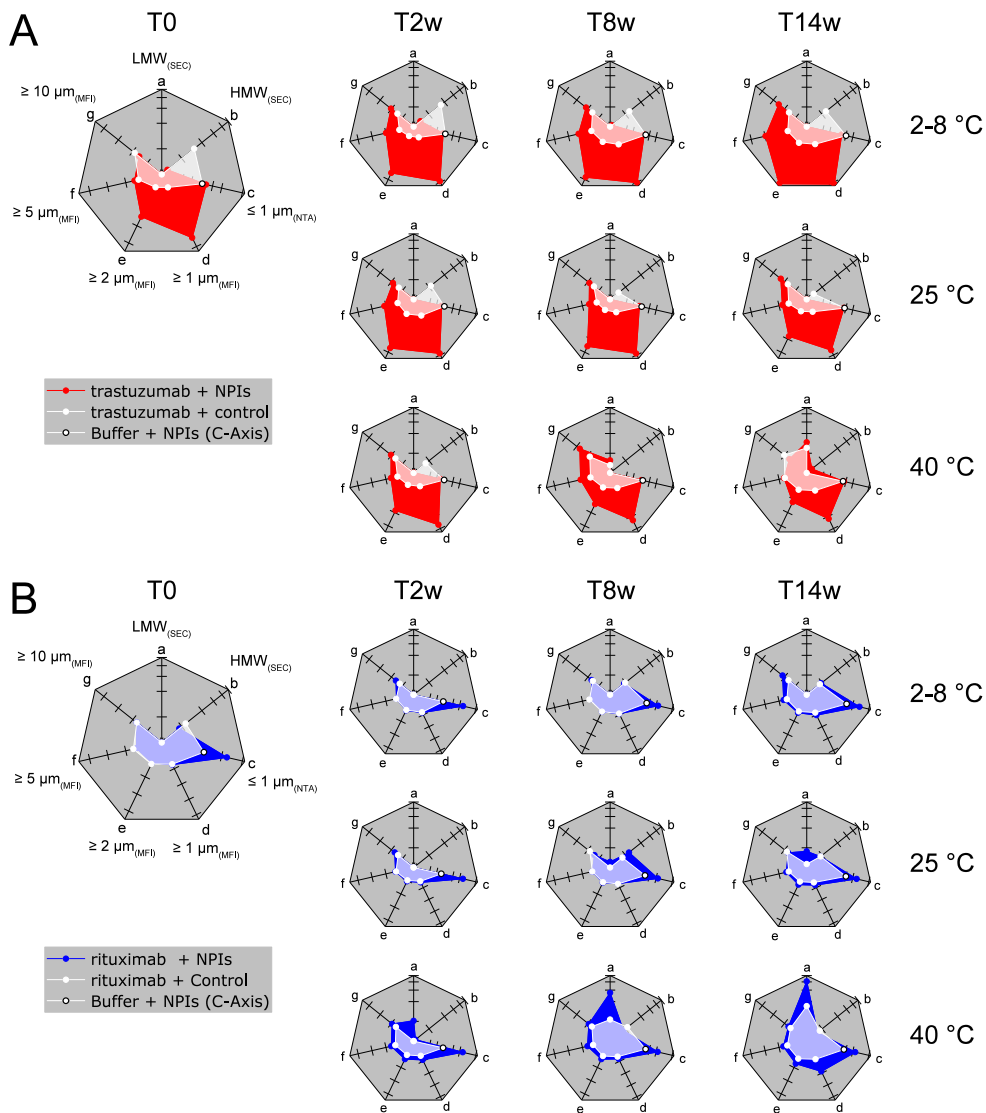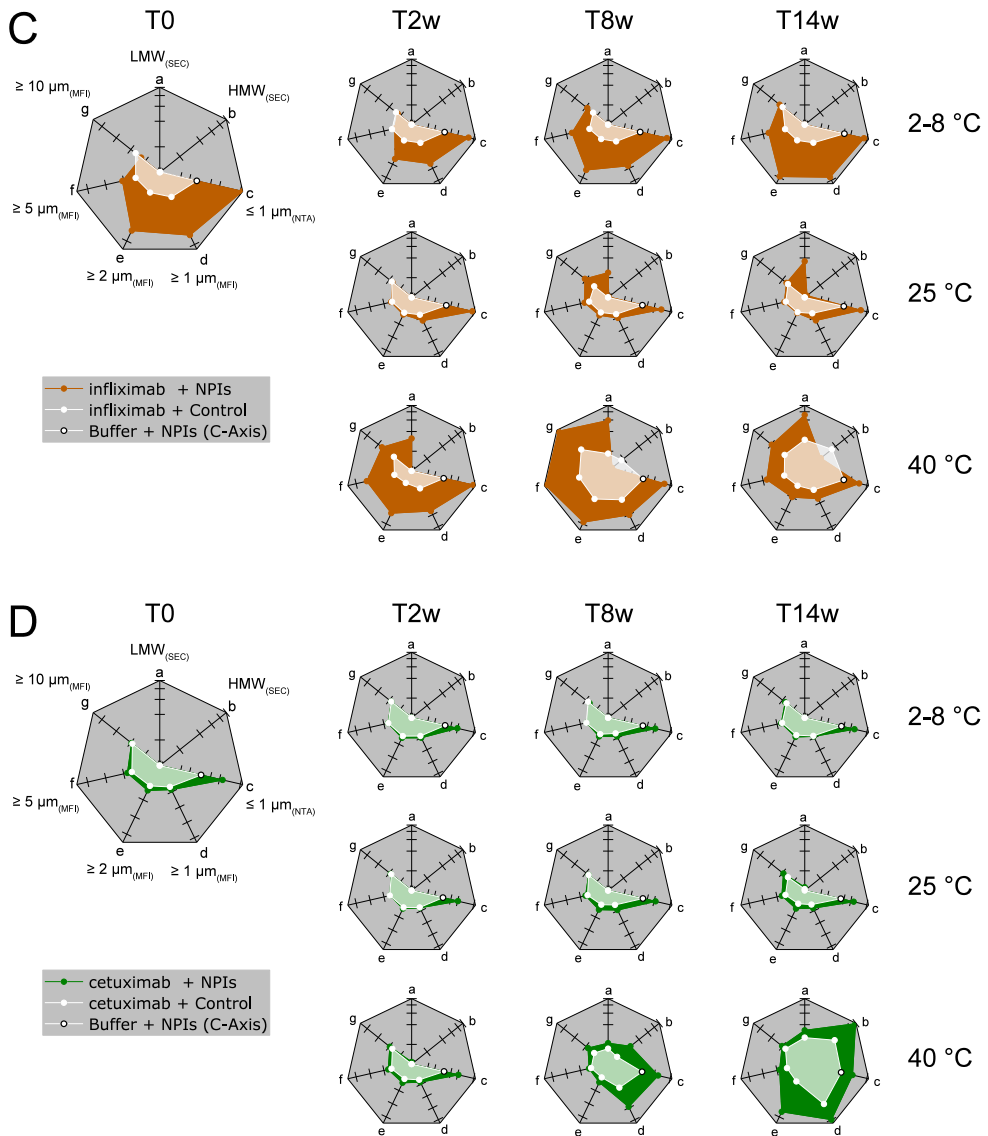
Figure 3: Results of the stability study of A) trastuzumab, B) rituximab, C) infliximab and D) cetuximab. The details of the radar plot axes are displayed in Figure 2. Radar plots show results for mAbs spiked with NPIs at a final concentration of $3.5x10^{10}$ particles/mL (colored graphs) and mAbs spiked with Control (white, semi-transparent graphs), where the data points on the C-axis show the respective formulation buffer spiked with NPIs at a final concentration of $3.5x10^{10}$ particles/mL (black circles).

Content of LMW species of rituximab and infliximab spiked with NPIs increased over time compared to the Control-spiked samples (Figure 3B, C, and 4A). Content of LMW species of trastuzumab and cetuximab spiked with NPIs did not change compared to the corresponding Control-spiked sample (Figure 3A and D). No difference in sample recovery was detected by SEC between the NPI-spiked and Control-spiked samples during the stability study (data not shown).

NPI-spiked cetuximab showed an increased content of HMW species upon storage at 40°C when compared to the Control-spiked sample (Figure 3D and 4B). For trastuzumab, the content of HMW species at T0 was higher in the Control-spiked sample than in NPI-spiked sample. This difference leveled out with increasing storage time and temperature. For rituximab, infliximab and cetuximab, NPIs did not induce the formation of HMW species (Figure 3 and 4).

NPI-spiked rituximab, infliximab, and cetuximab, but not trastuzumab, showed increased particle numbers in the nm-size range at T0 compared to the corresponding formulation buffer spiked with NPIs (Figure 3). Importantly, NTA (the analytical method used for the nm-size range) detects both, particles formed within the formulation and the spiked NPIs (11). Thus, formulation buffer spiked with NPIs was used as the appropriate reference rather than Control-spiked mAb samples (which contained negligible particle numbers in the nm-size range at T0 and any other time point and temperature during our studies; data not shown). There was no considerable change in particle numbers in the nm-size range during the stability study after T0 for all antibodies.

NPI-spiked trastuzumab and infliximab, showed turbidity, which was observed during visual inspection (data not shown) and increased particle numbers in the lower μm-size (MFI) range already at T0 (Figure 3). For NPI-spiked trastuzumab, a further increase in particle size and number over the μm-size range was observed during the stability study. Furthermore, the formation of visible particles was detected after 14 weeks at all storage temperatures. The Control-spiked samples did not show such a behavior. For NPI-spiked rituximab and cetuximab, there was no considerable change in particle numbers in the μm-size range at 2-8 and 25 °C. At 40 °C, however, rituximab spiked with NPIs showed clearly increased particle numbers in the lower μm-size range after 14 weeks when compared to the Control-spiked sample. Cetuximab spiked with NPIs showed an even more pronounced increase in μm-particle numbers at 40 °C compared the Control-spiked sample, which was accompanied by the appearance of turbidity. Infliximab samples spiked with NPIs behaved uncommonly during the stability study with respect to μm-particle numbers. While the particle numbers increased at 2-8 °C and particles grew in size at 40 °C, their numbers decreased dramatically upon storage at 25 °C. In addition, while the NPI-

spiked samples consistently showed turbidity at 2-8 and 40 °C with the appearance of visible particles after 8 weeks at 40 °C, the NPIs spiked samples stored at 25 °C were free of turbidity and visible particles. These observations support the results of MFI analysis. Additionally, cIEF analysis was performed throughout the stability study. However, no difference in charge variance between NPI-spiked and Control-spiked samples was observed (data not shown). Furthermore, conformational stability, monitored as the melting temperature (T_m) of the four tested mAbs measured by nDSF was not affected by the presence of NPIs (data not shown).
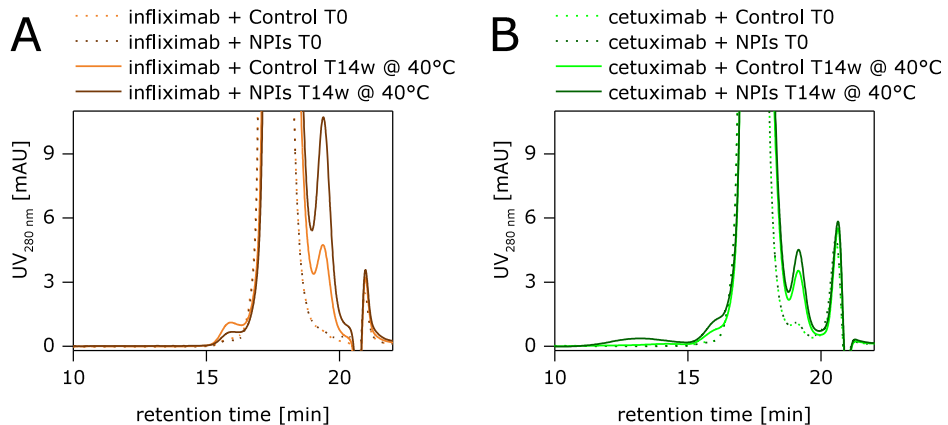

Figure 4: Examples of SEC-chromatograms of A) infliximab and B) cetuximab during the stability study. The peaks at a retention time of 17.5 min represent the monomer. Peaks with a retention time above 20 min are buffer related.

Effect of NPI concentration on mAb stability

Subsequent to the stability study, a NPI concentration dependent study was performed with three mAbs (trastuzumab, rituximab and infliximab). The tested NPI concentrations ranged from 0 to 3.5×10^{10} particles /mL. While the highest NPI concentration of 3.5×10^{10} particles/mL is the same as that used for the stability study, the NPI concentrations of 3.5×10^9, 3.5×10^8, and 3.5×10^7 particles/mL reflect high, medium, and low potential contamination of NPIs, respectively, in a hypothetical formulation containing 10% w/v sucrose, based on results of our previous study (11).

The destabilizing effects of the NPIs on trastuzumab, rituximab, and infliximab observed during the stability study could be reproduced for the highest concentration during the NPI concentration dependent study (Figure 5). For trastuzumab, it was further shown that only the highest NPI concentration affected trastuzumab stability negatively, regarding µm-particle numbers (Figure 5A), content of LMW species (Figure 5B), and turbidity (data

not shown). Consistent with the results from the stability study, content of HMW species (data not shown) and nm-particle numbers (data not shown) were not affected by the presence of NPIs. A small but significant decrease in sample recovery of about 2%, which was not detected in the stability study, was also observed for trastuzumab when spiked with the highest NPI concentration (Figure 5B).
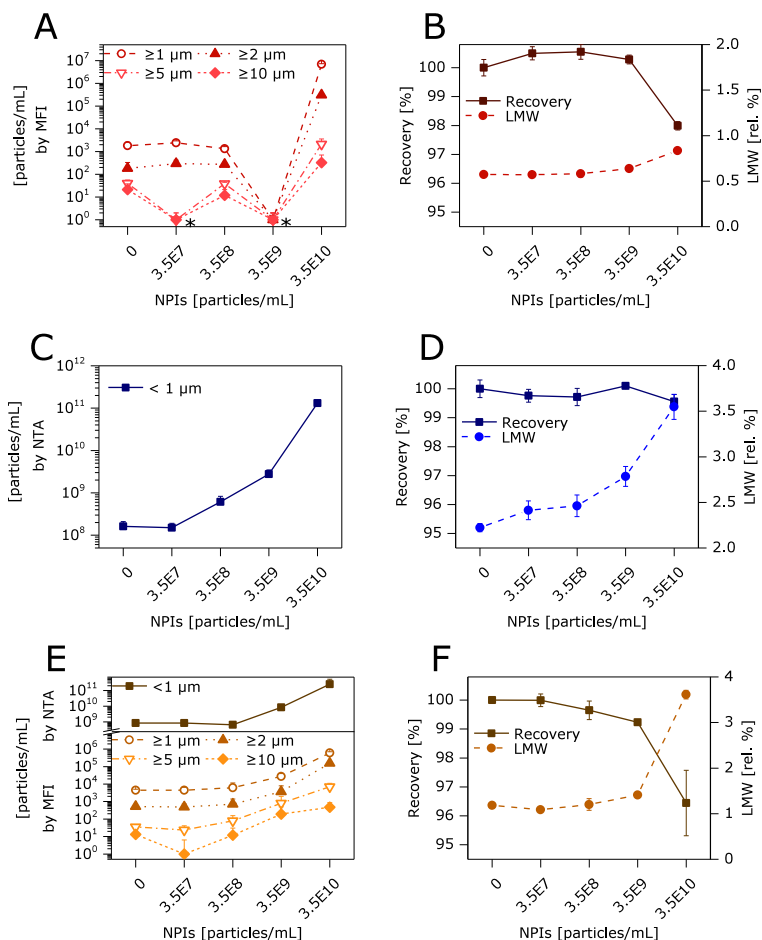
Figure 5: Concentration dependent effects of NPIs on A,B) trastuzumab, C,D) rituximab and E,F) infliximab. A,C,E) Particle concentration of mAb samples in relation to the spiked concentration of NPIs, as measured by MFI and/or NTA. For MFI, the values were corrected for the particle concentration obtained for mAb spiked with Control. For NTA, the values were corrected for the particle concentration obtained for the formulation buffer spiked with NPIs. Data points marked with * were negative after buffer correction and set to 1 for the purpose of illustration. B,D,F) Protein recovery as percentage of total peak area of the unstressed sample, LMW content as relative percentage of the total recovery (as measured by SEC). Symbols represent the arithmetic mean and error bars show standard deviations from triplicate preparations.

For rituximab, the elevated particle numbers in the nm-size range were consistently observed until a NPI concentration of 3.5×10^8 particles/mL (Figure 5C). Furthermore, the content of LMW species was elevated in the presence of NPIs even at concentrations as low as 3.5×10^7 particles/mL (Figure 5D). Consistent with the results from the stability study, sample recovery, content of HMW species and µm-particle numbers were not affected by the presence of NPIs (data not shown).

For infliximab, elevated particle numbers in the nm- and µm-size range were observed until a NPI concentration of 3.5×10^9 particles/mL (Figure 5E). Sample recovery was decreased and the content of LMW species was increased, but only when spiked with the highest NPI concentration of 3.5×10^{10} particles/mL (Figure 5F). Consistent with the results from the stability study, the content of HMW species was not affected by the presence of NPIs (data not shown).
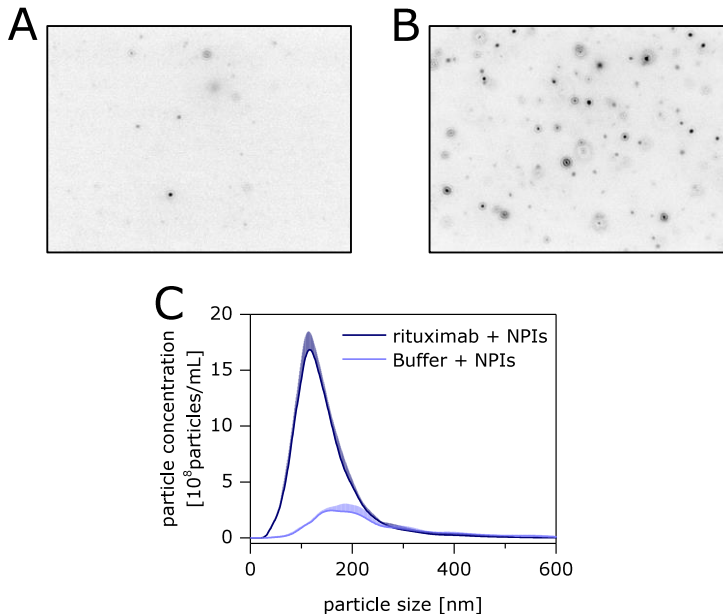
Figure 6: NTA images of A) rituximab formulation buffer and B) rituximab, both spiked with NPIs at a final concentration of 3.5×10^{10} particles/mL. The determined concentration for B) was about 2×10^{11} particles/mL. Images were captured in 100-fold diluted samples. Image colors were inverted for better visibility.

Interestingly, for those NPI-spiked mAb samples that showed elevated nm-particle numbers compared to the NPI-spiked formulation buffers (rituximab at NPI concentrations of 3.5×10^{10}, 3.5×10^9, and 3.5×10^8, and infliximab at NPI concentrations of 3.5×10^{10} and 3.5×10^9 particles/mL), we consistently found a decreased mean size by NTA of about 100 nm compared to the NPIs alone (representative example shown in Figure 6).

Discussion

All four mAbs included in our study, namely trastuzumab, rituximab, infliximab, and cetuximab, showed degradation upon exposure to NPIs, which was more pronounced as compared to the Control. Over the course of the study, we found distinct instability behaviors for each individual mAb when exposed to NPIs (Table 1). Formulation buffer controls have been included in all presented studies and did not show instabilities in any of the tested parameters throughout the study. It can thus be excluded that our observations are purely due to differences in formulation buffer composition or the result of excipient instabilities. Furthermore, the pH values measured immediately after sample preparation were within 0.1 pH units from those of the corresponding control samples, excluding pH shifts as the source of the observed instabilities.

Table 1 summarizes the observed effects of the NPIs on the stability of the tested mAbs and ranks the mAbs according to the severity of degradation (Sum of +'s). A higher score correlates to a more pronounced mAb degradation compared to the other tested mAbs. Following that score bottom-up, rituximab was affected to the lowest extent by the presence of the NPIs showing the immediate formation of high numbers of nm-sized particles as the main degradation product. Similarly, cetuximab showed the immediate formation of high numbers of nm-sized particles as the main degradation product. Cetuximab, however, was overall degraded more severely than rituximab. Trastuzumab in turn showed the formation of high numbers of µm-sized particles as the main degradation product and the appearance of turbidity. Infliximab was, among the tested mAbs, degraded to the greatest extent, showing high numbers of nm- and µm-sized particles as the main degradation product as well as the appearance of turbidity.

For rituximab and cetuximab, it was observed that the formation of nm-sized particles was not accompanied by the formation of HMW species or a simultaneous reduction of sample recovery by SEC. It was shown before that only small protein quantities, sometimes below the quantification limit of a SEC, are sufficient to form large numbers of subvisible particles (17). It could thus be assumed that minute amounts of protein have rapidly formed stable particles in the nm-size range. For both mAbs, these particles did not change detectibly in number or size over time. They were, however, followed by the formation of high numbers of µm-sized particles at elevated temperatures (Figure 3B and 3D). The similarities in behavior of rituximab and cetuximab suggests comparable aggregation mechanisms and by that potentially also a comparable mode of interaction with the NPIs. Despite all the similarities, though, small differences were observed. While rituximab formed LMW species at 25 and 40 °C, suggesting mAb fragmentation, cetuximab showed such behavior only at 40 °C to a small extent. Also, in contrast to

rituximab, cetuximab formed HMW species at 40 °C (Figure 4B). Importantly, rituximab showed degradation even when minor quantities of NPIs were present (Figure 5C and 5D).

Table 1: Influence of NPIs on the tested stability parameters of monoclonal antibodies.

Parameter	Method	trastuzumab	rituximab	infliximab	cetuximab
Visible particles	Visual inspection	+	–	+	–
Turbidity	Visual inspection	++	–	++	+
µm-particles	MFI	++	+	++	+
nm-particles	NTA	–	++	++	++
HMW species	SEC	–	–	–	+
Sample recovery	SEC	+	–	+	–
LMW species	SEC	–	+	+	–
Conformational Instability	nDSF	–	–	–	–
Charge variants	cIEF	–	–	–	–
	Sum of +'s	6	4	9	5

- = was not affected (relative to the control)

+ = was affected, but only at high concentrations of NPIs and/or not immediately (relative to the control)

++ = was highly and immediately affected and/or affected at NPIs concentrations potentially present in drug products (relative to the control)

Trastuzumab behaved differently to the presence of NPIs than rituximab and cetuximab. No increase in numbers of nm-sized particles was observed in any measurement. However, µm-particles formed immediately, as mentioned above, and grew in number and size, especially at 2-8 °C. This was accompanied by the presence of sample turbidity and resulted over time in formation of visible particles. Particle formation observed for trastuzumab was, different to rituximab, accompanied by a decrease in sample recovery by SEC (Figure 5B). Interestingly, HMW species of trastuzumab were not just absent in the presence of NPIs, but actually decreased compared to the Control-spiked sample. This could indicate that dimers are, besides the monomer, a potential source for particle formation and that, overall, a different type of interaction between trastuzumab and NPIs could have been at play. Other than observed for rituximab, trastuzumab showed signs of degradation only when exposed to NPI concentration above those potentially present in real-life drug products.

For infliximab, it appears as if the characteristics observed for rituximab as well as those observed for trastuzumab are present. High numbers of nm-sized particles as well as μm-sized particles formed immediately and even when exposed to smaller quantities of NPIs. Similar to rituximab, the nm-sized particles were continuously present and did not change detectibly in concentration and size over time and temperature. Additionally, degradation of infliximab also occurred in the presence of NPI concentrations potentially present in real-life drug products. Similar to trastuzumab, the μm-sized particles grew over time until the appearance of visible particles, which was accompanied by sample turbidity and a decreased sample recovery by SEC. It is not entirely clear, however, why this growth did not occur at 25 °C. Here, infliximab seems to show only the instability behavior observed for cetuximab and rituximab, while at 2-8 and 40 °C the instability behavior also observed for trastuzumab is additionally present. Potentially, there is more than one mechanism involved when it comes to the formation of μm-sized particles in presence of NPIs, with different temperature relationships.

It has been described previously that the presence of non-proteinaceous particles in the subvisible size range can affect the stability of a therapeutic protein. This is, because the activation energy for the formation of an aggregate can be dramatically lowered in the presence of solid surfaces (e.g., dust particles, container components, insoluble organic aggregates, etc.) (18,19). On the example of stainless-steel particles from piston pumps, silicone microdroplets from syringe coatings, and glass microparticles from glass containers, it was shown that heterogeneous nucleation occurs (i.e., particles that are comprised of proteinaceous and non-proteinaceous constituents) which negatively affect protein stability and could potentially increase protein immunogenicity (20–23). It is likely that the NPIs included in our study induced aggregation of the mAbs by presenting them a liquid-solid interface for heterogeneous nucleation.

Moreover, electrostatic interaction between mAbs and NPIs may have contributed as well, because NPIs are overall negatively charged, while the four mAbs are, due to their isoelectric point and buffer pH, positively charged. Whether other interactions could have contributed to the destabilizing effects of the NPIs cannot be concluded from our data. We could however show that no decrease in conformational stability, as measured by the melting temperature (Tm), or the formation of charge variants (e.g., though chemical modification played a role). A permanent association of the mAbs to the NPIs is not supported by our results, because NTA determined for the newly formed particles a smaller mean particle size than for the spiked NPIs alone (Figure 6). If association had occurred, one would expect a slight size increase. Even though this study cannot conclude with certainty on the underlying mechanisms responsible for the different behaviors of

the tested mAbs, it is clear that NPIs can indeed affect the stability of proteins and that the extent of destabilizing effects seems to depend on the mAb and the NPI concentration.

It has been shown before that nm- and μm-sized protein particles can trigger immunological reactions and thus increase the risk for side effects and other unwanted clinical events such as decreasing the therapeutic efficacy of the drug product (7–10). It could be that much lower concentrations of NPIs than the ones tested in this study lead to protein degradation, e.g., during long term storage, and that such degradation products could pose a risk for patients. We can expect NPIs to be present in at least some marketed drug products containing sugar, but there is no data or study available making a correlation between the safety of a drug product and its NPI concentration. However, it has been reported that during a clinical phase 1 study for a therapeutic protein that some of the healthy volunteers developed immunological side effects (24). These were marked by a dose-related transient fever and an elevation in total white blood cells, neutrophils, and C-reactive protein similar to an endotoxin-like exposure. The researchers could link this effect to impurities originating from the sucrose used in the formulation. They found the presence of (1-3)-β-glucan and could show that this was the root cause of the observed immunological side effects. This conclusion appears plausible, since these moieties are known immune-modulators (25). Additionally, the researchers found that the amount (1-3)-β-glucan could be decreased by filtering the sucrose solution through a 10-kDa filter. During their study, however, no further characterizations were made to identify the NPIs.

We tested our NPIs with the same assay and found high concentrations of (1-3)-β-glucan, just as described by Notarnicola et al. (24) (Figure 1). In addition, the values decreased markedly when the NPI samples were filtered through a 10-kDa membrane. This strongly indicates that the NPIs used in our study are comparable to the impurities that triggered the immunological side effects observed by Notarnicola et al. (24).

Conclusions

The presence of residual contaminants and impurities in (bio)pharmaceutical drug products should never be underestimated. In this study, we showed that NPIs negatively affected the stability of trastuzumab, rituximab, infliximab, and cetuximab. Although degradation profiles differed between the tested mAbs, destabilizing effects were observed at NPI concentrations that are, potentially, present in (bio-)pharmaceutical drug products formulated with sugar. Further studies are needed to identify the mechanism(s), protein characteristics, and formulation parameters involved in NPI-mediated protein

destabilization. We also showed that NPIs contained (1-3)-β-glucan, which is an immune-modulating molecule. Therefore, the presence of NPIs in therapeutic protein products is a potential risk factor for immunological side effects.

Acknowledgements

References

1. Jameel F, Hershenson S. Formulation and Process Development Strategies for Manufacturing Biopharmaceuticals. Hoboken, NJ, USA: John Wiley & Sons; 2010.

2. Carpenter JF, Manning MC. Rational Design of Stable Protein Formulations: Theory and Practice. New York, NY, USA: Kluwer Academic/Plenum; 2002.

3. Singh SK, Afonina N, Awwad M, Bechtold-Peters K, Blue JT, Chou D, et al. An industry perspective on the monitoring of subvisible particles as a quality attribute for protein therapeutics. J Pharm Sci. 2010;99(8):3302–21.

4. Narhi LO, Schmit J, Bechtold-Peters K, Sharma D. Classification of protein aggregates. J Pharm Sci. 2012 Feb;101(2):493–8.

5. Zölls S, Tantipolphan R, Wiggenhorn M, Winter G, Jiskoot W, Friess W, et al. Particles in therapeutic protein formulations, Part 1: overview of analytical methods. J Pharm Sci. 2012 Mar;101(3):914–35.

6. Narhi LO, Corvari V, Ripple DC, Afonina N, Cecchini I, Defelippis MR, et al. Subvisible (2-100 µm) particle analysis during biotherapeutic drug product development: Part 1, considerations and strategy. J Pharm Sci. 2015;104(6):1899–908.

7. Rosenberg AS. Effects of protein aggregates: an immunologic perspective. AAPS J. 2006 Jan;8(3):E501–7.

8. Carpenter JF, Randolph TW, Jiskoot W, Crommelin DJA, Middaugh CR, Winter G, et al. Overlooking subvisible particles in therapeutic protein products: gaps that may compromise product quality. J Pharm Sci. 2009 Apr;98(4):1201–5.

9. Jiskoot W, Randolph TW, Volkin DB, Middaugh CR, Schöneich C, Winter G, et al. Protein instability and immunogenicity: roadblocks to clinical application of injectable protein delivery systems for sustained release. J Pharm Sci. 2012 Mar;101(3):946–54.

10. Roberts CJ. Protein aggregation and its impact on product quality. Curr Opin Biotechnol. 2014;30:211–7.

11. Weinbuch D, Cheung JK, Ketelaars J, Filipe V, Hawe A, Den Engelsman J, et al. Nanoparticulate Impurities in Pharmaceutical-Grade Sugars and their Interference with Light Scattering-Based Analysis of Protein Formulations. Pharm Res. 2015;2419–27.

12. Rowe RC, Sheskey PJ, Cook WG, Fenton ME, Association AP. Handbook of Pharmaceutical Excipients. 7th ed. London: Pharmaceutical Press; 2012.

13. Lee JC, Timasheff SN. The stabilization of proteins by sucrose. J Biol Chem. 1981 Jul 25;256(14):7193–201.

14. Arakawa T, Timasheff SN. Stabilization of protein structure by sugars. Biochemistry. 1982 Dec 7;21(25):6536–44.

15.   Schwegman JJ, Hardwick L, Akers M. Practical Formulation and Process Development of Freeze-Dried Products. Pharm Dev Technol. 2005 May 1;10(2):151–73.

16.   Ph.Eur.2.9.20. General, particulate contamination: visible particles. In: The European Pharmacopoeia,. 7th ed. 2011.

17.   Kalonia C, Kumru OS, Prajapati I, Mathaes R, Engert J, Zhou S, et al. Calculating the Mass of Subvisible Protein Particles with Improved Accuracy Using Microflow Imaging Data. J Pharm Sci. 2014 Oct 9;1–12.

18.   Kamerzell TJ, Esfandiary R, Joshi SB, Middaugh CR, Volkin DB. Protein-excipient interactions: mechanisms and biophysical characterization applied to protein formulation development. Adv Drug Deliv Rev. Elsevier B.V.; 2011 Oct;63(13):1118–59.

19.   Chi EY, Weickmann J, Carpenter JF, Manning MC, Randolph TW. Heterogeneous nucleation-controlled particulate formation of recombinant human platelet-activating factor acetylhydrolase in pharmaceutical formulation. J Pharm Sci. 2005;94(2):256–74.

20.   Tyagi AK, Randolph TW, Dong A, Maloney KM, Hitscherich C, Carpenter JF. IgG particle formation during filling pump operation: A case study of heterogeneous nucleation on stainless steel nanoparticles. J Pharm Sci. 2009;98(1):94–104.

21.   Fradkin AH, Carpenter JF, Randolph TW. Glass particles as an adjuvant: a model for adverse immunogenicity of therapeutic proteins. J Pharm Sci. 2011 Nov;100(11):4953–64.

22.   Shomali M, Tanriverdi S, Freitag AJ, Engert J, Winter G, Siedler M, et al. Dose levels in particulate-containing formulations impact anti-drug antibody responses to murine monoclonal antibody in mice. J Pharm Sci. 2015;104(5):1610–21.

23.   Van Beers MMC, Gilli F, Schellekens H, Randolph TW, Jiskoot W. Immunogenicity of recombinant human interferon beta interacting with particles of glass, metal, and polystyrene. J Pharm Sci. 2012;101(1):187–99.

24.   Notarnicola S, Madden H, Browning J, Coots C, Eldredge J, Farrington G, et al. Poster Presentation: Investigation Of A Process Related Contaminant In a Clinical Drug Product. In: Recovery of Biological Products XI Conference. Banff Alberta, Canada; 2003.

25.   Williams DL. Overview of (1-->3)-beta-D-glucan immunobiology. Mediators Inflamm. 1997;6(4):247–50.

CHAPTER 9

SUMMARY AND PERSPECTIVES

Summary

Biopharmaceuticals have been highly successful in treating severe diseases and disorders that could not be treated by classical pharmaceutical compounds. A major obstacle for current research and development programs of biopharmaceutical drug products is the instability of the therapeutic protein, which may compromise safety and efficacy. For instance, the formation of aggregates, especially in the nm- and µm-size range, has been linked to immune reactions in patients, also known as unwanted immunogenicity. In the light of challenges regarding the analytical characterization of nm- and µm-particles, the aim of this thesis was to evaluate and improve established and emerging analytical techniques in this size range. These analytical techniques were then applied to characterize particles in the nm- and µm-size range present in protein formulations and to study the effect of nanoparticulate impurities on the stability of therapeutic proteins.

Chapter 2 introduced the concept of protein formulation development, which aims to assure the quality, safety, efficacy of a therapeutic protein product throughout the intended shelf life. Furthermore, various formulation strategies were outlined and challenges that can be encountered during the different stages of research and development for biopharmaceutical drug products are discussed.

Chapter 3 introduced the concept and underlying mechanisms of unwanted immunogenicity and gave guidance on how to select a suitable set of currently available immunogenicity prediction models during the different stages of research and development of biopharmaceutical drug products.

In **Chapter 4**, an improved version of the already established light obscuration technique was successfully applied to determine subvisible particle concentrations in formulations with high protein concentrations. It could further be shown how currently applied systems are limited in the analysis of viscous samples and that exceeding those limits could lead to an underestimation of particle counts.

Chapter 5 comparatively evaluated Micro-Flow Imaging (MFI) and Resonant Mass Measurement (RMM) as emerging techniques for the differentiation of protein particles and silicone oil droplets in biopharmaceutical formulations. The data showed that a customized morphological filter, developed specifically for this study, greatly improved the results delivered by the MFI instrument and enabled reliable discrimination of particles with a size as low as 2 µm. RMM showed highly accurate discrimination in the size range of about 0.5–2 µm. Therefore, it is recommended applying both techniques for a comprehensive analysis of biotherapeutics potentially containing silicone oil droplets and protein particles in the submicron and micron size range.

Chapter 6 compared four of the most relevant flow-imaging microscopy instruments and identified their differences, benefits and shortcoming to enable researchers the employment of the most suitable system for a given application. Based on the results, the systems were categorized into high-resolution systems, obtaining detailed morphology parameters enabling an accurate particle classification, and high-efficiency systems, delivering particle counts and sizes with high accuracy and precision.

In **Chapter 7**, it was shown that the interference of sugar-containing formulations with light scattering based analytical techniques is caused by the presence of a so far unknown type of nanoparticulate impurity in pharmaceutical-grade sugars. The results suggested them to be agglomerates of a variety of impurities (dextran, ash and aromatic colorants) not fully removed by the sugar refinement processes.

Chapter 8 investigated the effect of the nanoparticulate impurities discovered in Chapter 7 on the stability of four therapeutic monoclonal antibodies currently on the market. The stability of all antibodies was impaired by the presence of the nanoparticulate impurities resulting in the formation of aggregates, and nm- and µm-sized particles, however, to different extents among the antibodies. Furthermore, it was shown that the nanoparticulate impurities themselves contain immunomodulatory molecules potentially able to elicit immune responses in patients.

Perspectives

The work presented in this thesis aimed to support scientific efforts in making future biopharmaceutical products safer, by increasing the scientific understanding on the proper employment, strengths and limitations of crucial analytical techniques and by providing new insights into the nature and criticality of nm- and µm-sized particles. Future investigations and scientific studies should aim to improve particle characterization analytics, increase the fundamental understanding and optimize the prevention of aggregation, and to deliver further insights into the relationship between aggregate properties and immunogenicity.

Characterization of particles in biopharmaceutical products

The demand for novel and improved analytical techniques for the characterization of particles in the nm- and µm-size range has been expressed by many research groups in the past and is still valid (1–3). The "subvisible size gap" has been closed in part by the development of novel analytical techniques, some of which were evaluated in this thesis. In general, orthogonal methods employing truly different measurement principles are needed and should then be applied to overcome weaknesses and biases of instruments

relying on the same measurement principle. As an example, light-scattering based techniques NTA and DLS may be supported by emerging promising methods such as tailor dispersion analysis and flow cytometry, providing true orthogonality to commonly applied techniques (4–8).

Developments of new instruments for particle characterization should furthermore aim to address challenges presented by future biopharmaceutical drug products. The current trend, especially for monoclonal antibody products, goes towards highly concentrated preparations (e.g., above 100 mg/mL) for subcutaneous administration, due to the necessity of high doses (several mg/kg) with frequent dosing regimens (9). These products create new demands on current and future analytical technologies, such as small scale methods with low sample volume requirements and the ability to measure samples of high viscosity and high refractive index without the necessity of sample preparation (10–12). Some currently applied techniques would require a sample dilution step because of analytical limitations, which could alter a protein's aggregation state through a change in solvent composition and protein concentration, thereby affecting the reliability of test results (12).

Another trend for future biopharmaceutical drug products is the development of dedicated application devices and the use of prefilled syringes. These developments aim for a quicker and more accurate dosing, while enabling administration by non-professionals or self-administration (13). However, these developments come with new challenges. For example, the commonly applied process of siliconization of syringe surfaces for lubrication may lead to the presence of subvisible silicone oil droplets in some products (14–16). This creates the necessity for differentiation and identification of particles and demands novel analytical technologies and methodologies, some of which were evaluated during this thesis. While particles originating from primary packaging are not always harmful themselves, they can negatively affect the stability of the therapeutic protein (17,18). It is furthermore important to develop novel surface modification techniques that overcome the weaknesses of current container closure systems (13,19).

The combination of different measurement principles within one analytical device should also be in the focus of future development programs. For example, a device applying imaging microscopy or dynamic light scattering in liquid samples alongside Raman spectroscopy could establish a direct link between particle size and morphology and particle origin (20–23). Such insights would be highly valuably during biopharmaceutical development and troubleshooting.

Understanding and prevention of aggregation

A highly active field of research aims to understand the fundamental mechanisms underlying protein aggregation and the formation of nm- and µm-particles. Many different aggregation mechanisms have been identified, but it is not yet possible to predict which pathways will be predominant for a certain protein in a particular formulation (24). Furthermore, different pathways can exist in parallel and their occurrence depends on the molecular nature of the protein, the protein environment (e.g., formulation and primary container) and the applied stress conditions. If the molecular nature makes a protein prone to aggregation because of the presence of potential aggregation hot-spots, one could attempt to change the protein's sequence and structure by protein engineering (24,25). This, however, may not eliminate the formation of aggregates, since factors other than primary and secondary structure are important in this context. For some proteins, aggregation pathways in relation to pH and ionic strength have been identified (26–29). Unfortunately, these can in most cases not be directly applied to other proteins. Furthermore, it is currently not fully understood how proteins aggregate when exposed to solid-liquid and liquid-air interfaces (30,31). Thus, formulation developers still rely mostly on empirical data and scientific experience to find suitable formulation conditions and the (or a) right combination of stabilizing excipients. A correlation of protein characteristics to a range of potentially optimal formulation conditions, including suggestions for type and concentration of excipients, would enable a faster and more focused formulation-, and thereby product development.

Relationship between aggregate properties and immunogenicity

It is clear that the presence of protein aggregates, especially in the nm- and µm-size range, can dramatically increase the risk for unwanted immunogenicity and the occurrence of adverse effects in patients. Still, there is currently little understanding as to which specific properties of aggregates and particles are involved in immunogenicity (32). Studies have shown that the amount of aggregates and particles determined in drug products does not necessarily correlate to the presence, type, or severity of immunological reactions in patients (33). Thus, besides number and size of aggregates and particles, there must be many other attributes important for immunogenicity, such as the arrangement and content of T-cell and B-cell epitopes on the aggregates' surface, protein conformation within the aggregate, type and extent of chemical modifications accompanied with aggregation, and aggregate density and morphology. It is an active field of research to understand the contribution of each of those attributes to the overall immunogenicity of a biopharmaceutical drug product. These efforts, however, are often impaired by the availability of clinical data and the ability to compare quality attributes among the

different products, related to the lack of standardized particle analytics (34,35). Thus, improved techniques for the analysis of aggregates and particles, utilized in a standardized way, will contribute to the investigation of unwanted immunogenicity.

References

1. Narhi LO, Jiang Y, Cao S, Benedek K, Shnek D. A critical review of analytical methods for subvisible and visible particles. Curr Pharm Biotechnol. 2009 Jun;10(4):373–81.

2. Carpenter JF, Randolph TW, Jiskoot W, Crommelin DJA, Middaugh CR, Winter G, et al. Overlooking subvisible particles in therapeutic protein products: gaps that may compromise product quality. J Pharm Sci. 2009 Apr;98(4):1201–5.

3. Ríos Quiroz A, Lamerz J, Da Cunha T, Boillon A, Adler M, Finkler C, et al. Factors Governing the Precision of Subvisible Particle Measurement Methods - A Case Study with a Low-Concentration Therapeutic Protein Product in a Prefilled Syringe. Pharm Res. 2016;33(2):450–61.

4. Hawe A, Hulse WL, Jiskoot W, Forbes RT. Taylor dispersion analysis compared to dynamic light scattering for the size analysis of therapeutic peptides and proteins and their aggregates. Pharm Res. 2011 Sep;28(9):2302–10.

5. Cipelletti L, Biron JP, Martin M, Cottet H. Measuring Arbitrary Diffusion Coefficient Distributions of Nano-Objects by Taylor Dispersion Analysis. Anal Chem. 2015;87(16):8489–96.

6. Latunde-Dada S, Bott R, Hampton K, Leszczyszyn OI. Application of the Exact Dispersion Solution to the Analysis of Solutes beyond the Limits of Taylor Dispersion. Anal Chem. 2015;87(15):8021–5.

7. Lubich C, Malisauskas M, Prenninger T, Wurz T, Matthiessen P, Turecek PL, et al. A Flow-Cytometry-Based Approach to Facilitate Quantification, Size Estimation and Characterization of Sub-visible Particles in Protein Solutions. Pharm Res. 2015;(2):2863–76.

8. Nishi H, Mathäs R, Fürst R, Winter G. Label-Free Flow Cytometry Analysis of Subvisible Aggregates in Liquid IgG1 Antibody Formulations. J Pharm Sci. 2013 Nov 11;103(1):1–10.

9. Shire SJ, Shahrokh Z, Liu J. Challenges in the development of high protein concentration formulations. J Pharm Sci. 2004 Jun;93(6):1390–402.

10. Molloy S, Fesinmeyer RM, Martinez T, Murphy PD, Pelletier ME, Treuheit MJ, et al. Optimized UV Detection of High-Concentration Antibody Formulations using High-Throughput SE-HPLC. J Pharm Sci. 2015;104(2):508–14.

11. Hawe A, Schaubhut F, Geidobler R, Wiggenhorn M, Friess W, Rast M, et al. Pharmaceutical feasibility of sub-visible particle analysis in parenterals with reduced volume light obscuration methods. Eur J Pharm Biopharm. Elsevier B.V.; 2013 Feb 27;85(3 PART B):1084–7.

12. Zölls S, Gregoritza M, Tantipolphan R, Wiggenhorn M, Winter G, Friess W, et al. How subvisible particles become invisible-relevance of the refractive index for protein particle analysis. J Pharm Sci. 2013 Mar 5;102(5):1434–46.

13. Yoshino K, Nakamura K, Yamashita A, Abe Y, Iwasaki K, Kanazawa Y, et al. Functional evaluation and characterization of a newly developed silicone oil-free prefillable syringe system. J Pharm Sci. 2014 Mar 18;103(5):1520–8.

14. Majumdar S, Ford BM, Mar KD, Sullivan VJ, Ulrich RG, D'souza AJM. Evaluation of the effect of syringe surfaces on protein formulations. J Pharm Sci. 2011 Jul;100(7):2563–73.

15. Krayukhina E, Tsumoto K, Uchiyama S, Fukui K. Effects of syringe material and silicone oil lubrication on the stability of pharmaceutical proteins. J Pharm Sci. 2015 Sep 24;104(2):527–35.

16. Gerhardt A, Mcgraw NR, Schwartz DK, Bee JS, Carpenter JF, Randolph TW. Protein aggregation and particle formation in prefilled glass syringes. J Pharm Sci. 2014 Jun;103(6):1601–12.

17. Thirumangalathu R, Krishnan S, Ricci MS, Brems DN, Randolph TW, Carpenter JF. Silicone oil- and agitation-induced aggregation of a monoclonal antibody in aqueous solution. J Pharm Sci. 2009 Sep;98(9):3167–81.

18. Jones LS, Kaufmann A, Middaugh CR. Silicone oil induced aggregation of proteins. J Pharm Sci. 2005 Apr;94(4):918–27.

19. Depaz R a, Chevolleau T, Jouffray S, Narwal R, Dimitrova MN. Cross-linked silicone coating: A novel prefilled syringe technology that reduces subvisible particles and maintains compatibility with biologics. J Pharm Sci. 2014 Mar 18;103(5):1383–93.

20. Li B. A Comprehensive Technology of Particle Characterization that Automatically Measure Particle Size, Shape and Chemical Identity in One Single Platform. In: Cai X, Heng J, editors. Particle Science and Engineering. Cambridge: Royal Society of Chemistry; 2014. p. 126–30.

21. Saggu M, Liu J, Patel A. Identification of Subvisible Particles in Biopharmaceutical Formulations Using Raman Spectroscopy Provides Insight into Polysorbate 20 Degradation Pathway. Pharm Res. 2015;2877–88.

22. Lewis EN, Qi W, Kidder LH, Amin S, Kenyon SM, Blake S. Combined dynamic light scattering and raman spectroscopy approach for characterizing the aggregation of therapeutic proteins. Molecules. 2014;19(12):20888–905.

23. Zhou C, Qi W, Lewis EN, Carpenter JF. Characterization of Sizes of Aggregates of Insulin Analogs and the Conformations of the Constituent Protein Molecules: A Concomitant Dynamic Light Scattering and Raman Spectroscopy Study. J Pharm Sci. Elsevier Ltd; 2016;105(2):551–8.

24. Roberts CJ. Therapeutic protein aggregation: mechanisms, design, and control. Trends Biotechnol. Elsevier Ltd; 2014 Jul;32(7):372–80.

25. Wu SJ, Luo J, O'Neil KT, Kang J, Lacy ER, Canziani G, et al. Structure-based engineering of a monoclonal antibody for improved solubility. Protein Eng Des Sel. 2010;23(8):643–51.

26. Li Y, Ogunnaike BA, Roberts CJ. Multi-variate approach to global protein aggregation behavior and kinetics: effects of pH, NaCl, and temperature for alpha-chymotrypsinogen A. J Pharm Sci. 2010 Feb;99(2):645–62.

27. Brummitt RK, Nesta DP, Chang L, Chase SF, Laue TM, Roberts CJ. Nonnative aggregation of an IgG1 antibody in acidic conditions: part 1. Unfolding, colloidal interactions, and formation of high-molecular-weight aggregates. J Pharm Sci. 2011 Jun;100(6):2087–103.

28.   Sahin E, Grillo AO, Perkins MD, Roberts CJ. Comparative effects of pH and ionic strength on protein-protein interactions, unfolding, and aggregation for IgG1 antibodies. J Pharm Sci. 2010 Dec;99(12):4830–48.

29.   Kim N, Remmele RL, Liu D, Razinkov VI, Fernandez EJ, Roberts CJ. Aggregation of anti-streptavidin immunoglobulin gamma-1 involves Fab unfolding and competing growth pathways mediated by pH and salt concentration. Biophys Chem. Elsevier B.V.; 2013 Feb;172:26–36.

30.   Campioni S, Carret G, Jordens S, Nicoud L, Mezzenga R, Riek R. The presence of an air-water interface affects formation and elongation of α-synuclein fibrils. J Am Chem Soc. 2014 Jan;136(7):2866–75.

31.   Perevozchikova T, Nanda H, Nesta DP, Roberts CJ. Protein Adsorption, Desorption, and Aggregation Mediated by Solid-Liquid Interfaces. J Pharm Sci. 2015 Jun;104(6):1946–59.

32.   Filipe V, Schellekens H, Jiskoot W. Aggregation and Immunogenicity of Therapeutic Proteins. In: Wang W, Roberts C, editors. Aggregation of Therapeutic Proteins. 2010.

33.   Moussa EM, Panchal JP, Moorthy BS, Blum JS, Joubert MK, Narhi LO, et al. Immunogenicity of Therapeutic Protein Aggregates. J Pharm Sci. Elsevier Ltd; 2016;105(2):417–30.

34.   Hermeling S, Crommelin DJ a, Schellekens H, Jiskoot W. Structure-immunogenicity relationships of therapeutic proteins. Pharm Res. 2004 Jun;21(6):897–903.

35.   Jiskoot W, Kijanka G, Randolph TW, Carpenter JF, Koulov A V., Mahler HC, et al. Mouse Models for Assessing Protein Immunogenicity: Lessons and Challenges. J Pharm Sci. Elsevier Ltd; 2016;105(5):1567–75.

Nederlandse samenvatting

Biofarmaca worden succesvol ingezet bij het behandelen van ernstige ziekten en aandoeningen die niet te behandelen zijn met klassieke geneesmiddelen. Echter, een grote belemmering voor hedendaags onderzoek naar nieuwe biofarmaca betreft de instabiliteit van therapeutische eiwitten, wat een schadelijke invloed kan hebben op de veiligheid en werkzaamheid. Zo is de vorming van aggregaten – met name in de nanometer en micrometer schaal – in verband gebracht met immuunreacties in patiënten. Dit fenomeen staat beter bekend als ongewenste immunogeniciteit.

In **Hoofdstuk 2** wordt het formuleringsproces van therapeutische eiwitten geïntroduceerd. Dit proces vormt een essentieel onderdeel van de ontwikkeling van biofarmaca, omdat het tracht het therapeutische en commerciële succes van veelbelovende producten te waarborgen. Het verzekeren van de kwaliteit, veiligheid en werkzaamheid gedurende de houdbaarheid van het product is daarbij het hoofddoel. Omdat het formuleringsproces plaatsvindt tijdens het gehele ontwikkelingsproces van biofarmaca, bestaat het formuleringsproces uit verschillende fases. Bovendien vereist elk biofarmacon een unieke formulering om een aantal redenen: verschillende vatbaarheden voor bepaalde degradatiemechanismen, specifieke karakteristieken van het actieve bestanddeel (het therapeutische eiwit), bepaalde eisen om de therapietrouw te verhogen en diverse marketingoverwegingen. Daarnaast kan het formuleringsproces op verschillende manieren worden aangepakt. Zo kan er, gebaseerd op een rationele aanpak, gebruik worden gemaakt van wetenschappelijke kennis die verkregen is door het systematisch analyseren van eiwitten met behulp van diverse analytische technieken. Dit hoofdstuk geeft een introductie over het formuleringsproces van therapeutische eiwitten. Hierbij zullen huidige formuleringsstrategieën en uitdagingen worden behandeld.

Omdat alle therapeutische eiwitten de potentie hebben om immunogeen te zijn, zal in **Hoofdstuk 3** ongewenste immunogeniciteit en onderliggende mechanismen besproken worden. Antilichamen tegen therapeutische eiwitten kunnen namelijk de werkzaamheid verminderen, wat kan leiden tot een toename in de kosten van een therapie. In zeldzame gevallen kan het zelfs resulteren in levensbedreigende situaties. Vandaar dat het belangrijk is om therapeutische eiwitten te ontwikkelen met een minimale immunogeniciteit. Het voorspellen van immunogeniciteit speelt daarom al vroeg in het ontwikkelingsproces een belangrijke rol. Verschillende in silico-, in vitro- en in vivo-modellen kunnen gebruikt worden om immunogeniciteit te voorspellen. Dit biedt de mogelijkheid om immunogene eigenschappen te identificeren en om een selectie te maken van eiwitten met een lage immunogeniciteit. Hoewel dergelijke modellen volop worden gebruikt, zijn er verschillen in de voorspellende waarde. Zo is er nog onvoldoende kennis over het type immuunreactie op therapeutische eiwitten dat ongewenste

immunogeniciteit tot gevolg heeft. Daarnaast verkennen modellen verschillende componenten van het immuunsysteem en is er een gebrek aan een geïntegreerde klinische validatie. In dit hoofdstuk bespreken we welke modellen tegenwoordig in gebruik zijn en welke aspecten van immunogeniciteit deze modellen vertegenwoordigen. Daarnaast bediscussiëren we de toegevoegde waarde en beperking van elk model.

Light obscuration (LO) is tegenwoordig een standaardtechniek om subvisuele (microscopisch fijne) deeltjes te analyseren tijdens de kwaliteitscontrole van geneesmiddelen die parenteraal worden toegediend, zoals therapeutische eiwitten. In sommige gevallen hebben zulke geneesmiddelen een hoge viscositeit door een hoge eiwitconcentratie. Dit kan leiden tot foutieve LO-metingen. In **Hoofdstuk 4** wordt omschreven hoe een verhoogde viscositeit van vloeibare monsters, vanaf 9 centipoise (cP), leidde tot een onderschatting in het aantal subvisuele deeltjes. Het toepassen van een overdruk op monsters met een hoge viscositeit bleek de betrouwbaarheid van de LO-metingen te herstellen zonder dat extra monstervoorbewerkingen vereist waren. Daarnaast werd duidelijk dat huidige analytische technieken niet goed in staat zijn om viskeuze samples te analyseren. Wanneer hier geen rekening mee wordt gehouden kan dit leiden tot een onderschatting in het aantal deeltjes.

In **Hoofdstuk 5** wordt omschreven hoe *Micro-Flow Imaging* (MFI) en *Resonant Mass Measurement* (RMM) gebruikt kunnen worden om siliconenoliedruppels en eiwitdeeltjes van elkaar te onderscheiden. Het kunnen onderscheiden van dergelijke deeltjes – op nanometer- en micrometer-schaal – is essentieel voor de ontwikkeling van biofarmaca, met name bij voorgevulde injectiespuiten. In dit onderzoek werd gebruikgemaakt van kunstmatig verkregen siliconenoliedruppels en eiwitdeeltjes. Daarnaast werden deze deeltjes gemengd in verschillende verhoudingen om te onderzoeken in hoeverre de technieken in staat zijn om deze deeltjes te onderscheiden. De ingebouwde MFI-software was in staat om siliconenoliedruppels en eiwitdeeltjes van elkaar te onderscheiden wanneer de deeltjes groter waren dan 2 μm en er een mengverhouding van 70:30-30:70 werd gebruikt. Tevens werd er een MFI-softwarefilter ontwikkeld dat de prestaties aanzienlijk verbeterde; zelfs wanneer er extreme mengverhoudingen werden gebruikt van 95:5-15:85. Daarentegen bleek RMM in staat te zijn om siliconenoliedruppels en eiwitdeeltjes van 0.5 tot 2 μm van elkaar te onderscheiden, onafhankelijk van de mengverhouding die werd gebruikt. Kortom, zowel MFI als RMM waren in staat om deeltjes van elkaar te onderscheiden. Daarom adviseren we om beide technieken te gebruiken bij het analyseren van biofarmaca die mogelijk siliconenoliedruppels en/of eiwitdeeltjes bevatten.

Flow Imaging Microscopy (FIM) is een aantal jaren geleden geïntroduceerd en is sindsdien steeds belangrijker geworden voor het analyseren van eiwitdeeltjes. **Hoofdstuk 6**

omschrijft een vergelijking van vier relevante FIM-apparaten (MFI4100, MFI5200, FlowCAM VS1 en FlowCAM PV) voor het analyseren van biofarmaca. Voor deze vergelijking werden verschillende deeltjes gebruikt, namelijk polystyreen standaarddeeltjes, eiwitdeeltjes (gemaakt van monoklonale antilichamen) en siliconenoliedruppels. Naast de kwantificering en karakterisering is onderzocht hoe goed de apparaten in staat zijn om verschillende type deeltjes van elkaar te onderscheiden. Bovendien is er gekeken naar de gebruiksvriendelijkheid en kwaliteit van de verkregen afbeeldingen van de deeltjes. De FlowCAM-apparaten, met name de FlowCAM VS1, creëerden afbeeldingen in een hoge resolutie. De FlowCAM PV gaf de meest precieze kwantificering van het aantal eiwitdeeltjes, zelfs wanneer er sprake was van suboptimale omstandigheden door een verhoogde brekingsindex van de formulering. Bovendien was dit systeem het beste in staat om eiwitdeeltjes van siliconenoliedruppels te onderscheiden. Ook de MFI-apparaten konden accuraat de deeltjesgrootte- en concentratie van samples met polystyreen standaarddeeltjes vaststellen. De MFI5200 bleek hierin het best in staat. Dit apparaat was, net als de FlowCAM PV, ook in staat om eiwitdeeltjes te detecteren, zelfs wanneer er sprake was van een verhoogde brekingsindex. In vergelijking met de FlowCAM-apparaten waren de MFI-apparaten gebruiksvriendelijker en bleek het gemakkelijker om gestandaardiseerde metingen en data-analyses uit te voeren. De belangrijkste conclusie van dit onderzoek is dat de selectie van het meest geschikte FIM-systeem sterk afhankelijk is van de voornaamste output parameters met betrekking tot het doel van het onderzoek.

Hoofdstuk 7 beschrijft de hoofdoorzaak en consequentie van het interferentiesignaal (100-200 nm) dat zich manifesteert bij *Dynamic Light Scattering* (DLS) en *Nanoparticle Tracking Analysis* (NTA) analyses van suikerhoudende oplossingen. In dit onderzoek zijn verschillende suikers met variërende zuiverheden en van diverse leveranciers geanalyseerd met DLS en NTA. Ook is het effect van ultrafiltratie en diafiltratie bestudeerd. Verder zijn *Fourier Transform Infrared* (FTIR) *Microscopy*, *Scanning Electron Microscopy Coupled Energy-dispersive X-ray Spectroscopy* (SEM-EDX) en *Fluorescence Spectroscopy* gebruikt. De intensiteit van het interferentiesignaal was afhankelijk van het type suiker en zuiverheid, en de leverancier en productiepartij. Ultrafiltratie van monsters met een 0.02-μm filter verwijderde het interferentiesignaal. Het interferentiesignaal bleek veroorzaakt te worden door nanodeeltjes – bestaande uit dextranen, mineralen en aromatische kleurstoffen – die niet volledig verwijderd waren tijdens het suikerraffinage proces. Kortom, het interferentiesignaal werd veroorzaakt door nanodeeltjes die als verontreiniging aanwezig zijn in farmaceutische suikers. Verder in deze samenvatting zal er naar deze nanodeeltjes gerefereerd worden als *Nano-Verontreinigingen* (NVs).

In **Hoofdstuk 8** wordt omschreven welk effect de eerder omschreven NV's hebben op de stabiliteit van verschillende monoklonale antilichamen. Eerst zijn NV's verkregen uit

farmaceutische graad sucrose (saccharose). Vervolgens zijn de verkregen NV's toegevoegd aan trastuzumab-, rituximab-, infliximab- en cetuximab-formuleringen. De stabiliteit van de monoklonale antilichamen is onderzocht door middel van *Visual Inspection*, FIM, NTA, *Size-exclusion Chromatography* (SEC), *Capillary Isoelectric Focusing en Intrinsic Differential Scanning Fluorimetry* als functie van opslagtijd, temperatuur en NV-concentratie. Ook zijn de NV's gekarakteriseerd met behulp van laser Doppler electrophorese en de Glucatell assay om de ζ-potentiaal en het (1-3)-β-glucaangehalte te bepalen. NV's bleken een schadelijke invloed te hebben op alle onderzochte monoklonale antilichamen. Na het toevoegen van NV's aan trastuzumab werden de formuleringen troebel en ontstonden er grote aantallen microdeeltjes. In rituximab- en cetuximabformuleringen vormden zich alleen hoge aantallen nanodeeltjes. Na het toevoegen van NV's aan infliximab ontstonden er zowel nanodeeltjes als microdeeltjes. Bovendien werd het infliximab-mengsel troebel. Hoewel de stabiliteit van trastuzumab en infliximab vrijwel direct na het toevoegen van NV's al verminderde, was dit bij rituximab en cetuximab pas detecteerbaar na een opslagtijd van 14 weken en een verhoogde opslagtemperatuur. Bovendien werd de stabiliteit van rituximab en infliximab al beïnvloed door een NV-concentratie die mogelijk in commerciële producten aanwezig is. De stabiliteit van trastuzumab werd alleen beïnvloed bij hogere concentraties NV's. NV's bleken ook een hoog gehalte te hebben aan (1-3)-β-glucaan, een immuunstimulerende stof. Samengevat vormt de aanwezigheid van NV's in farmaceutische suikers een risico op stabiliteitsproblemen en ongewenste immunogeniciteit.

Gezien de problemen met betrekking tot het karakteriseren van deeltjes in de nanometer- en micrometer-schaal zal dit proefschrift hopelijk leiden tot een verbetering van bestaande en opkomende analytische technieken om subvisuele deeltjes te onderzoeken. Daarnaast kunnen wetenschappers die werkzaam zijn bij bedrijven of universiteiten de verkregen inzichten toepassen om analytische technieken zo effectief mogelijk te gebruiken. Dit proefschrift laat ook zien dat farmaceutische suikers NV's bevatten die niet alleen interfereren met analytische technieken, maar ook een schadelijk effect bleken te hebben op de stabiliteit van monoklonale antilichamen. De resultaten gepresenteerd in de voorgaande hoofdstukken dragen dus bij aan de mondiale inspanning om veilige en effectieve geneesmiddelen te ontwikkelen.

Abbreviations

%	percent
%RH	Percent relative humidity
°C	Degree Celsius
µg	Microgram
µL	Microliter
µm	Micrometer
ABD	Area based diameter
ACS	American Chemical Society
ADA	Anti-drug antibody
AF4	Asymmetric flow field flow fractionation
Al	Aluminum
ANN	Artificial neuronal networks
APC	Antigen-presenting cell
API	Active pharmaceutical ingredient
Asp	Asparagine
AU	Absorption unit
AUC	Analytical ultracentrifugation
C	Carbon
Ca	Calcium
CD4+	Cluster of differentiation 4 positive
CFR	Code of federal regulations
cIEF	Capillary isoelectric focusing
cP	Centipoise
cSt	Centistokes
CTA	Clinical trial authorization
DLS	Dynamic light scattering
DNA	Deoxyribonucleic acid
DP	Drug product
DS	Drug substance
DSC	Differential scanning calorimetry
DSF	Dynamic scanning fluorimetry
ECD	Equivalent circular diameter
EDX	Energy dispersive X-ray spectroscopy
ELISA	Enzyme-linked immunosorbent assay

Exp.	Expiration date
FDA	Food and Drug Administration
Fe	Iron
FTIR	Fourier transform infrared spectroscopy
g	Gram
Glu	Glutamine
h	Hour(s)
H	Hydrogen
H_2O_2	Hydrogen peroxide
HCl	Hydrogen chloride
His	Histidine
HLA	Human leukocyte antigen
HMW	High molecular weight
HPLC	High performance liquid chromatography
HTF	High throughput formulation
ICH	International Council for Harmonization
IgG	Immunoglobulin G
IgG1	Immunoglobulin G1
IgM	Immunoglobulin M
IL	Interleukin
INF	Interferon
K	Potassium
kDa	Kilo Dalton
LA	License application
LDE	Laser Doppler electrophoresis
LMW	Low molecular weight
LO	Light obscuration
LOD	Limit of detection
mAb	Monoclonal antibody
MDa	Mega Dalton
MFI	Micro-Flow Imaging
mg	Milligram
Mg	Magnesium
MHC	Major histocompatibility complex
min	Minute(s)
mL	Milliliter

mM	Millimolar
mm	Millimeter
MS	Mass spectrometry
NaCl	Sodium chloride
nDSF	Intrinsic dynamic scanning fluorimetry
ng	Nanogram
NIST	National Institute of Standards and Technology
NK	Natural killer cells
nm	Nanometer
NPI	Nanoparticulate impurities
NTA	Nanoparticle tracking analysis
O	Oxygen
P	Phosphorus
Part./mL	Particles per milliliter
PBMC	Peripheral blood mononuclear cells
PDI	Polydispersity index
Ph.Eur.	European Pharmacopeia
PK/PD	Pharmacokinetics / pharmacodynamics
pKa	Acid dissociation constant
PVDF	Polyvinylidene fluoride
QC	Quality control
R^2	Coefficient of determination
RI	Refractive index
RMM	Resonant mass measurement
RNA	Ribonucleic acid
rpm	Rounds per minute
s	Second(s)
S	Sulfur
SEC	Size-exclusion chromatography
SEM	Scanning electron microscopy
Si	Silicon
SLS	Static light scattering
SMR	Suspended microchannel resonator
TCR	T cell receptor
TFF	Tangential flow filtration
Tg'	Glass transition temperature of the frozen state

Tm	Melting temperature
TNF	Tumor necrosis factor
UPLC	Ultra performance liquid chromatography
US	United States
USP	United States Pharmacopeia
UV	Ultra-violet
v/v	Volume per volume
w/v	Weight per volume
w/w	Weight per weight
λ	Wavelength

List of publications

Weinbuch D*, Zölls S*, Wiggenhorn M, Friess W, Winter G, Jiskoot W, Hawe A. Micro-flow imaging and resonant mass measurement (Archimedes) - complementary methods to quantitatively differentiate protein particles and silicone oil droplets. *Journal of Pharmaceutical Sciences* 2013 Jul;102(7):2152-65.

Brinks V, **Weinbuch D**, Baker M, Dean Y, Stas P, Kostense S, Rup B, Jiskoot W. Preclinical models used for immunogenicity prediction of therapeutic proteins. *Pharmaceutical Research* 2013 Jul;30(7):1719-28.

Zölls S*, **Weinbuch D***, Wiggenhorn M, Winter G, Friess W, Jiskoot W, Hawe A. Flow imaging microscopy for protein particle analysis--a comparative evaluation of four different analytical instruments. *AAPS Journal* 2013 Oct;15(4):1200-11.

Weinbuch D, Jiskoot W, Hawe A. Light obscuration measurements of highly viscous solutions: sample pressurization overcomes underestimation of subvisible particle counts. *AAPS Journal* 2014 Sep;16(5):1128-31.

Weinbuch D, Cheung JK, Ketelaars J, Filipe V, Hawe A, den Engelsman J, Jiskoot W. Nanoparticulate impurities in pharmaceutical-grade sugars and their interference with light scattering-based analysis of protein formulations. *Pharmaceutical Research* 2015 Jul;32(7):2419-27

Weinbuch D, Hawe A, Jiskoot W, Friess W. Introduction into formulation development of biologics. In: *Challenges in Protein Product Development* by Mahler HC & Warne NW (editors). Manuscript accepted for publication.

Weinbuch D, Fogg M, Ruigrok M, Jiskoot J, Hawe A. Nanoparticulate impurities in pharmaceutical-grade sucrose are a potential threat to protein stability. Manuscript submitted for publication.

*shared first authors

Curriculum vitae

Daniel Weinbuch was born on May 1st 1985 in Illertissen, Germany. In September 2004, he started his career by earning an associate degree as a pharmaceutical production technician at Merckle in Ulm, Germany and further gained experience in fill-finishing processes by working at the validation/qualification department for sterile dosage forms at ratiopharm in Blaubeuren, Germany, until August 2015. He subsequently pursued an academic study in Pharmaceutical Biotechnology at the Biberach University of Applied Sciences in Germany from which he graduated in January 2010. During this study, he wrote his Bachelor thesis on the development of human monoclonal antibodies by phage display at Boehringer Ingelheim in Ridgefield, CT, USA. He further worked as a scientist at the Kobe Pharma Research Institute in Japan in 2010 before earning his Master's degree in Biopharmaceutical Sciences from the Leiden University in the Netherlands in September 2012, where he focused on protein aggregation and unwanted immunogenicity. In February 2013, Daniel Weinbuch started his PhD project under the supervision of Prof. Dr. Wim Jiskoot at the Leiden Academic Centre for Drug Research (LACDR) in the Netherlands in collaboration with Dr. Andrea Hawe at Coriolis Pharma in Munich, Germany. While focusing on the topic "pharmaceutical aspects of subvisible particles in protein formulations", he (co-)authored seven peer-reviewed publications and gave podiums presentations at international conferences on several occasions. During the PhD project-collaboration, Daniel Weinbuch worked part-time as a formulation scientist at Coriolis Pharma. Since March 2016, he is employed as the Manager GRP (Good Research Practice) at Coriolis Pharma.